# Assessment of Runoff Regime in Wang Chhu River Basin, Bhutan by Snow cover mapping and stream flow modelling.

SONAM LHAMO
February,2015

SUPERVISORS:
DR. ING. T.H.M (TOM) RIENTJES
DR.IR.C (CHRISTIAAN). VAN DER TOL

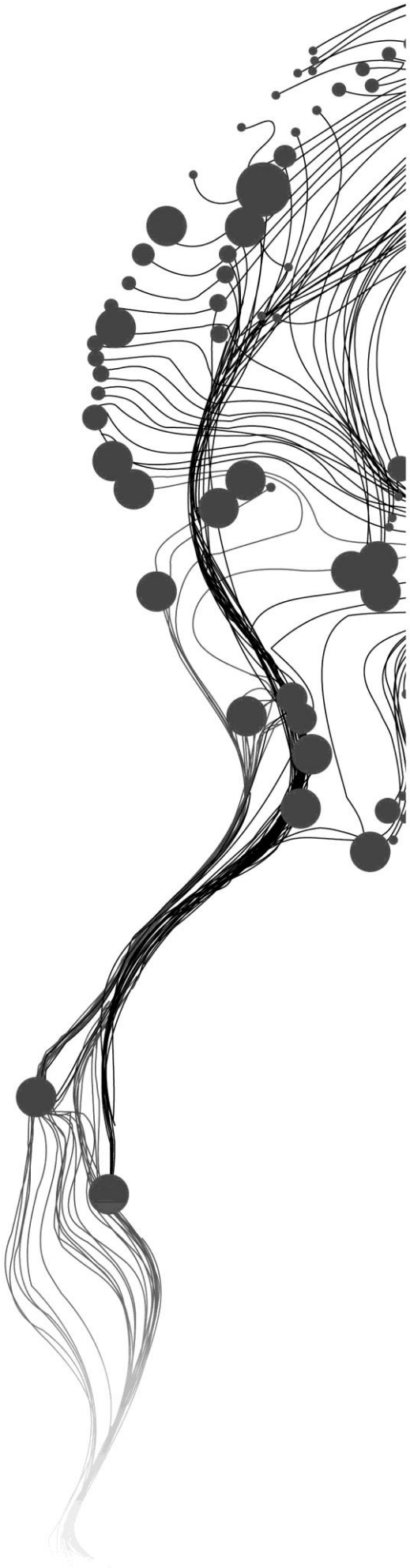

# ASSESSMENT OF RUNOFF REGIME IN WANG CHHU RIVER BASIN, BHUTAN BY SNOW COVER MAPPING AND STREAM FLOW MODELLING.

SONAM LHAMO
Enschede, The Netherlands, [February,2015]

Thesis submitted to the Faculty of Geo-Information Science and Earth Observation of the University of Twente in partial fulfilment of the requirements for the degree of Master of Science in Geo-information Science and Earth Observation.
Specialization: Water Resources and Environmental Management

SUPERVISORS:
DR. ING. T.H.M (TOM) RIENTJES
DR.IR.C (CHRISTIAAN). VAN DER TOL

THESIS ASSESSMENT BOARD:
Prof. Dr. Z. (Bob) Su (Chair)
Prof. Dr. P. Reggiani (University of Siegen)
Dr. T.H.M. Rientjes
Dr. C. van der Tol

# ABSTRACT

Snow and its dynamics play an important role in the Global water cycle. The Northern frontiers of Bhutan have large areas under snow cover and glaciers which feed most of the river systems in the country. Understanding the runoff regime of these basins are important for various hydrological purposes. This thesis investigates the use of remote sensing snow products for snow cover mapping in the Wang Chhu Sub basin in Bhutan, daily and eight day composite MODIS TERRA snow products were used for the snow cover mapping and analysis. MODIS an optical sensor on board NASA's Earth Observation system's Terra and Aqua satellite is desirable because of its high temporal and spatial resolution and also because it is easily accessible and because of its high accuracy reported from other regions.

The snow cover maps derived from the MODIS snow products show a large percentage of cloud cover and therefore to analyse the snow cover data various steps and processes were adopted for the proper analysis of the snow cover area. Overall the average cloud percentage for the snow cover maps derived from the daily MODIS Terra snow product was found to be over 50% for the entire study period of eight years (2003-2008).To develop relationship between the snow cover area and the runoff the basin was divided into catchments and regression analysis were carried out, though the strength of correlation of the regressions were weak, the general pattern was increase in snow cover resulted in decrease in the stream flow. To check for the spatial and temporal variability of the snow cover area in the basin, the basin was divided into elevation zones and snow cover for each elevation zone was calculated and also depletion curves helped in understanding the spatial and temporal variability of snow cover in the study area.

Next the HBV-96 model was used to calibrate and validate the streamflow of the study area for the years 2003 to 2010, where 2003 being the warm up period, 2004-2008 the calibration period and 2009-2010 the validation period. The manual calibration with the optimized parameters yielded in a Nash Sutcliffe (NSE) value of 0.80 and a NSE of 0.75 for the validation period.The HBV model simulation represented the snow cover area fairly whereby the timing of melt and accumulation of snow was comparable to the snow cover data from the MODIS snow product.

Key words: Snow cover mapping, MODIS snow products, calibrate, mapping, remote sensing, and validation.

# ACKNOWLEDGEMENTS

I would like to extend my sincere thanks to my first supervisor Dr. T.H.M. Rientjes for his unwavering support,encouragement and for all the advices,this thesis would not have been possible without his guidance.

I would also like to thank my second supervisor Dr. C. Van der Tol for his support and valuable comments throughout the thesis period.

I am grateful for the enormous support,resources and help provided to me by the staff and Lecturers in the Department of Water Resources,ITC for a very fulfilling and active learning throughout the course of my study.I present my gratitude to Mr Chimmi Dorji from the Department of Hydromet Services, Bhutan for all his timely assistance in collecting the data for this research work.

I would like to give my special thanks to the Netherlands Fellowship Programme(NFP) for providing me this opportunity to study at ITC.And finally I would like to acknowledge my classmates in the Core Module and in the Water Resources Department for all their co operation and support and most of all for making school life fun.

# TABLE OF CONTENTS

# LIST OF FIGURES

# LIST OF TABLES

# 1. INTRODUCTION

## 1.1. Background

Ice and snow on land surfaces and sea collectively called the cryosphere is one of the most important component of the earth's climate system. Snow cover forms one of the largest component of the cryosphere covering approximately one third of the earth's surface every year ("Snow and Climate | National Snow and Ice Data Centre," 2014). About 70% of the world's fresh water resources are stored in ice and snow (UNEP, 2007).Snow has a large influence on the water balance and the energy balance. Seasonal snow melt is one of the main contributors to runoff in many mountainous regions and it is the main source of water for irrigation and water supply for billions of people living in these regions. The energy balance is affected since snow has very high albedo and low thermal conductivity (Hall & Riggs, 2007). Because of its physical properties, snow cover plays a very important role in influencing global and regional energy cycle as well as the water and carbon cycle (after FAO, 2009). Over the last four decades, snow cover has globally decreased substantially (UNEP, 2007) and is attributed to global warming (IPCC, 2007).The decrease in spatial snow cover extent and increased snow cover melt is expected to continue for the decades ahead by projected increases in global temperature. Changes in snow cover potentially could have very serious impacts on ecology, water resources, agriculture, and economic activities including hydropower generation, industry, transportation and other social impacts. Therefore monitoring of snow cover has been identified to be of prime importance for better understanding of global and regional climates, and assessment of water resources(FAO, 2009).At the international level snow cover has been declared as an essential climate variable for Global climate observing system(GCOS) of the World Meteorological Organization(GCOS,2010).

The Hindu Kush Himalayan (HKH) region extending from Afghanistan in the east to Myanmar in the west, covers an area of approximately 4.19 million square kilometres (ICIMOD, 2011) and contains the largest concentration of ice and snow cover outside the Polar region. The area forms one of the largest storehouses of fresh water sources and in the higher altitude (above 3000m) a substantial amount of the annual precipitation falls as snow (Gurung et al., 2011). The HKH region is the source of some of the largest Asian river systems like Indus, Ganges, Brahmaputra and Mekong among others( Kulkarni et al.,2011) .These major rivers originate from the mountainous regions which have their catchments in snow covered areas and snow melt is one of the major component of stream flow. The large population living in these river valleys depend on the rivers for their livelihood and the ever increasing demand for fresh water has initiated the need to predict the amount of melt water contributing to the stream flow for better management of water resources in the HKH region.

Bhutan has always been following a conservation centred development policy which has resulted in maintaining and preserving the country's natural resources. Currently Bhutan has a forest cover of approximately 70.46%(NSB, 2013).As a result of the good forest cover and an average annual precipitation of about 2200 mm, the country is endowed with abundant water resources. Almost all the valleys in Bhutan have a swiftly flowing river which are fed by snow/glacial melt and rainfall during the summer monsoon or both. Bhutan has one of the highest total renewable water resources per capita in the South East Asian region estimated at 109,294 cubic meter per capita per year(2009)("UN Water: KWIP," 2014).Almost 80 % of the total population depends on agriculture and livestock farming for their livelihood, the farmers depend on the rivers, springs and rainfall for irrigation purposes. The steep

mountains, deep valleys and swiftly flowing rivers are the source of the country's hydro power generation, which is one of the major contributors to the country's economy.

Even if endowed with rich and plentiful water resources, Bhutan still faces localized and seasonal water shortages for both drinking and agricultural purposes. Only 78% of the population has excess to clean drinking water and 12.5% of arable land is irrigated(NEC,2003.).Precipitation is unevenly distributed spatially, river sediment loads have drastically increased over the years and there is a wide variation in river flows during dry and monsoon seasons. To aggravate problems further pressure on water resources is increasing due to water demands from various growing sectors like industries, increasing population apart from agricultural purposes.

Like in the other parts of the Himalayas, Bhutan's rivers are fed by glacier and snowmelt. Agriculture is the main source of livelihood for about 80% of the people. Hydro power is one of the largest contributor to the kingdom's economy generating over 45% of the national revenue (NSB, 2013).In Bhutan snow and glacier melt contributes substantially to stream flow more so during the dry season, there are indications that climate change have serious impacts on seasonal and annual runoff (IPCC, 2007).Studies show that in recent times glaciers have been melting which will eventually have long term effect on the amount of snow and glacier melt causing reduction in the stream flow during the dry season which can have serious impacts on the hydro power sector of the economy (Rupper et al., 2012a). Dietz, et al., (2012) describe that it is crucial to have an accurate snow cover and snow water equivalent map for assessing the contributions of snow and glacier melt to stream flow for better management of hydro power and better understanding, planning and development of the water resources in the country.

In the last few decades many hydrological models have been in use for various applications. Singh, (1995) has documented most popular computer models of watershed hydrology. Singh& Frevert, (2002a, 2002b) published a 2 volume book with a comprehensive account of 38 models for large and small watershed hydrology. The World Meteorological Organization was among the first ones to carry out inter-comparisons of hydrological models (WMO, 1982) and also snowmelt models (WMO, 1986). Hydrological models facilitates in understanding the influence of variability of snow cover on various other aspects of climate. In areas where the primary source of runoff in the stream flow is from snow melt, snowmelt runoff modelling has become an inevitable tool for water resource management. Snow cover area and snow water equivalent which is the liquid water which would be released upon complete melting of the snowpack are the important inputs for modelling snowmelt (Mhawej et al., 2014).

Traditionally the inputs for hydrological models are obtained from ground point-measurements of precipitation, temperature and other climatic variables from hydro-meteorological stations but with improvement in technology and with the advent of remote sensing, near real time data with good spatial and temporal resolution have become available(. Hall &Martinec, 1986). Remote sensing techniques have been widely used for snow cover mapping, monitoring and snow melt runoff studies globally at various temporal and spatial scales (Williams & Ferrigno, 2005).One of the first applications of remote sensing for snow related studies was reported from Eastern Canada in April 1960 with the TRIOS-1 satellite (Kulkarni, et al., 2006a).Since then, the use of operational remote sensing based mapping has been improving over the decades with the development of higher temporal frequency and improved sensors at higher spatial resolution. Remote sensing is an inevitable tool in monitoring snow cover and its processes especially in areas where there is scarcity of in-situ field measurements like in the Himalayas (Jain, et al., 2010).Mapping and monitoring of snow related processes is vital for modelling of snow melt runoff processes, hydrological analysis and water resources evaluation. Accurate and timely measurement of snow cover area and duration are important for modelling stream flow because snow cover area depletion

controls the runoff regime (Ferguson, 1999). Snow water equivalent is an important input for hydrological modelling and runoff prediction. Snow cover data acquired by remote sensing has been used as inputs for stream flow modelling and it has resulted in improved simulation of snowmelt runoff (Foster & Rango, 1989)

## 1.2. Problem Statement

Scientific studies carried out in the Bhutan Himalayas were mostly focused on glaciers, glacial lakes, glacial lake outburst floods and their dynamics because of the fact that the country faces huge threat from these disasters. This since there have been several incidences of Glacial Lake outburst floods in the last 50 years with the most recent one in 1994 with major socio-economic impacts (Ageta,et al., 2000), (Komori, 2008), (Rupper et al., 2012), (Naito, et al., 2012) and (Tadono & Kawamoto, 2012). Glaciers and their dynamics received much attention, while snow cover and its contribution to runoff has been largely neglected in scientific studies in Bhutan.

In Bhutan snowmelt is one of the major contributors to stream flow but there are studies or assessments where contributions are quantified. Since seasonal snow cover is important in assessing the availability of water in the rivers (Kulkarni,et al. 2006), it is therefore very important to map the areal extent of snow and water equivalent for various climatological and hydrological applications.

In other Himalayan regions remote sensing has been widely used in assessing snow cover and many recent studies on snow cover and its variability in the Himalayan region have shown decline in snow cover area, it has been reported by (Rikiishi & Nakasato, 2006) that snow cover in the Himalayas have decreased by about one third and the snow cover duration by 23 days between 1996 and 2001 at elevations of 4000-6000m. Study by (Prasch,et al., 2013) state that in a central Himalayan basin, Lhasa river basin, more than 50 % of runoff is from snowmelt. Similarly (Tahir,et al., 2011) reported that in the Upper Indus basin, more than 65% of the annual flow of the Upper Indus river is from seasonal and permanent snowfields above 3500m. Unlike the above mentioned studies, work of (Siderius et al., 2013) in the Ganges basin, India states that annual snowmelt contribution to runoff accounts for approximately between 1% to 5%.These findings may or may not hold true for the case of Bhutan but climate data and information is sparse and not well documented(NEC, 2008) in Bhutan which contributes to a lot of uncertainties in the researches carried out. Of the very few studies carried out in Bhutan, a recent study by (Ghedira,et al., 2011), used MODIS snow products to study snow cover status and trends in Bhutan, they concluded that both inter-annual and seasonal trend for snow cover area showed a declining trend for the period 2002-2010. However it has not been investigated as to how the declining snow cover area affected the runoff in the stream flow. And keeping in view Bhutan's Hydro power sector, the backbone of the economy which depends on the runoff in the rivers, it is of utmost importance to have an idea of the contribution of snowmelt in the stream flow. Hydrological stream flow modelling studies in Bhutan has been carried out only for the purpose of hydro power and climate change studies(Beldring & VoksØ, 2012) and is not been used as a tool for sustainable water resource management. Studies have always stated that the contribution of snowmelt to the stream flow in the rivers in Bhutan are substantial but there are no studies which gives a precise and definitive estimate of snowmelt contribution to stream flow, incorporation of satellite products and hydrological modelling would help in understanding the snowmelt component of stream flow.

Therefore as a pilot basin, the Wang Chhu basin located in the western part of Bhutan is selected for this research. An integrated approach to hydrological modelling and monitoring that combines both ground and satellite derived observations would help characterize the hydrological processes in the basin. For this

study, first a snow cover map will be produced using satellite remote sensing and then the well-known HBV Hydrological model will be used to simulate stream flow.

## 1.3. Objectives and research questions.

### 1.3.1. Main objective:

- The main objective of this study is to assess the runoff regime in the Wang Chhu basin by snow cover mapping and stream flow modelling..

### 1.3.2. Specific objectives:

- Snow cover mapping using MODIS snow product in the Wang Chhu Basin.
- Analyse relationship between MODIS derived snow cover distribution with ground station data.
- Identify spatial and temporal pattern of snow covered area.
- Evaluate the potential use of MODIS for snow cover mapping in Bhutan.
- HBV Model calibration using measured runoff and comparison with the derived snow cover maps.

### 1.3.3. Research questions.

Following are the research questions to meet the above objectives:

- Determine the most advantageous satellite snow data available in terms of quality and cost.
- How can MODIS snowfall products be processed in order to obtain the snow cover maps?
- How does snow spatial variability relate to runoff generation in a large range of elevation in Wang chhu basin?
- How does snow cover area change with altitude?
- Can snow cover area and temperature be related ?
- Comparison of snow cover maps to simulated runoff in the basin.

## 1.4. Thesis outline:

This thesis is divided into seven chapters,chapter 1 gives the introduction th the study area,the problem statement and the research objectives and questions.Chapter 2 provides an extensive literature review on snow hydrology and the physical characteristic of snowpacks followed by snowmelt modelling approaches with brief review on remotesensing of snow.Chapter 3 introduces the study area and the datasets used for this research work.Chapter 4 discusses the snow cover mapping and hydrological modelling approaches followed by methodology adopted for this research in chapter 5.Chapter 6 gives the results and sdiscussions and finally in chapter 7 the conclusions and recommendations are made.

# 2. LITERATURE REVIEW

## 2.1. Snow Hydrology

### 2.1.1. Introduction:

An understanding of snow hydrology is essential to hydrological modelling of snow melt. Snowfall and the resulting seasonal snow cover is an important source of water in many parts of the world. Even if their volumetric amount contributes very little to the world's fresh water source, they are of very great hydrological importance( Engman & Gurney, 2000). When the accumulated snow pack melts, the melt water recharges the groundwater and replenishes surface water storage thereby playing an important role in the water cycle. Excessive and untimely snowmelt runoff can cause flooding while inadequate snowmelt often is the reason for droughts(Eamer & Prestrud, 2007). From snowfall to snowmelt the processes play a major role in the hydrological cycle and the runoff regime leading to a pronounced seasonal variation in temperate to cold regions and sometimes in the mountainous basins of tropical regions.

### 2.1.2. The physics of snow formation:

The process of snow formation begins in atmospheric clouds from minute ice particles called 'nuclei', these ice nuclei are particles that causes ice crystals to form through either direct freezing of cold droplets or freezing of water deposited on the particle surfaces as vapour. For the formation of snow, two atmospheric conditions should be met, firstly the atmospheric temperature should be at or below the freezing point (0 degrees Celsius) and there should be a minimum amount of moisture in the air (National Snow and Ice Data Center, 2014). The growth of ice crystals leads to the formation of snow crystals. A snow crystal is a large particle having a very complex shape and visible to the human eye. A snow crystal develops by sublimation and deposition sometimes with the added freezing of surrounding water droplets. The snow crystals continue their growth until they reach a mass at which they are too heave to remain suspended in the cloud, when they reach this critical mass, they fall, more or less joined into snowflakes. If the atmospheric temperature remains sufficiently cold all the way down to the ground the snowflakes formed reaches the ground as snow.

Snow on the ground is a dynamic medium. The properties of snow which reach the ground and form snowpack's changes constantly as a function of energy fluxes, wind, moisture and pressure. The physical properties of snow changes over time and also can vary hugely over small distances, both vertically within snowpack and horizontally over space. Snow on the ground differs greatly from the ice crystals that are formed in the atmosphere(Geographica, 2012). Ice crystals are of various shapes and sizes which by the time they reach the ground surface have undergone a lot of changes resulting from growth, disintegration and agglomeration.

The ice particles deposited on the ground are called snow grains and form snowpack's, the shape and size of the snow grains change dramatically by a process called snow metamorphism where changes in form occurs due to heat flow and pressure. Snow grains bonds with their neighbours and these bonded snow grains acts as an ice skeleton to provide structural strength to the snowpack. As a result of numerous events of snowfall, snow packs develops. Each snowfall event may occur with different meteorological conditions which results in horizontally stratified snowpack which can be vertically heterogeneous or anisotropic. Also the meteorological conditions in between different snowfall events change the physical properties of the snowpack(UNEP, 2007).

### 2.1.3. Physical properties of snow packs:

Snow on the ground is a mixture of water in three phases which are ice, liquid water and water vapour. Air is a major component of fresh snow falling on the ground forming more than 95% of the volume, also solutes and particulates within the snowpack can influence some properties of the snow such as the albedo of the snow.Figure 1 shows the characteristics of snowpacks.

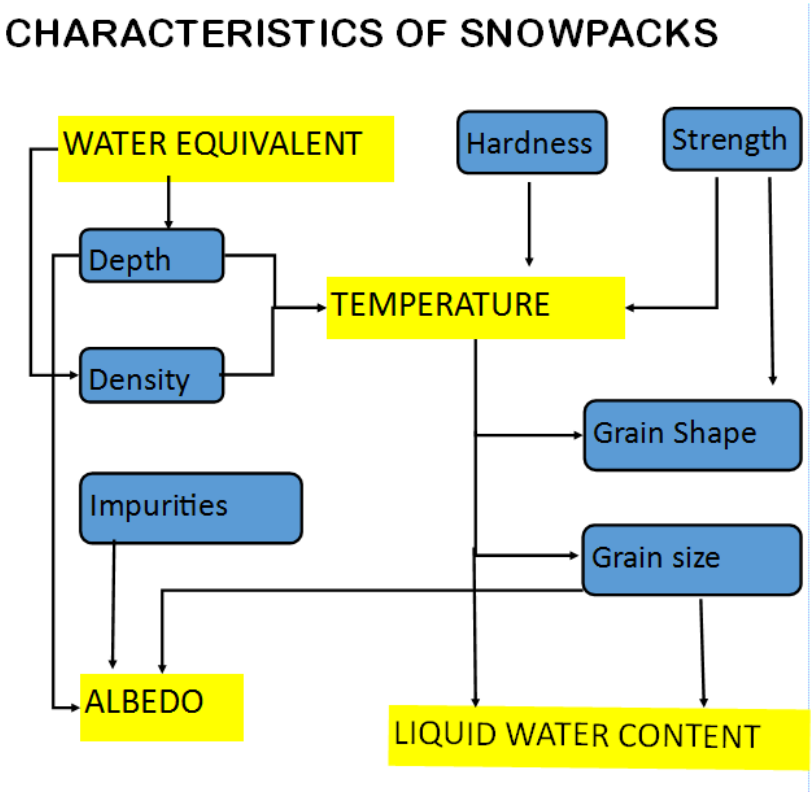


Figure 1 Characteristics of snowpack's.

Some of the physical parameters used to characterize snowpack are as follows:

1. **Snow water equivalent(mm)**
   Snow water equivalent is an important property of a snowpack. The water equivalent of snow pack represents the amount of liquid water that will be released when snow pack is completely melted.It takes into consideration any liquid water that may be stored in the snow pack along with the ice crystals at the time of measurement. Snow water equivalent is measured directly in the field or can be computed from the measurements of depth and the density of snowpack ( after Jonas et al., 2009)as:

$$SWE = d(\rho_s/\rho_w) \qquad \text{Equation 1}$$

Where:

SWE: water equivalent (m)

d: snowpack depth (m)

$\rho_s$: Snowpack density ($kgm^{-3}$)

$\rho_w$: Density of liquid water, approximately 1 x $10^3$($kgm^{-3}$)

2. **Albedo**

Albedo is an important characteristic of a snowpack. Snow albedo is the fraction of incident solar radiation that is reflected away from the snow. It controls the radiation balance, affecting the timing and intensity of snowmelt as well as the climate(Fernandes et al., 2009). Albedo is usually averaged over the visible short-wave radiation of the electromagnetic spectrum(0.4-0.7 μm).Snow albedo is highly variable, generally albedo of fresh newly fallen snow is as high as 95% but tends to decrease with time as metamorphosis of the snow pack changes the snow grains. As the snow ages, it comes in contact with dust and air pollution thereby gets contaminated and albedo reduces to as low as 25%(Gardner & Sharp, 2010).This high variability makes it important to actually measure the albedo of snow packs since small errors in albedo cab translate into large errors in energy estimates.

3. **Liquid Water content of snow:**

Liquid water content of a snowpack represents all liquid water retained in the snowpack including water in transit from rain or melt and also water that is stored against gravitational forces(Brubaker, 2001). During the onset of snowmelt, the meltwater produced will first be retained in the snowpack as liquid water before being produced as runoff. Only after exceeding the retaining capacity of the snowpack which is normally 5-10% liquid water content per unit volume, additional snowmelt will be released from the snowpack as runoff. The liquid water content will vary over time due to surface melting and rain(Techel & Pielmeier, 2011).The liquid water content affects the amount of water released during melt per unit of energy input. A unit of energy input at the time of high liquid water content will release more water than at the time of low liquid content because of the release of water already held in the snow pack as well as water from the melt(Denoth, 2003) Liquid content of snow is expressed in two ways, either as the volume of liquid water per unit volume of snow or as the mass of liquid water per unit mass of snow pack. And the two measures are related as (A. Rango, 1993):

$$\theta_v = \theta_m(\rho_s/\rho_w) \qquad \text{Equation 2}$$

Where:

$\boldsymbol{\theta_v}$**:** Volumetric liquid water content ($m^3$ of liquid per $m^3$ of snow)

$\boldsymbol{\theta_m}$**:** Liquid water content on mass basis (kg of liquid water per kg of snow)

$\boldsymbol{\rho_s}$**:** Snowpack density ($kgm^{-3}$)

$\boldsymbol{\rho_w}$**:** Liquid water density ($10^3 kgm^{-3}$)

4. **Snow Density($g/cm^3$ or $kg/m^3$)**

Snow density is an important physical property of snow which establishes relationship between snow depth and the water content of snow. When snow water equivalent is given in mm of water and snow depth in m, then the units of snow density is expressed in $kg/m^3$.An average density of freshly fallen snow can be assumed as $100kg/m^3$, which gives 1 unit of water for each 10 units of snow depth. Density of freshly fallen snow varies widely depending on the amount of air present within the lattice of the snow crystals. Snow densities vary greatly from one snowfall event to another and also varies within a single snowfall event depending on the convective nature. Snow densities vary roughly from $10kg/m^3$ to roughly $350kg/m^3$ (Kirkbride, 2011).Lower snow densities are generally found in snowfalls formed under cold, dry conditions and higher densities in wet snows at warm temperatures. The density of snowpack ultimately controls the pore space available for storage and transmission of

liquid water and gases. Snow density can be expressed by a relationship between snow and water content. Average density of snow pack also varies seasonally.

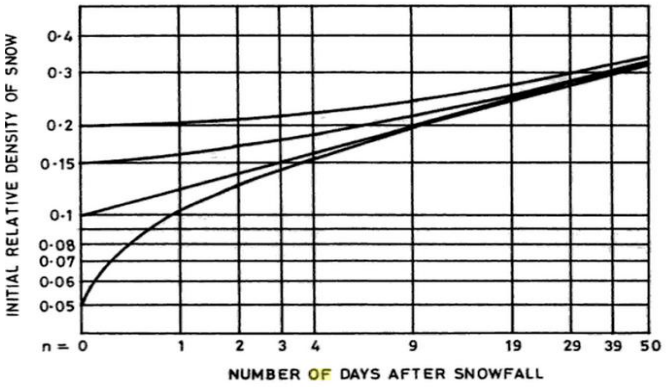


Figure 2 Increase of snow density with time for snow layers with different initial densities (after Martinec, 1977)

### 2.1.4. SNOWMELT AND MELT WATER PRODUCTION

In the worldwide scheme of the water cycle, runoff from snowmelt plays a major role in the global movement of water(Lemke et al., 2007). The importance of snowmelt varies geographically, in the warmer tropical climates snowmelt does not directly play a role in water availability unlike in the colder climates where much of the spring time runoff and stream flow in rivers and streams is a result of melting snow and ice (Yerdelen, 2005).Snowmelt is an important surface water input of great concern to other aspects of hydrology like water sufficiency, flood control and erosion among others. Numerous studies have been carried out in the past to understand the thermodynamics of snowmelt. Some of the very early works were conducted by (Clyde,1931), (Wilson, 1941) and one of the most detailed studies on snowmelt thermodynamics was carried out by the U.S.Army Corps of Engineers in 1956 which is still regarded as a standard and is the source of equation for practical modelling, they developed the SSARR (Stream flow Synthesis and Reservoir Regulation) which provides hydrological simulations on snowmelt dominated river systems for planning, design and other operational water control works. In recent years with the advent of geo information systems, remote sensing technology and spatial data sets of elevation, vegetation, soils and other hydro meteorological variables, energy balance snowmelt models have been developed to operate on a spatially distributed basis.

Snowmelt is primarily driven by exchange of energy at the snow-air interface. The whole process of snowmelt is closely linked to the flow and storage of energy into and through the snowpack. To understand the behaviour of snowmelt like the amount and timing during a melt event, it is important to know the energy sources(Gelfan et al., 2004). The net energy available at the surface of the snow and the thermal state of the snowpack are the two primary factors of snowmelt. Some of the other secondary factors that affect the snow melt processes are wind, rain, heat absorption properties of the ground, sun zenith angle and snow depth and density among others. Whenever there is sufficient energy available, some snow will start melting and form liquid water. The process of snowmelt can be classified into three basic phases:

1. **The warming phase:** During this phase the absorbed energy raises the average snowpack temperature to a point at which the snowpack is isothermal (temperature remains constant) at 0°C.
2. **The ripening phase:** The already absorbed energy is used to melt but the meltwater is retained in the snowpack since the physical structure of the snow pack is a porous matrix and the melt water is held as liquid water in the interstices between the snow grains which gradually increases the snow

density and snow water content. At the end of this phase, the snowpack is saturated and cannot retain any more liquid water, it is then said to be 'ripe'.

3. **The output phase**: With further absorption of energy, the capacity of the snowpack interstices to hold liquid water is exceeded some of the snowmelt will move as snowmelt runoff. Also some portion of the melt water may infiltrate into the ground, infiltration depends on inherent soil characteristics, soil moisture content as well as whether the ground is frozen or not.

This phase is a much idealized sequence because in most cases melting will typically occur at the surface of the snowpack before the ripening phase. The melt water may percolate into deeper layers where the snow temperature is below 0°C and refreezes forming ice layer and lenses. There is also the typical diurnal freeze-thaw

## 2.2. Modelling snowmelt

Snow melt modelling is an important component in the process of predicting runoff from snow covered or glacier covered basins and also to study changes in the cryosphere related with climate change. Computation of snowmelt from a watershed is usually made using an energy balance approach or some empirically defined snow melt index approach.

### 2.2.1. Models based on Energy balance approach:

The energy balance approach is based on the fundamental physical principles of conservation of energy and mass for calculating snowmelt at shorter time steps. This method is highly data intensive but it is the most through and accurate method for calculating snowmelt. This method considers and quantifies the energy fluxes on the interface of the atmosphere-snow and the earth surface. It involves the accounting of incoming energy, outgoing energy and the change in energy storage for the snowpack at a given time. The energy is then expressed as the heat equivalent of snowmelt (Yerdelen, 2005). The melting of snow is an overall result of different heat transfer processes. Sun is ultimate source of energy for snowmelt but in between there is a complex interaction of the incoming radiation, the atmosphere and the land surface. The energy balance of the snowpack for any given time interval can be expressed by the following equation:

$$Q_m = Q_{sn} + Q_{ln} + Q_h + Q_e + Q_p + Q_g \pm \frac{dU}{dt} \qquad \text{Equation 3}$$

Where:

$Q_m$: The net energy available for melt

$Q_{sn}$: Net shortwave radiation flux absorbed by the snow

$Q_{ln}$: Net long wave radiation flux at the snow air interface

$Q_h$: Convective transport of sensible heat between air and the snowpack

$Q_e$: Latent heat released by the condensation, evaporation or sublimation of water vapour on the snowpack.

$Q_g$: Conduction of heat to the snowpack from the ground

$Q_p$: Advection of heat to the snowpack through rainfall

$\frac{dU}{dt}$ Rate of change of internal energy per unit surface area per unit time

The different components of energy in the above equation are all units are expressed in MJ $m^{-2}day^{-1}$ and considered in terms of energy flux that is the amount of energy received on a horizontal snow surface of unit area over a unit time. The rate of change of internal energy of the snow pack is made up of the amount of energy required to melt the ice portion of the snowpack, freeze the liquid water in the snow

and change the temperature of the snow (Encyclopaedia of Snow, Ice and Glaciers, 2011). Positive value of the $Q_m$ will result in snowmelt. Therefore amount of energy available to cause snowmelt depend on the magnitude of various energy inputs to the snowpack and is very dynamic. The sum of all the energy sources represents the total amount of energy available for melting the snowpack and can be expressed at a point by the following equation:

$$M = \frac{Q_m}{h_f \rho_w B} \qquad \text{Equation 4}$$

**M:** the depth of meltwater (mm/day)
$Q_m$**:** Net energy flux computed from equation 1(Kj/m$^2$*day)
$h_f$: Latent heat of fusion of ice (Kj/kg)
$\rho_w$:Density of water (kg/m$^3$)
$B$**:** Thermal quality of snow (B≤1)

The thermal quality of the snow is the fraction of ice in a unit mass of wet snow and it depends on the amount of free water content and temperature of the snowpack. A snow pack that contains no free water has a thermal quality equal to 1, with the onset of melting some free water is held within the matrix of the snow which reduces the thermal quality. The energy required to release 1g of water is less than the latent heat of fusion of water(334.9 Kj/kg or 80 cal/g for pure ice).The value of thermal quality of snow that is thermally ripened for melting containing 3-5% of liquid water in snow generally ranges in between 0.95-0.97.

The main advantage of energy balance model is the possibility to implement it in several climatic conditions. And also the possibility to describe in detail all the processes and physical nature of snow accumulation and metamorphism. Difficulty in implementing an energy balance model for the purpose of predicting snowmelt arises due to the variability of the heat transfer processes both over time and space. Also disadvantage of this model arises from the difficulty in obtaining the input data necessary for parameterization, calibration and validation of the model (Geographica, 2012).

### 2.2.2. Models based on temperature index method

For this study the temperature index method is used to estimate snowmelt and runoff. Temperature index models assumes an empirical relationship between air temperatures and melt rate(Hock, 2003). Temperature index model was derived by (Finsterwalder and Schunk, 1887) for glaciological studies in the Alps. The method has wide application in prediction of melt for operational flood forecasting and hydrological modelling and various other applications and till date temperature index approach is widely used Because of the complexity in determining the individual energy fluxes in the energy balance models, temperature index models are widely used in snowmelt estimation. The method makes use of the air temperature which is generally considered to be the best index of heat transfer processes associated with snowmelt. Air temperature is a meteorological variable observed by in-situ meteorological gauging stations and is broadly used in hydrological modelling since it gives a simplified description of energy exchange at the atmosphere-snowpack and ground surface interface. Air temperature expressed in degree-days is used for snowmelt calculations as an index of the complex energy balance tending to snowmelt (Encyclopaedia of Snow, Ice and Glaciers, 2011) and this method is also referred to as the degree-day method. Degree-day is a unit expressing the amount of heat in terms of persistence of temperature for a 24 hour period of 1 $^0$C departure from a reference temperature. The most common and simplest expression relating snowmelt to air temperature can be expressed as in equation 3:

$$M = D_f(T - T_C) \quad \text{Equation 5}$$

$$M = 0 \quad \text{When } T < T_C$$

**M:** snowmelt (mm/day)

$\boldsymbol{D_f}$**:** Degree day factor (mm/day/$^0$C), this is the snow water equivalent decrease in a day caused by the air temperature change of 1$^0$C compared to the critical temperature value.

**T:** mean air temperature ($^0$C)

$\boldsymbol{T_C}$ **:**Critical air temperature at which snow starts melting ($^0$C)

Neither the degree day factor nor the critical temperature can be constant because air temperature is only one among many other meteorological parameters that influence snow melt, other parameters commonly used are relative humidity, snow albedo, wind speed and short wave radiation. Literature provides with different values for degree-day factor and the critical temperature, generally the critical temperature is set as a constant at 0$^0$C, without a huge loss in model performance. The value of the degree day factor is understood to range in between 2-15 mm/day/$^0$C depending on the physical properties of snow or global radiation but normally the value varies between 3-6 mm/day/$^0$C(Killingtveit & Sælthun, 1995).

In various studies, degree-day model has been modified in a number of ways to fit localized climatic conditions and catchment characteristics(Garen and Marks,2005; Magnusson et.al,2011:Uhlmann et.al,2009:Fierz et.al,2003;Sensoy et.al,2006;Hock,1999). One of the most common version of the degree-day method is the addition of short wave radiation and snow albedo, with the addition of new variables equation 3 can be modified and can be expressed as equation 4.

$$M = D_f(T - T_c) + b(1 - \alpha)S \quad \text{Equation 6}$$

**M:** snowmelt (mm/day)

$\boldsymbol{D_f}$**:** Degree day factor (mm/day/$^0$C)

**T:** mean air temperature ($^0$C)

$\boldsymbol{T_c}$ **:**Critical air temperature at which snow starts melting ($^0$C)

**b:** Radiation index (mm/day/W/m$^2$)

**α:** snow albedo

**S:** short wave incoming radiation (W/m$^2$)

Works of (Pellicciotti, Buergi, Immerzeel, Konz, & Shrestha, 2012) concludes that with the use of the modified degree-day approach almost 80-90% of the energy balance terms can be derived.(Hock, 2003) lists the advantages of using the temperature index models as the easy availability of temperature data, relatively easy interpolation and forecasting possibilities of air temperature and good model performance and computational simplicity. The main drawbacks of this approach is firstly the accuracy of this method decreases with increasing temporal resolution and also intensity of snowmelt has a huge spatial variability depending on many factors like topography, slope and land cover. These variability's are quite difficult to express using temperature index models.

### 2.3. Operational snowmelt models:

During the last few decades numerous snow melt models were developed which satisfied the purpose of describing snow melt processes. These models have proved to be an instrumental tool for water balance studies, managing and mitigating disasters related to water. The World Meteorological organization was among the first ones to compile and carry out an intercomparision of snowmelt models (World

Meteorological Organization, 1982). Most snowmelt models are rainfall runoff models with extra routines added to the stores and melt precipitation which falls as snow but there are few snowmelt models not for use in non-snowy environments. The part of the model that deals with snowmelt has to achieve three main operations at every time step: To extrapolate available meteorological data to the snowpack to

- Calculate rates of snowmelt at different points of time and then to
- Integrate snowmelt over the current area of snowpack in order to estimate the total volume of new meltwater.

The melt water and rainfall if any is then routed to the basin outlet. Moving to the next time step the model has to take into consideration any changes in the snow covered area. With air temperature above zero °C, snow cover generally decreases over time and areas become snow free.. Snow cover and initial snow depth is spatially not uniform and is one of the causes that snowmelt also not uniform and thus snowmelt runoff changes over time. However any fresh snow that falls during the melt season causes temporary expansion of the snowpack (Ferguson, 1999), (Day, 2009) in his work reviewed 5 of the commonly used snowmelt models namely the SNTHERM model, Snowmelt Runoff Model(SRM),University of British Columbia(UBC)model, Precipitation Runoff Modelling System(PRMS0 and the Hydrologiska Byrans Vattenbalansavedelning (HBV) model. He discussed the input data needed, the advantages and the disadvantages of these models.(Anand Verdhen & Bhagu R. Chahar & Om P. Sharma, 2014) did a review on the snow melt algorithms used in some popular snowmelt models in the Himalayas and have concluded that such studies are important in determining which snowmelt models perform best for different regions over a long time and to provide insights into what level of complexity is warranted in a snowmelt model with limited data. The following table shows a list of models and their characteristics.

Table 1: Comparison of runoff models adapted from (WMO, 1986) & (Russell, 2006)

| | Name of the model | Author/authors(Year) | Required data |
|---|---|---|---|
| 1 | Stream flow Synthesis and Reservoir Regulation (SSARR) | Anderson (1973) | Temperature, precipitation, discharge |
| 2 | National Weather Service (NWS) | Burnash (1973) | Temperature, precipitation, discharge |
| 3 | TANK | Sugawara et.al. (1974) | Temperature,precipitationEvapotranspiration,, discharge, evapotranspiration |
| 4 | Hydrologiska Byrans Vattenbalansavedelning (HBV) Model | Bergstrom (1975) | Temperature, precipitation, discharge, evapotranspiration |
| 5 | Snowmelt Runoff Model(SRM) | Martinec (1975) | Temperature, precipitation ,discharge evapotranspiration |
| 6 | University of British | Quick (1976) | Temperature, precipitation and discharge |

| | | | |
|---|---|---|---|
| | Columbia Model (UBC) | | |
| 7 | CEQUEAU | Charbonneau (1977) | Temperature, precipitation, discharge, Snowfall |
| 8 | NAM | Gotleib (1980) | Temperature, precipitation , discharge |
| 9 | ERM | Turcan (1981) | Temperature, precipitation, discharge |
| 10 | Precipitation Runoff Modelling System (PRMS) | Leavesley (1983) | Temperature, precipitation, olar radiation |
| 11 | Coupled Routing and Excess Storage (CREST) | University of Oklahoma and NASA SERVIR (2008) | Potential evapotranspiration, precipitation. |

**HBV-96 MODEL**

The Hydrologiska Byrans Vattenbalansavedelning (HBV) model was developed by Dr. Sten Bregstrom and his colleagues at the Swedish Meteorological and Hydrological Institute (SMHI) in the 1970's.It is regarded as a semi distributed conceptual precipitation runoff model in which the catchment can be divided into sub basins and using elevation zoning used to simulate runoff processes in a catchment using precipitation, air temperature and potential evaporation as input data. The model computes snow accumulation, snow melt, actual evapotranspiration, storage in soil moisture and ground water and the runoff from the catchment. Today the concept if HBV model is widespread, it has been modified several times and exist in different versions and has been applied in more than 50 countries(SHMI,2008,manual version 6.2) with different climatic conditions, varying catchment sizes varying in size from small research basin to large continental scale and different elevation zones. HBV is used as a standard method for hydrological forecasting in many countries used for research studies, design and mitigation of water related disasters.

The main principles behind the HBV model are as follows:

- The model must be based on a sound scientific foundation
- It must be possible to meet the data demand in most areas.
- Its complexity must be justified by its performance
- It must be properly validated
- The user must be able to understand the model.

This model is discussed in depth in chapter 4.

## 2.4. Remote Sensing of Snow.

An innovative technique in the field of snow hydrology is remote sensing. Remote sensing techniques have proven to be instrumental in the field of snow hydrology by lack of adequate information on spatial and temporal coverage of snow characteristics and data. . Remotely sensed data supplements the conventional in-situ (i.e, point data) observations in various unique aspects. Remote sensing technique has advantage to observe and measure spatial information at specified time interval (or use recurrently) and the state of the earth's surface over large and remote areas. Remote sensing of snow and ice permits to monitor and measure …..in real time and year round (Ko & Winther, 2001). The fact that measurement can be repeated over time by has been of great importance in studying and monitoring of spatial and temporal variability of snow cover (Nolin, 2010). Some of the very early attempts to incorporate remote sensing in the field of snow Hydrology was carried out by Rango et.al (1977) which focused on the effective application of remote sensing data to predict runoff.(Seidel & Martinec, 2004) in their book "Remote Sensing in Snow Hydrology: Runoff Modelling, Effect of Climate Change" have extensively discussed the role of remote sensing in snow hydrology, it summarizes the attempts at snow cover mapping using remote sensing data, usefulness of the satellite derived snow cover for hydrological modelling and the methods of using satellite images for snow cover mapping. The use of various satellite derived snow products for snow cover mapping and monitoring activities for various purposes from across the globe has been reported, (Paper, 2014) gives an overview on the current status of satellite based snow products in the European region, (Immerzeel et. al, 2009) explains the use of remote sensing in identifying spatial-temporal trends in snow cover in the Himalayan river basin.(Taylor et al,2012) gives an overview of the methods of snow cover mapping.

From the remote sensing perspective, snow cover is one of the readily identifiable measures of water resources from satellite imagery. In the electromagnetic spectrum all objects in all the wavelengths emits radiation as shown in the figure 3.For the purpose of snow and ice remote sensing, sensors that operate from gamma rays wavelength to very high frequency microwave potions have been used, however the visible and near infrared region and the microwave region of the electromagnetic spectrum has been commonly used for snow cover mapping (Kelly & Hall, 2008). Due to its unique reflectance characteristic snow reflects a high proportion of radiation in the visible part of the electromagnetic spectrum(Taylor et al., 2012). As seen in the figure 4, fresh snow has a very high reflectance in the visible part of the electromagnetic spectrum which gradually decreases as the snow ages. The decrease in the reflectivity of snow with age is caused because of many factors, firstly the impurities of snow cover which increases over time and secondly the melting and refreezing processes within the snow which leads to increase in grain size.

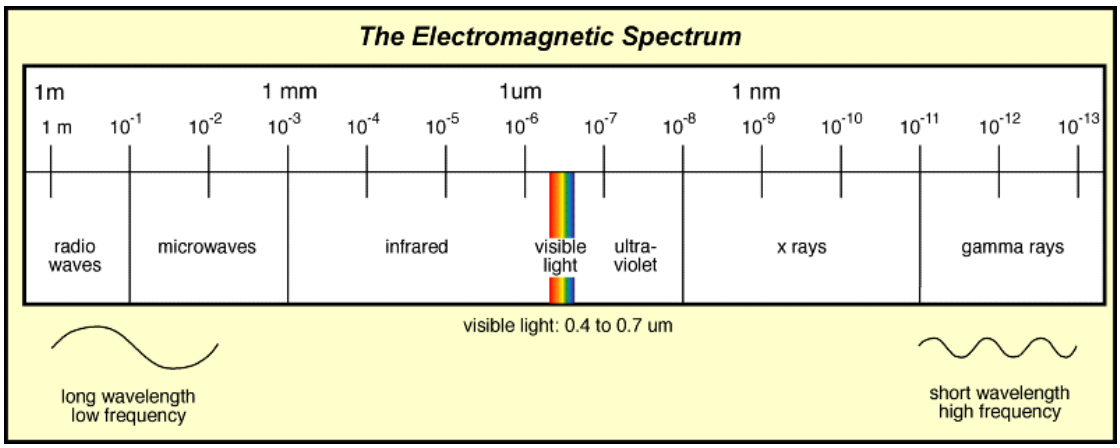


Figure 3: Electromagnetic spectrum.

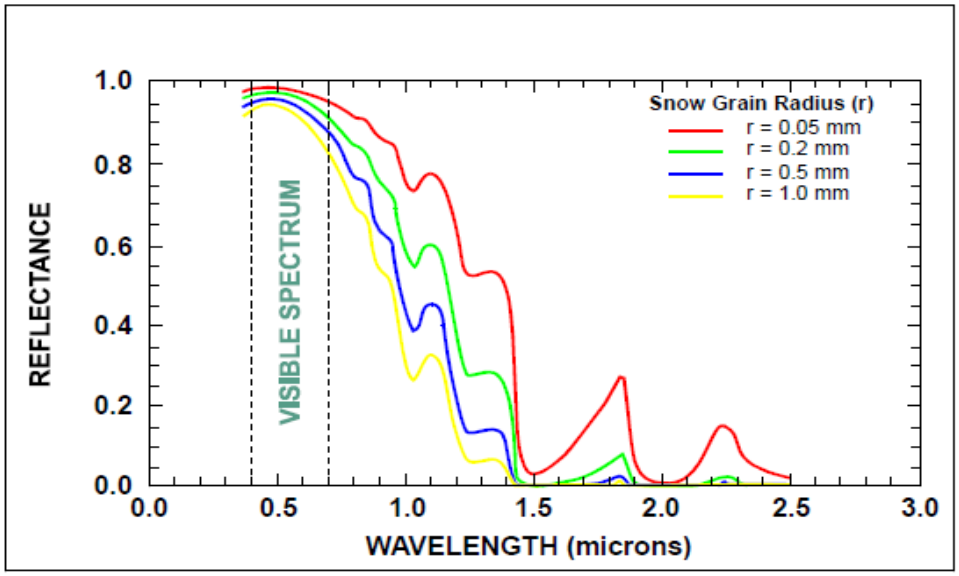


Figure 4: Reflective properties of snow (John Hopkins University IR Spectroscopy Lab).

In the visible and the near infrared region properties of snow cover like snow cover extent, snow surface temperature, albedo and sometimes snow depth can be can be determined by satellite remote sensing. The visible and infrared region is affected by cloud cover but measurements from these regions have the best spatial resolution (Taylor et al., 2011). Thermal infrared region of the electromagnetic spectrum measures the radiation emitted by the earth's surface which is in turn dependent on the surface temperature so this channel is mostly used for measuring the snow surface temperature, in this region cloud affects the measurements and limits the usability of these images. In the microwave region, the snow depth and the snow water equivalent, liquid water capacity, grain size, shape and stratification are some of the physical properties that can be estimated because in this region active (backscattering) or passive (emission) signals respond to the bulk properties of the snowpack in addition to the variations in the surface and subsurface features of snow(Dai, Che, Wang, & Zhang, 2012). All the regions of the electromagnetic spectrum used for snow and ice remote sensing has their own advantages and drawbacks. One of the main difference between optical and microwave observations is the fact that microwave observations can be carried out under all weather and illumination conditions(Kelly & Hall, 2008),however the microwave observations are subjected to lower spatial resolution as compared to the optical observations. Table 2 shows the relationship between snow properties and the spectral bands followed by table 3 showing snow properties which affects its reflectance( Engman & Gurney, 2000) (Meier, 1979)

Table 2:Relationship between snow properties and spectral bands[Adapted after ( Engman & Gurney, 2000) (Meier, 1979)]

| Property | Visible/near infrared | Thermal | Microwave |
|---|---|---|---|
| Snow cover area | Yes | Yes | Yes |
| Depth | If very shallow | Weak | Moderate |
| Snow water equivalent | If very shallow | Weak | Strong |
| Stratigraphy | No | Weak | Strong |

| | | | |
|---|---|---|---|
| Albedo | Strong | No | No |
| Liquid water content | Weak | Weak | Strong |
| Temperature | No | Strong | Weak |
| All weather capability | No | No | Yes |
| Current best resolution | Few meters | Hundreds of meters | Tens of metres |

Table 3: Properties of snow affecting its reflectance [Adapted after (Engman & Gurney, 2000) (Meier, 1979)]

| **Property** | **Visible reflectance** | **Near Infrared Reflectance** | **Thermal Infrared Emissivity** | **Microwave Emissivity** |
|---|---|---|---|---|
| Grain size | | Yes | No | Yes |
| Sun Zenith Angle | No | Yes | Yes | Yes |
| Depth | Yes | No | No | Yes |
| Contaminants | Yes | No | No | |
| Liquid Water content | No | | No | Yes |
| Temperature | No | No | No | Yes |
| Density | No | No | No | Yes |

The most efficient way of monitoring the dynamic seasonal snow cover changes on a large scale is through satellite remote sensing ( A. Rango, 1994) and in mountainous areas snow cover mapping is demanding because of the topography. There are various factors like wavelength, spatial and temporal resolutions and other important factors which should be taken into consideration while selecting the best possible sensor for the use of snow cover mapping(Hall and Martinec, 1985).For monitoring snow cover change due to melt and accumulation the very first necessity is a sensor with a frequent temporal resolution with a moderate spatial resolution for achieving cloud free images, the best application for snow remote sensing has been found in the visible and the near infrared regions of the electromagnetic spectrum. With the use of microwave data the cloud cover issue is resolved but it comes with the cost of lower spatial resolution (Basist et al., 1996).(Frei et al., 2012) give an extensive review of the global satellite derived snow products. Table 4 lists the satellites and their characteristics currently in orbit for snow cover mapping, a comprehensive study of space borne missions and sensors have been compiled by ( Kramer, 2002).

Table 4:List of satellites for snow cover mapping[adapted after (Seidel & Martinec, 2011) and (Kramer, 2002)

| Satellite | Sensors | Spatial resolution | Temporal resolution | Mission Launched by/year |
|---|---|---|---|---|
| Meteosat-7 | VIS/IR | 2.5 km ×x 2.5 km | 0.5 hours | EUMETSAT/1997 |
| Meteosat-8 | VIS/IR | 1km × 1 km | 0.25 hours | EUMETSAT/1997 |
| NOAA-14,-16 | AVHRR | 1km × 1 km | 12-24 hours | NOAA/2000 |
| TERRA/AQUA | MODIS-XS | 250m, 500m,1000m | 1-2 days | NASA/1999,2002 |
| ENVISAT | MERIS | 300m × 300m | 3 days | ESA/2002 |
| Landsat-4,-5 | MSS | 57m × 79m | 16 days | NASA/1972,1984 |
| | TM | 30m × 30m | | |
| Landsat -7 | ETM+ | 30m × 30m | 16 days | NASA/1999 |
| | PAN | 15m × 15m | | |
| SPOT -2,-3,-4 | XS | 20m × 20m | 26 days | CNES,France/1990,1993,1998 |
| | PAN | 10m × 10m | | |
| SPOT -5 | XS | 10m × 10m | 26 days | CNES,France/2002 |
| | PAN | 5m × 5m | | |
| IRS -1C | PAN | 5.8m × 5.8m | 5 days | ISRO,India/1995 |
| | LISS-3 | 23m × 23m | | |
| | WIFS | 188m × 188m | | |
| IRS-P3 | WIFS | 188m × 188m | 24 days | IRSO,India/1996 |
| | MOS | 520m × 520m | | |
| IKONOS | XS | 4m × 4m | 3 days | Digital Globe,USA/1991 |
| | PAN | 1m × 1m | | |
| QUICKBIRD-2 | XS | 2.44m × 2.88m | 3 days | Digital Globe,USA/2001 |
| | PAN | 0.61m × 0.72m | | |

The list of satellites in table 4 can be classified into high and medium resolution optical Imagers. The medium resolution optical imagers have the advantage of high repetition rate sometimes allowing almost

near real time access to data, therefore medium resolution optical sensors are very suitable for regular and efficient snow cover mapping purposes(Ko & Winther, 2001).In larger basins the use of these medium resolution optical imagers are limited but mapping snow cover at regional and continental scales can be immensely benefitted from wide areal coverage and low costs. Medium optical imagery satellites have been widely studied and used for studying snow cover dynamics as demonstrated by a huge number of literature on this topic. AVHRR has been the most and the longest utilized medium resolution optical imager among the available medium resolution optical imagers (Chokmani et al., 2006).For the northern hemisphere snow cover maps are available since 1966 from the website of National Oceanic and Atmospheric Administration(US Department of Commerce, NOAA, 2015).The NOAA-AVHRR derived snow cover maps are usually used for small scale areas and for larger scale studies higher resolution multi spectral sensors like sensors on board Landsat, SPOT and quick bird satellites are used (Hyvärinen, 2006).With the launch of Moderate Resolution Imaging Spectroradiometer (MODIS) by NASA as a part of the Earth Observation System platform is of special significance for snow hydrology. The snow cover maps derived from MODIS data has been proven to represent potential improvements as compared to other hemispheric scale snow maps available mainly because of its improved spatial resolution and snow/cloud discrimination capabilities and also their frequent global coverage (D. K. Hall & Riggs, 2007).A detailed description of MODIS can be found in chapter 4.

# 3. STUDY AREA AND MATERIALS

## 3.1. Study area: Wang Chhu basin

The Wang Chhu basin is located in western Bhutan within 27$^{o}$ 5' -27$^{o}$ 51' north latitude and 89$^{o}$ 6' - 89$^{o}$ 46'east longitude as shown in figure 5 below. The total drainage area of the basin is approximately 3590 km$^2$(MOAF,2011). The total length of the basin is 137 kilometres. Wang chhu is one of the four major rivers in Bhutan and it has three main tributaries, Haa chhu, Pa chhu and Thim chhu. Wang Chhu originates from the snow covered mountains in the north and flows south easterly. The river is known as Raidak River when it reaches India and is one of the tributaries of the Bharamaputra River. This basin is the most populated region of the country with about 26% of the total population living in the basin. Two functional hydro power plants are located in the Wang Chhu basin, namely Chhukha Hydropower plant with an installed capacity of 336 MW and generating an average of 1745 million units of energy per annum and Tala Hydro power plant 3 kilometres downstream of Chhukha Hydropower plant with an installed capacity of 1020 MW and generating an average of 4500 million units of energy per annum(NSB, 2013).

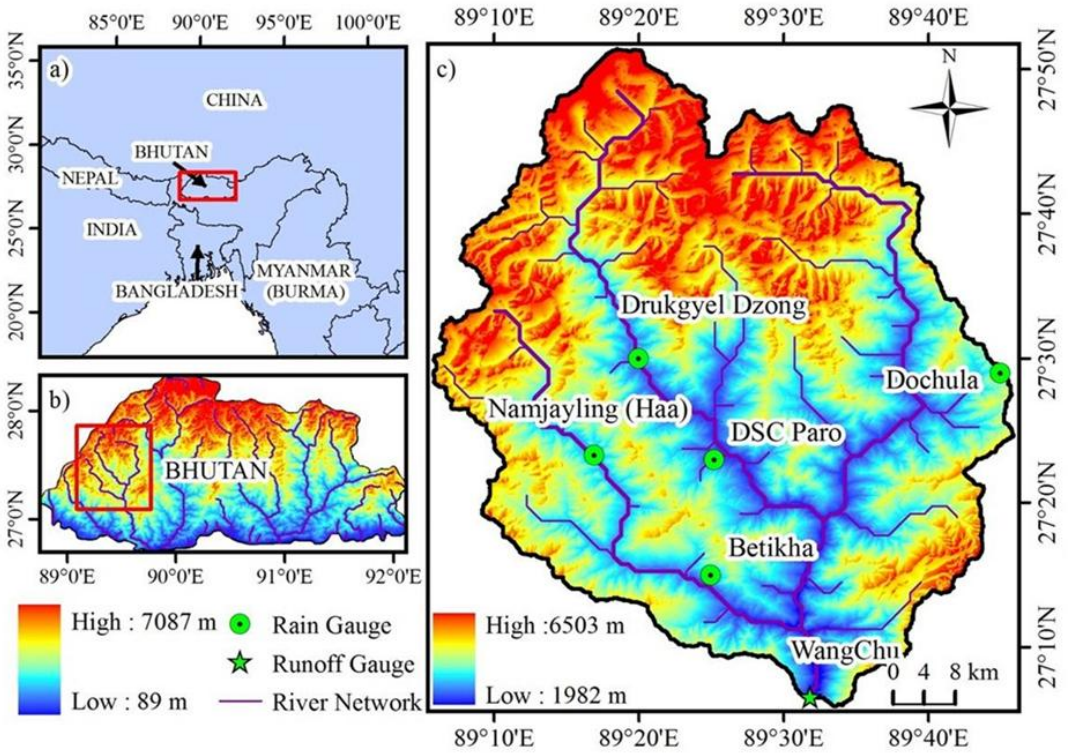


Figure 5: Location of the study area.

### 3.1.1. Topography

The basin is characterized by rugged mountainous topography with high internal relief in most part of the basin especially in the north. The altitude in the basin ranges from about 90m above mean sea level in the south to over 7000m above mean sea level in the north. This huge elevation gradient affects precipitation and temperature values in the basin. The northern periphery of the Basin maintains an annual snowpack and approximately 4.4% of the area is covered by glaciers or permanent snow(Beldring et al., 2013). The

basin has an average slope of 26.5 $^{o}$ .Of the total 677 glaciers and 2674 glacial lakes in Bhutan,36 glaciers and 221 glacial lakes lies in the head waters of Wang Chhu basin(Mool,et al., 2001).

## 3.2. Climate

The climate in the basin is as varied as its altitude and is affected by the summer monsoon from the Bay of Bengal. The monsoon season starts from June and lasts up till September and the dry season from October till May. The climate of the basin is divided into three zones, sub-tropical in the Southern foothills, warm temperate in the mid hills and arid alpine in the extreme north of the basin, with mean annual temperature varying from 15 $^{o}$ c to 30$^{o}$ c in the southern foothills. Mean annual rainfall varies from 2500 to 5500mm in the southern foothills, 1000 to 2500mm in the mid valleys and 500 to 1000mm in the northern part of the basin. The basin is equipped with five rain gauge stations and a stream flow gauge at the outlet of Chhukha Dam hydrological station, as shown in figure 1

### 3.2.1. Land cover and land use

The main land cover type in the Wang chhu basin is forest, covering approximately 45% of the basin area. The other land cover types include woodland(17.8%),open shrub land(9.7%),wooded grassland(8.2%),grassland(7.6%) and other land use types(less than 10%)(Hansen et al, 2000).Farming system in the basin include agriculture, horticulture and livestock. The basin has a total arable land of 32,489 acres .The main croplands consists of rice, potatoes, maize, apple and orange orchards.
Due to the high population density in the basin, there is a significant pressure on the forest. Forest degradation is one of the major issues in the basin, the major reasons being construction of roads and infrastructure development and also forest fires(MoAF,Bhutan, 2011).

## 3.3. Datasets

### 3.3.1. Data collected from offices

The Department of hydro-met services under the Ministry of Economic Affairs, Bhutan provides weather, water, climate and other related environmental services to a wide range of sectors, available hydro-meteorological data like precipitation, temperature, humidity, wind speed and river discharge for the study area were collected from the Department of Hydro met services.(Table5).These collected data will be used as in put and to calibrate the HBV model. During the field visit for data collection, it was explained by the officers in charge that the river gauges get submerged during the peak seasons and causes difficulty in reading them correctly and also other factors like instrument breakdown and other technical problems sometimes causes days without observations. Therefore the streamflow data(table 6) is not free from observational errors. Other data like the land use, land cover maps were collected from the National Soil service center, Bhutan.

Table 5: Available meteorological stations in the basin.

| Station name | Co ordinates | elevation | Data available period |
|---|---|---|---|
| Drugyel | 27.5 N,89.33 E | 2720 | 2003-2000 |
| H | 27.38 N,89.28 E | 2547 | 2003-2000 |
| Paro | 27.38 N,89.42 E | 2406 | 2003-2000 |
| Simtokha | 27.43 N,89.67 E | 2310 | 2003-2000 |
| Gidagom | 27.38 N,89.57E | 2210 | 2003-2000 |
| Betikha | 27.25 N,89.41 E | 2660 | 2003-2000 |
| Chapcha | 27.20 E,89.55 E | 2450 | 2003-2000 |
| Chhukha | 27.06 N,89.56 E | 1380 | 2003-2000 |

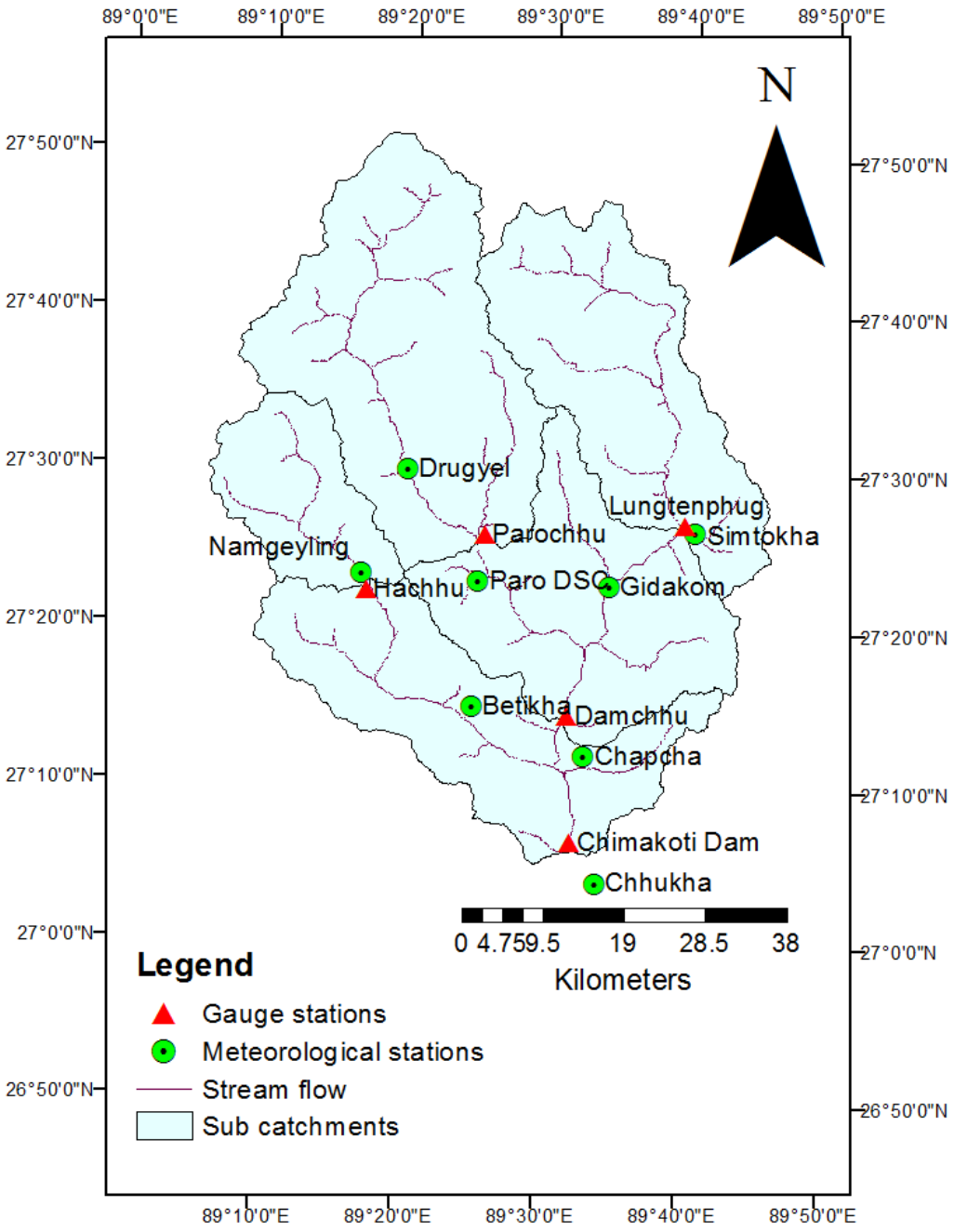


Figure 6: Meteorological and gauge stations in the station.

Table 6: List of discharge stations in the basin.

| Station name | Co ordinates | elevation | Available data |
|---|---|---|---|
| **Lungten phu** | 27.44 N,89.66E | 2260 | 2003-2010 |
| **Chhukha** | 27.10 N.89.53 E | 1820 | 2003-2010 |
| **Paro** | 27.43 N,89.42 E | 2255 | 2003-2010 |
| **Haa** | 27.37 N,89.28 E | 2700 | 2003-2010 |
| **Damchu** | 27.24 N,89.52 E | 1990 | 2003-2010 |

### 3.3.2. Land cover maps:

The land cover maps used for the study area was extracted from the Land cover atlas of Bhutan (2012) published by the National Soil and Service Centre, Bhutan. These land cover maps were derived from Landsat TM satellite imagery (2000) by performing a hierarchical classification technique and updated through digital image processing of multispectral ALOS images (AVNIR-2) using the winter seasons from 2006-2009 along with other available reference materials and also extensive ground truthing and accuracy assessment had been carried out. The land cover types are divided into 28 land cover sub classes which can be grouped together into 11 broad land cover classes as shown in table 7 below.

Table 7: Land cover classes and sub classes.

| Land cover Class | Sub-class |
|---|---|
| FORESTS | Fir Forest |
| | Mixed Conifer Forest |
| | Blue Pine Forest |
| | Chir Pine Forest |
| | Broad Leaf Forest |
| | Broad Leaf &Conifer Forest |
| SHRUBS | Shrubs |
| MEADOWS | Meadows |
| CULTIVATED AGRICULTURAL LAND | Chhuzhing(Irrigated agricultural land) |
| | Kamzhing(non -irrigated agricultural land) |
| | Apple Orchard |
| | Citrus Orchard |
| | Areca nut plantation |
| | Cardamom Plantation |
| | Others |
| BUILT UP | Built up area |
| NON-BUILT UP | Non Built up areas |
| SNOW COVER | Snow cover |
| BARE AREAS | Rock Outcrops |
| | Scree |
| | Bare Soils |
| WATER BODIES | Lakes |
| | Reservoirs |
| | Rivers |
| MARSHY LAND | Marshy areas |
| DEGRADED AREAS | Landslides |
| | Gullies |
| | Moraines |

### 3.3.3. MODIS snow product:

For the snow cover mapping MODIS daily snow products have been used. The MODIS daily TERRA snow cover maps are downloaded from the NASA REVERB ECHO website (http://reverb.echo.nasa.gov/reverb/#utf8=%E2%9C%93&spatial_map=satellite&spatial_type=rectangle), this website has a full collection of MODIS land products. Downloading the MODIS snow product from this website is a three step process as shown in figure 7:

- Step 1: Select search criteria: For the select Search criteria, the area of interest needs to be specified this can be done by drawing a box on the map to spatially define the search area. Then a search term needs to be entered, in this case MOD10A1 is entered for the MODIS TERRA daily 500m snow cover product, the time frame of the data required can be entered.
- Step 2: Select datasets, here the specific dataset can be checked and proceed to the next step.
- Step 3: Discover granules: Here the list of relevant data is populated and once the dataset required is fully described then click the search for granules and then on the next page the list of chosen data appears and it can be viewed ,inspected and then put the chosen data in the shopping cart and then can be downloaded.

  The MODIS snow products are discussed in detail in chapter 4.

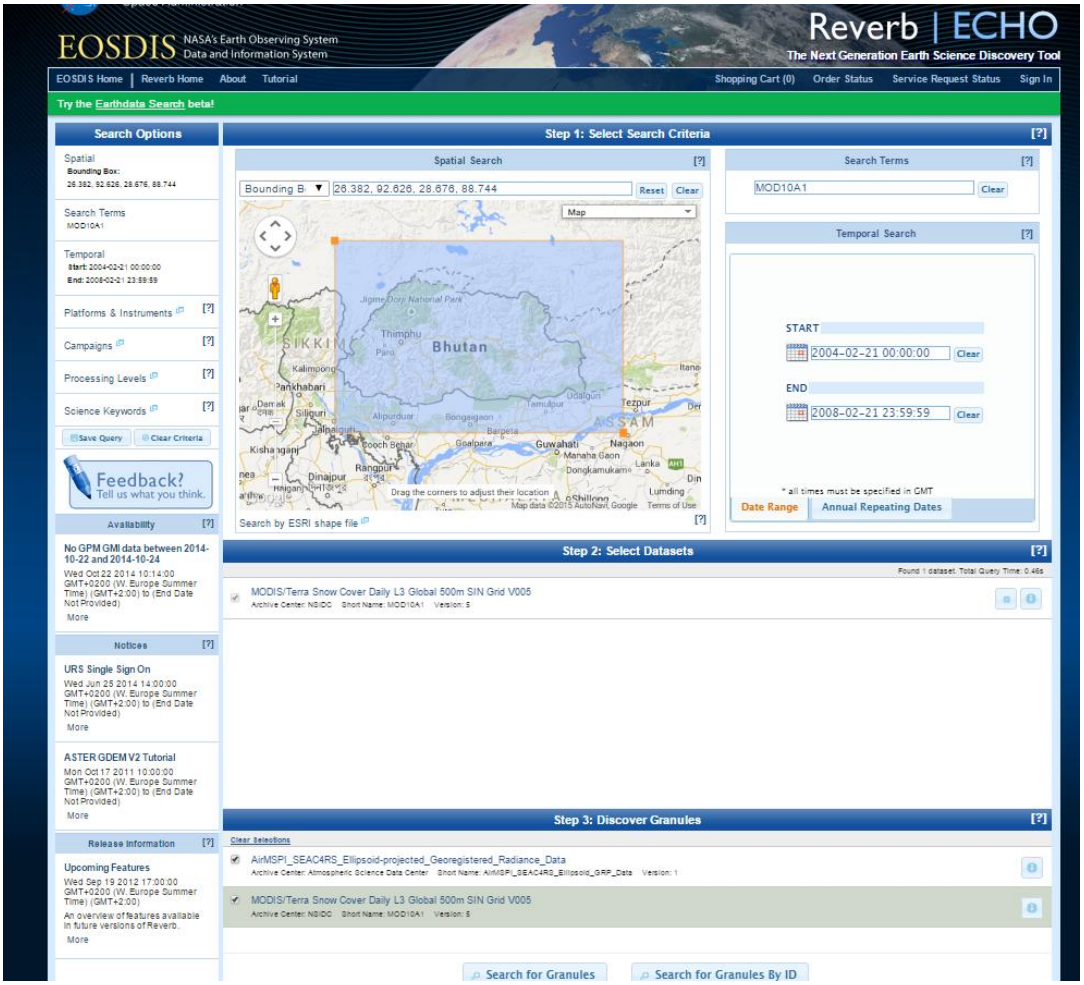


Figure 7: Downloading data from REVERB EC HO website.

# 4. SNOW COVER MAPPING AND HYDROLOGICAL MODELLING

## 4.1. MODIS snow products for snow cover mapping

MODIS snow products have been applied to various aspects of water resource sciences like hydrology, meteorology, climatology and ecological sciences among others (Chelamallu et. al., 2013). They have been proven to be of immense value for studying and monitoring snow process dynamics throughout the world. Evaluation of the applications of MODIS snow products in snow cover mapping and for use in hydrological models have been carried out in many regions of the world like Austria (Parajka & Blöschl, 2008a),the Patagonia(Lopez et al., 2008),Lebanon (Mhawej et al., 2014),Canada (Pouliot et al., 2014),USA(Franz & Karsten, 2013) ,Tibetan plateau (Gao et al., 2012),China (Yang et al., 2012),the Himalayan region(Maskey et al., 2011),(Safari Shad et al., 2013) and also at the global level( Salomonson et al., 1998)In the studies carried out so far the accuracy of the MODIS snow cover maps varies from as low as 21% to even up to 99% in few cases ,the accuracy of the product largely depends on the cloud cover, the land cover types, seasonal snow cover types and the elevation(Parajka & Blöschl, 2008b),(Salomonson & Appel, 2004),(Tekeli, et al., 2005) .In the Himalayas especially in remote and high altitude areas where there is little or no ground based data at all,MODIS snow product data have been instrumental in establishing a benchmark and carrying out snow cover mapping (Maskey et al., 2011).MODIS snow cover products are preferred over other products for studying mapping snow cover in the Bhutan Himalayas because of its high temporal resolution, free and easy data accessibility ,relatively higher spatial resolution and its good performance in other Himalayan basins(Sharma et al., 2012).

### 4.1.1. Moderate Resolution Imaging Spectroradiometer (MODIS)

The MODIS instruments on the Terra platform was launched on 18th December 1999 and on the Aqua Platform on 4th May,2002 by the Earth Observation Systems at the Gordon Space flight Centre in Greenbelt, MD(Hall et al., 2002).Terra passes from north to south across the equator in the morning while Aqua passes from south to north in the afternoon. MODIS provides imageries of the earth surface and clouds in 36 discrete ,narrow spectral bands from approximately 0.4 to 14.0 μm with temporal resolutions from 1 to 2 days and a spatial resolution of 250m in bands 1to 2,500m from bands 3 to 7 and 1000m in bands 8-36.A detailed list of bands corresponding to their wavelengths and resolutions can be found in table 7.The main objective of MODIS data is to improve our understanding of global processes and dynamics occurring on the land, in the sea and in the lower atmosphere.

There is a very hardworking, dedicated team force working behind MODIS consisting of various Universities, institutes and organizations under the directives of NASA. The MODIS science team is divided into four main categories: Atmosphere, Calibration, Land and Ocean from which 44 standard MODIS products are generated. Table 8 shows the available MODIS data products.Table 9 gives the summary of MODIS data products.

Table 8:MODIS Spectral bands with its characteristics[Adapted from National Snow and Ice Data Centre(http://nsidc.org/data/docs/daac/modis_v5/spectral_bands.html)]

| Band | Bandwidth | Resolution(m) | Primary use |
|---|---|---|---|
| 1 | 620-670 nm | 250 | Land/Cloud/Aerosols |
| 2 | 841-876 nm | 250 | Boundaries |
| 3 | 459-479 nm | 500 | |
| 4 | 545-565 nm | 500 | Land/Cloud/Aerosols |
| 5 | 1230-1250 nm | 500 | Properties |
| 6 | 1628-1652 nm | 500 | |
| 7 | 2105-2155 nm | 500 | |
| 8 | 405-420 nm | 1000 | |
| 9 | 438-448 nm | 1000 | |
| 10 | 483-493 nm | 1000 | |
| 11 | 526-536 nm | 1000 | Ocean Colour |
| 12 | 546-556 nm | 1000 | Phytoplankton |
| 13 | 662-672 nm | 1000 | Biogeochemistry |
| 14 | 673-683 nm | 1000 | |
| 15 | 743-753 nm | 1000 | |
| 16 | 862-877 nm | 1000 | |
| 17 | 890-920 nm | 1000 | |
| 18 | 931-941 nm | 1000 | Atmospheric Water Vapour |
| 19 | 915-965 nm | 1000 | |
| 20 | 3.660-3.840 μm | 1000 | |
| 21 | 3.929-3.989 μm | 1000 | Surface/Cloud Temperature |
| 22 | 3.929-3.989 μm | 1000 | |
| 23 | 4.020-4.080 μm | 1000 | |
| 24 | 4.433-4.498 μm | 1000 | Atmospheric Temperature |
| 25 | 4.482-4.549 μm | 1000 | |
| 26 | 1.360-1.390 μm | 1000 | Cirrus Clouds |
| 27 | 6.535-6.895 μm | 1000 | Water Vapour |
| 28 | 7.175-7.475 μm | 1000 | |
| 29 | 8.400-8.700 μm | 1000 | Cloud Properties |
| 30 | 9.580-9.880 μm | 1000 | Ozone |
| 31 | 10.780-11.280 μm | 1000 | |
| 32 | 11.770-12.270 μm | 1000 | Surface/Cloud Temperature |
| 33 | 13.185-13.485 μm | 1000 | |
| 34 | 13.485-13.785 μm | 1000 | |
| 35 | 13.785-14.085 μm | 1000 | |
| 36 | 14.085-14.385 μm | 1000 | Cloud Top Attitude |

Table 9: Summary of MODIS data products [Adapted from USGS website(https://lpdaac.usgs.gov/products/modis_products_table)]

| |
|---|
| **Calibration:** |
| **MOD 01** - Level-1A Radiance Counts |
| **MOD 02** - Level-1B Calibrated Geo located Radiances |
| **MOD 03** - Geolocation Data Set |
| **Atmosphere:** |
| MOD 04 - Aerosol Product |
| MOD 05 - Total Precipitable Water (Water Vapour) |
| MOD 06 - Cloud Product |
| MOD 07 - Atmospheric Profiles |
| MOD 08 - Gridded Atmospheric Product |
| MOD 35 - Cloud Mask |
| **Land:** |
| MOD 09 - Surface Reflectance |
| MOD 11 - Land Surface Temperature & Emissivity |
| MOD 12 - Land Cover/Land Cover Change |
| MOD 13 - Gridded Vegetation Indices (Max NDVI & Integrated MVI) |
| MOD 14 - Thermal Anomalies, Fires & Biomass Burning |
| MOD 15 - Leaf Area Index & FPAR |
| MOD 16 - Evapotranspiration |
| MOD 17 - Net Photosynthesis and Primary Productivity |
| MOD 43 - Surface Reflectance |
| MOD 44 - Vegetation Cover Conversion |
| **Cryosphere:** |
| MOD 10 - Snow Cover |
| MOD 29 - Sea Ice Cover |
| **Ocean:** |
| MOD 18 - Normalized Water-leaving Radiance |
| MOD 19 - Pigment Concentration |
| MOD 20 - Chlorophyll Fluorescence |
| MOD 21 - Chlorophyll_a Pigment Concentration |
| MOD 22 - Photosynthetically Available Radiation (PAR) |
| MOD 23 - Suspended-Solids Concentration |
| MOD 24 - Organic Matter Concentration |
| MOD 25 - Coccolith Concentration |
| MOD 26 - Ocean Water Attenuation Coefficient |
| MOD 27 - Ocean Primary Productivity |
| MOD 28 - Sea Surface Temperature |
| MOD 31 - Phycoerythrin Concentration |
| MOD 36 - Total Absorption Coefficient |
| MOD 37 - Ocean Aerosol Properties |
| MOD 39 - Clear Water Epsilon |

**MODIS snow products:**

The MODIS snow products are provided as a sequence of products beginning with a swath product, and progressing, through spatial and temporal transformations, to a monthly global snow product(Hall et al., 2002). The MODIS snow data products are produced as a series of seven products as listed in table 10.The sequence begins as a swath (scene) at a spatial resolution of 500m.

Table 10:MODIS snow data products [Adapted from (Hall et al., 2002)]

| Earth Science Data Type(ESDT) | Product level | Nominal data array dimension | Spatial Resolution | Temporal resolution | Map Projection |
|---|---|---|---|---|---|
| MOD10_L2 | L2 | 1354 km by 2000km | 500m | Swath(scene) | None(lat-long referenced) |
| MOD10_L2G | L2G | 1200 km by 1200km | 500m | Day of multiple coincident swaths | Sinusoidal |
| MOD10A1 | L3 | 1200 km by 1200km | 500m | Day | Sinusoidal |
| MOD10A2 | L3 | 1200 km by 1200km | 500m | Eight days | Sinusoidal |
| MOD10C1 | L3 | $360^0$ by $180^0$(global) | $0.05^0$ by $0.05^0$ | Day | Geographic |
| MOD10C2 | L3 | $360^0$ by $180^0$(global) | $0.05^0$ by $0.05^0$ | Eight days | Geographic |
| MOD10CM | L3 | $360^0$ by $180^0$(global) | $0.05^0$ by $0.05^0$ | Month | Geographic |

MODIS snow products are archived in Hierarchical Data Format-Earth Observing System (HDF-EOS) file formats, HDF is the standard archive format for EOS Data Information System(EOSDIS).The snow product file consists of two files namely the global attribute file that is the metadata and the scientific datasets(SDSs) that is the data arrays with local attributes (Hall et al., 2002).The snow products are archieved and distributed from the National Snow and Ice Data Centre(NSIDC) Distributed Active Archive Centre(DAAC) at the Univerisity of Colarado in Boulder,Colorado http://nsidc.org and the snow products can be downloaded and ordered from http://nsidc.org/NASA/MODIS.

**MODIS Snow Detection Algorithm:**

The snowmap(snow mapping) algorithm of MODIS identifies snow,lakeice and sea ice by their reflectance and emmitance properties and produced global daily and 8 day composite snow products(D. Hall & Riggs, 2001).The main technique used in the algorithms for snow mapping are threshold based criteria tests,the normalized difference between the bands and some decesion rules.The bands used as inputs to the snow cover algorithm are bands 1,2,4,6,31 and 32.

MODIS snow mapping algorithm is based on Normalized Difference Snow Index(NDSI) and a set of thresholds.NDSI is a measure of the relative magnitude of the characteristic reflectance difference between the visible and the short wave infra red reflectance of snow as shown in the equation below and is useful for identifying snow and ice and for separating snow/ice and most cumulus clouds. NDSI is insenstitive to a wide range of illumanation conditions and is partially normalized for atmospheric effects and does not depend on reflectance in a single band (D. Hall & Riggs, 2001)

$$NDSI = \frac{MODIS\ Band\ 4 - MODIS Band\ 6}{MODIS\ Band\ 4 + MODIS Band\ 6}$$ Equation 7

High reflectance of snow in the visible compared to mid infrared portion of the electromagnetic spectrum results in higher values for NDSI for snow as compared to other surface materials. After numerous researches and tests comparing MODIS snow products with Landsat TM by the scientists involved in the snow mapping algorithm, the NDSI threshold for snow is found to be greater than 0.4 but water may also have an NDSI of 0.4, therefore to discriminate between snow and water an additional test is necessary. Snow and water can be discriminated by using MODIS Band 2(0.841-0.876 μm), the reflectance of water in this band is less than 11%,so therefore if the reflectance of MODIS Band 2 is ≥ 11% and NDSI ≥ 0.4 then the pixel is initially mapped as snow(D. Hall & Riggs, 2001).
Pure snow has a very high NDSI but it decreases as other feature appears in a pixel, values of NDSI of snow in a mixed pixel is less than that for pure snow. Forested areas causes problems in classification of snow since these regions are usually dark and have NDSI lower than 0.4.To overcome this problem the Normalized Difference Vegetation Index(NDVI) which is an effective method for monitoring global vegetation codditions is used along with the NDSI to classify between snow free and snow covered forests.NDVI for MODIS is calculated using MODIS Band 1 and Band 2 as shown in the equation below.Therefore by using NDVI and NDSI togather it is possible to lower the NDSI threshold in forested areas without affecting the algorithm performance in other land cover types.

$$NDSI = \frac{MODIS\ Band\ 2 - MODIS Band\ 1}{MODIS\ Band\ 2 + MODIS Band\ 1}$$ Equation 8

Snow and cloud are discriminated by the snowmap algorithm based on the difference of their reflectance and emmitance properties,clouds are highly variable and have high reflectance in the visible and near infrared parts of the electromagnetic spectrum while reflectance of snow drops in the short wave infrared part of the spectrum.NDSI can separate snow from most obscuring clouds but it does not always identify optically thin cirrus clouds from snow therefore the clouds needs to be masked, it is done so using the MODIS cloud mask product.

A thermal mask was implemented in 2001 to overcome problems of cloud intrusion,aerosol effect,coastline and sand confusion to improve the overall accuracy of MODIS snowmap algorithm.For this sake a split window technique which uses MODIS Band 31 (10.78-11.28 μm) to estimate the surface temperature,this band was selected because it represents an atmospheric window in which little of the eliminated thermal rdiation is absorbed by the atmosphere.Also a tentative threshold of 277k has been set so in this process a pixel is not mapped as snow if the estimated surface temperature is greater than 277k, it has been reported that by using this technique especially in the tropical regions the snow covered areas improved greatly (D. Hall & Riggs, 2001).

Detailed technical specification,data collection,algorithm and other characteristics on the MODIS snow product can be found from the MODIS snow product webpage (http://modis.gsfc.nasa.gov/data/dataprod/dataproducts.php?MOD_NUMBER=10) and from "Algorithm theoretical basis document (ATBD) for the MODIS snow and sea ice-mapping algorithms" (D. Hall & Riggs, 2001), "MODIS Snow Products User Guide to Collection 5" (Riggs et al., 2006)) and "MODIS snow-cover products"(D. Hall et al., 2002)among others.

### 4.1. Model selection for stream flow Simulation

One of the most important task in hydrological modelling is selecting the most appropriate model. Selection is mostly based on simplicity, input data requirements, output reliability, robustness and the computational capacity among other factors(Marshall et al., 2005).Before using any hydrological model, it

is vital to understand the hydrological processes in the catchment. As stated in the document "Teaching aids in Hydrology" (UNESCO, 1985), the main purpose of using hydrological models is not to duplicate the complicated hydrological process in detail by a more sophisticated model, but to demonstrate the principal elements of the process, their combination into a simple or comprehensive model, and the importance of the model in solving typical problems of engineering hydrology.

Today there are numerous models available for calculating the response of the catchment to rainfall, snowmelt and other climatic variables. The hydrological models can be widely classified into two groups namely physically based distributed models and conceptually based lumped models. Physically based distributed hydrological models are based on our understanding of the physics of the hydrological processes which control catchment response and are expressed using mathematical equations to describe these hydrological processes by solving mass conservation and momentum equations. Examples of fully distributed models are the SHE model (Abbott et al., 1986)DHSVM(Wigmosta & Nijssen, 2002) and the IHDM((Beven et al., 1987).As pointed out by (Beven, 1989) practical difficulties arises in these fully distributed models because in practice the parameter values are heterogeneous and also due to the huge differences in the actual measurements and the model grid size leading to the problems in the validation of the models ( Feyen et al.,2000).

On the other hand, the conceptually based lumped hydrological models simplify the complex hydrological processes by simple book keeping procedures to quantify the physical processes (Yu ,2002).The advantage of these lumped models is that the conceptual parameterization is simple and therefore leading to efficient computation. In these conceptually based lumped models, the complexity is simplified by the introduction of optimization of model parameters which is very difficult to measure directly In the field, these parameters can be optimized by parameter calibration using the various available tools and they remain constant as long as the catchment property is not changed (Rientjes et al., 2013)(Bormann, et al, 2009).Examples of these models are the HBV model (Bergstrom, 1997) and the Sacramento model (Burnash, 1995) among others. Since these models are less data demanding ,are robust and gives good results they are widely used,HBV is widely used and was tested in over 40 countries(Bergstrom, 1997). Using a fully distributed hydrological model would be ideal when input data is available adequately but in data sparse areas like Bhutan, it would be a huge challenge at the cost of the model efficiency, on the contrary using a lumped conceptual model wold be more beneficial. As per the above discussed criteria's and characteristics the HBV-96 model is selected for this research and is discussed in detail below. Table11 lists down the major differences between physically based distributed models and the conceptually based lumped models.

Table 11: Differences between lumped and distributed hydrological models [Adapted after (Bormann et al., 2009).

| Characteristics | Distributed models | Lumped Models |
|---|---|---|
| Effort for model set up | High | Low |
| Spatial structures | Yes | No |
| Model results | Distributed water fluxes and integral response | Integral response |
| Model parameterization | Mainly a priori estimation of parameters, calibration is difficult or sometimes impossible. | Manual or automatic. |
| Model validation | Integral response, distributed water flows and state variables. | Only integral response. |
| Main source of uncertainty | Input data, parameters (dependent on scale) | Simple lumped concept. |

### 4.1.1. HBV MODEL

The Hydrologiska Byrans Vattenbalansavedelning (HBV) model was developed by Dr. Sten Bregstrom and his colleagues at the Swedish Meteorological and Hydrological Institute (SMHI) in the 1970's.It is regarded as a semi distributed conceptual precipitation runoff model in which the catchment can be divided into sub basins and using elevation zoning used to simulate runoff processes in a catchment using precipitation, air temperature and potential evaporation as input data. The model computes snow accumulation, snow melt, actual evapotranspiration, storage in soil moisture and ground water and the runoff from the catchment. Today the concept if HBV model is widespread, it has been modified several times and exist in different versions and has been applied in more than 45 countries(Bergstrom, 1997) with different climatic conditions, varying catchment sizes varying in size from small research basin to large continental scale and different elevation zones.HBV is used as a standard method for hydrological forecasting in many countries used for research studies, design and mitigation of flood related disasters.
The main principles behind the HBV model are as follows:

- The model must be based on a sound scientific foundation
- It must be possible to meet the data demand in most areas.
- Its complexity must be justified by its performance
- It must be properly validated
- The user must be able to understand the model.

### 4.1.2. The HBV Model structure

HBV is classified as a semi distributed conceptual model which is based on representation of few main components of the model on the land phase of the hydrological cycle, sub basins are used as primary hydrological units, an area-elevation distribution and land use classification is used. In the case of geographically and/or climatologically heterogeneous basins and in cases of presence of large lakes the sub basin option is usually used. For basins of considerable elevation range, a subdivision into elevation zones is made. Runoff is computed using meteorological data mainly precipitation, air temperature and potential evapotranspiration. For computing the runoff the model computes the water balance for the main storage types and shows how these storages changes in response to the varying meteorological inputs. The model adopts a daily time step although a shorter time step option is available. The graphical representation of the HBV model structure is as shown in figure 8.

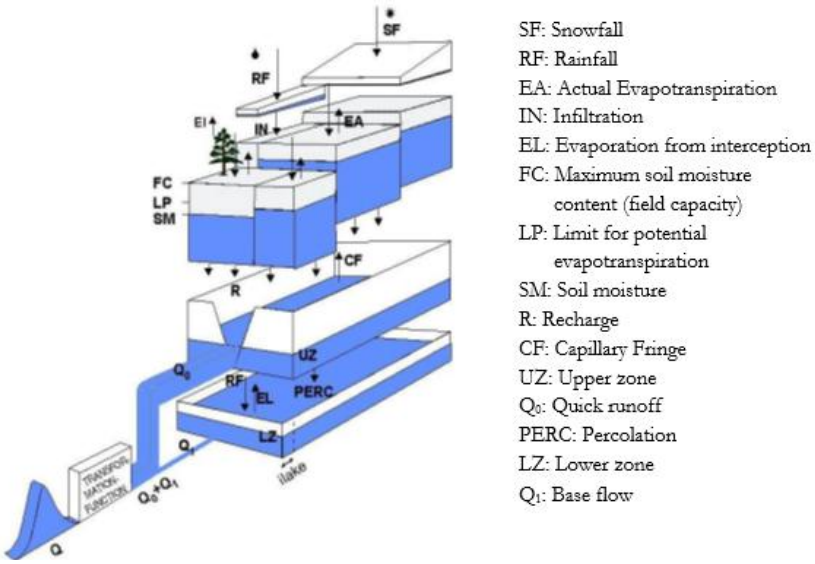


Figure 8: Schematic representation of the HBV model for one sub basin [Source: SMHI Manual version 6.2, 2011].

The HBV Model consists of four main routines. They are precipitation and snow routine, soil moisture routine, runoff generating routine and a routing routine. These routines are discussed in detail below.

The input data to the model are observations of precipitation, air temperature, vapour pressure, wind speed and estimates of potential evaporation, the values of the evapotranspiration are long term monthly averages. Air temperature, vapour pressure and wind speed are used for calculation of snow accumulation and melt. Observations of discharge are used to calibrate the model, verify and correct the model before a runoff forecast. (IHMS Manual version 6.2,2011).

#### 4.1.2.1. Precipitation and snow accumulation routine:

Precipitation is the main factor in simulating stream flow, a threshold temperature is used to differentiate between snow and rainfall:

$$RF = pcorr \cdot rfcf \cdot P \text{ if } T > tt \qquad \text{Equation 9}$$

$$SF = pcorr \cdot sfcf \cdot P \text{ if } T < tt \qquad \text{Equation 10}$$

RF = rainfall
SF = snowfall
P = observed precipitation (mm)
T = observed temperature ($^{o}$C)
*tt* = threshold temperature ($^{o}$C)
*rfcf* = rainfall correction factor
*sfcf* = snowfall correction factor
*pcorr* = general precipitation correction factor.

There are separate rainfall and snowfall correction factors because observed precipitation values are often affected by observational losses. The precipitation correction factor accounts for systematic errors that may be caused by non-representative precipitation input. To adjust precipitation to current altitude, lapse rate parameter *pcalt* is used.

**Snow routine:**
The snow routine of the model deals with snow accumulation and melt. The snowmelt routine is based on a simple degree day approach, based on air temperature. Precipitation is assumed to accumulate as snow when air temperature drops below a threshold temperature (tt) which is usually close to $0^{0}$C.

Snowmelt = *cfmax* .(T - *tt*) where T is temperature, *tt* the threshold temperature and *cfmax* the melting factor.

Snow accumulation is adjusted by snow correction factor to account for under catch of snow and winter evaporation. Temperature and precipitation lapse rate is provided according to elevation. Snow melt starts when temperature is above the threshold temperature in accordance with a simple degree-day factor which is assumed to remain constant throughout the melt season. The snow pack is assumed to retain the melt water as long as the amount does not exceed a certain water holding capacity of snow (given by parameter *whc*), after which runoff is generated. When temperature falls below the threshold temperature this water gradually refreezes according to the formula:

$$\text{Refreezing melt water} = cfr \,.cfmax \cdot (tt - T) \qquad \text{Equation 11}$$

Where *cfr* is the refreezing factor.

With the division of the catchment into elevation zones the model simulates elevation dependent variability in snow storage. Higher elevation receives more snow and precipitation compared to lower areas which results in an elevation dependent snow storage distribution in the catchment. In the snow routine the main results are the following three variables which are computed for each elevation zone and time step:

- Snow storage in mm of water equivalent.
- Free/liquid water content in snow(mm)
- Snowmelt(mm)

Glacier melt will occur only in the glacier zone and is taken into account by the model in the same way as snowmelt by the following formula, no glacier melt occurs as long as there is snow in the current zone.

Glacier melt = *gmelt* · (T - *ttm*) Equation 12

T = observed temperature (°C)
*gmelt* = glacier melting factor (mm/°C · day)
*ttm* = threshold temperature for snow melt (°C)

#### 4.1.2.2. Soil moisture routine:

Soil moisture accounting of the HBV model is based on a modification of the tank approach, it assumes a statistical distribution of storage capacities in a basin. The input to the soil moisture routine is rainfall or snowmelt from the snow routine and then it computes the storage of water in soil moisture, actual evapotranspiration and the runoff which will be the input to the response routine. The soil moisture routine is primarily based on three empirical parameters Beta (β), LP and FC as shown in figure 7 below. Beta (β) controls the contribution to the runoff response function (ΔQ/ΔP), and the increase in the soil moisture storage for each millimetre of rainfall or snowmelt (1-ΔQ/ΔP). The equation is nonlinear when β is not equal to 1 and usually the value of β is in the range of 2-3, which makes the equation strongly nonlinear.The ratio ΔQ/ΔP is also known as the runoff coefficient and ΔQis often called the effective precipitation.

$$\frac{\Delta Q}{\Delta P} = \left(\frac{SM}{FC}\right)^{\beta} \quad \text{Equation 13}$$

$$R = IN * \left(\frac{SM}{FC}\right)^{\beta} \quad \text{Equation 14}$$

There is a small percentage of contribution to runoff when the soil moisture content is low and higher contribution when soil moisture content is high. FC is the maximum soil moisture storage in the model, if the soil moisture storage is filled up to the FC, no more precipitation or snowmelt can be stored as soil moisture and all further input to soil moisture storage will be transformed as runoff which will lead to high runoff even during the times of moderate rainfall.The soil moisture routine is depicted in figure 9.

The soil moisture storage is depleted by evapotranspiration. The model is run with monthly data of long term mean potential evapotranspiration, based on the Penman formula (Penman, 1948).The calculation of actual evapotranspiration is a function of potential evapotranspiration and the relative soil moisture storage(SM/FC).If the soil moisture exceeds a threshold value (LP), actual evapotranspiration equals the potential evaporation and if soil moisture us below LP then the actual evapotranspiration decreases linearly with the decrease in storage. Beta (β), LP and FC are all free parameters which must be determined by model calibration.

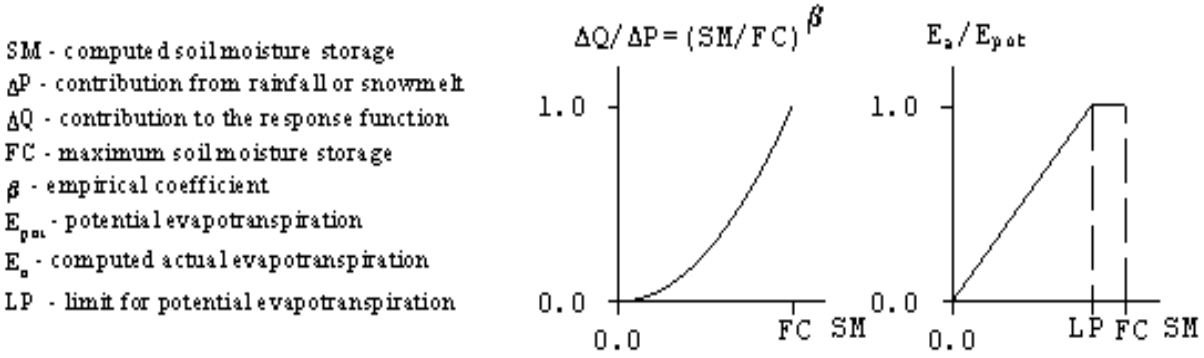


Figure 9: The soil moisture routine [Source: SMHI Manual version 6.2, 2011]

#### 4.1.2.3. The response routine:

The runoff generation routine is the response function which transforms excess water from the soil moisture routine into runoff, it also includes the effect of direct precipitation and evapotranspiration on a part which represents lakes, rivers and other wet areas. Two reservoirs the upper nonlinear and the lower ,linear reservoirs are the origin of the quick (superficial channel) and slow (base flow) runoff components of the hydrograph. The effect of the runoff response function is very similar to the use of a unit hydrograph whereby a sequence of net precipitation values are transformed into a runoff hydrograph. Each sub basin has its own response functions.

The upper zone represents the quick runoff components from overland flow and groundwater drained through inter flow. When the input of net precipitation from the soil moisture zone exceeds the percolation capacity (*perc*), the upper zone storage starts to fill up and gets simultaneously drained through the lower outlet. The drainage speed is determined by the recession coefficient of the lower outlet (k.UZ) as shown in figure 10. The lower zone represents the groundwater storage of the catchment which contributes to the base flow. The out flow from the upper and the lower reservoir is defined by a set of equations as shown in figure 8.

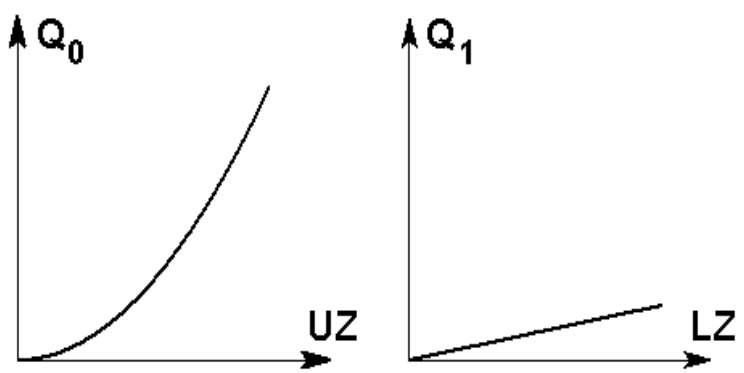


Figure 10: The response routine [Source: SMHI Manual version 6.2, 2011

**Outflow from upper non-linear reservoir:**

$Q_0 = k \cdot UZ^{(1+ alfa)}$

$Q_0$ = reservoir outflow upper reservoir (mm)

UZ = reservoir content upper reservoir (mm)

k = recession coefficient upper reservoir

here 'alfa' is a measure of non-linearity.

**Outflow from the lower linear reservoir:**

$Q1 = k4 \cdot LZ$

Q1 = reservoir outflow lower reservoir (mm)

LZ = reservoir content lower reservoir (mm)

k4 = recession coefficient upper reservoir

#### 4.1.2.4. Routing routine/Transformation Function:

In order to get a proper shape of the resulting hydrograph at the outlet of the sub basin, the runoff [illegible] e transformation figure 11 below,

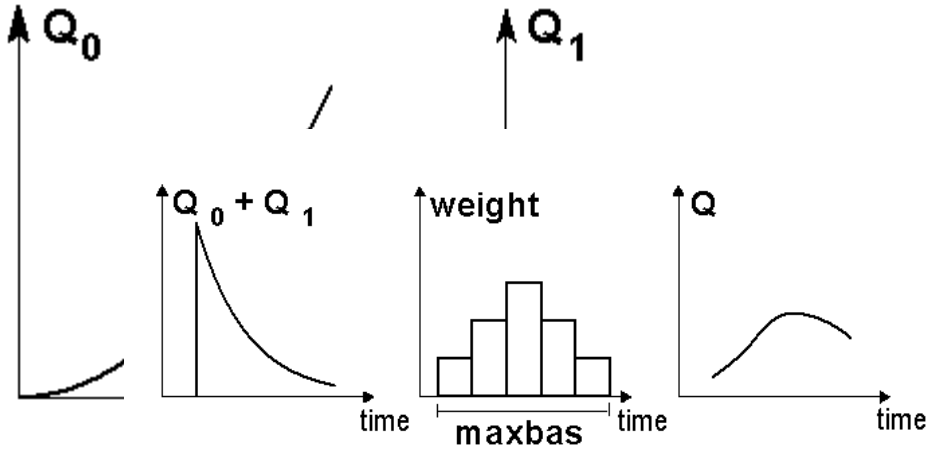


Figure 11: The transformation function [Source: SMHI Manual version 6.2, 2011].

# 5. RESEARCH METHODOLOGY

## 5.1. Snow cover mapping

For this research work the MODIS/Terra Snow Cover Daily L3 Global 500m Grid (MOD10A1) and MODIS/Terra Snow Cover 8-Day L3 Global 500m grid (MOD10A2) have been used, Since the TERRA satellite passes from north to south across the equator during the mornings it was preferred over the AQUA satellite which passes south to north over the equator during the afternoon because cloud cover obscuration is less during the mornings. This MODIS product contains snow cover, snow albedo, fractional snow cover, and Quality Assessment (QA) data in compressed Hierarchical Data Format-Earth Observing System (HDF-EOS) format (Riggs et al., 2006) which stores raster data, in raster representation area is divided into grids of equal sizes often called cells/pixels. Each of these pixels are assigned their unique properties .For remotely sensed data their resolution is described by pixels, a pixel is defined as the smallest element in an image that can be individually processed, the resolution of an image is described by the size of the pixel in the image. In the case of MOD10A1 the pixel size of snow extent is of 500 m by 500 m which in the study area, the Wang Chhu Basin translates to approximately 16710 pixels.

### 5.1.1. Downloading data:

The MODIS Snow and Ice data products are distributed by the National Snow and ice Data Centre (NSIDC) based in Colorado, they provide links to various product data sources and NASA REVERB ECHO website was the source of data for MODIS snow and ice data products. The REVERB ECHO website stores entire archived data for MODIS products as well as data from other Earth observation System Data and Information System (EOSDIC) data from other satellites and sensors. MODIS /Terra snow cover daily L3 global 500m SIN Grid V005 were downloaded for 8 years from the year 2003 to 2010 using a file transfer protocol (FTP) pull over the internet which is an easy way for users to copy files over the internet. V005 is the latest version of available data with advanced pre-processing and with an improved method of identifying and classifying snow and clouds (Riggs et al., 2006) The downloaded images needs to be processed and clipped to the area of interest. The following processes were carried out to come up with the snow cover maps.

### 5.1.2. Data Processing:

Once the MODIS Terra snow cover product (MOD10A1) has been downloaded, it is important to know the projection of the data because it is known that different projection systems store various aspects of the image. There are different projection systems like equidistant, equal area and conformal projections among others. The type of projection needed will depend on the information requirements and for the purpose of snow cover mapping an equal area projection is required. The MOD10A1 has a sinusoidal projection which is an equal area projection displaying proper areas which is equal to their corresponding areas on the globe however the sinusoidal projection( Hall et al., 2002) distorts the image of the land masses but it is not a problem in this analysis because it is just a visual drawback.

The coordinate system used is the Universal Transverse Mercator (UTM), it divides the earth into grids into 60 longitudinal zones which are 6 degrees wide ,extending from 80 degrees south to 84 degrees north and uses a specific secant transverse Mercator projection in each zone. The transverse Mercator projection has the capability of mapping a region of large north-south extent with low distortion. Each zone is divided into 20 latitude bands which are 8 degrees wide extending north and south from the equator and

are numbered by alphabets starting from C to X (alphabets I and O are omitted because of their similarity to numbers 1 and 0) (Snyder, 1987).The study area, Wang Chhu basin is located in zone 46N as shown in figure 12 below.

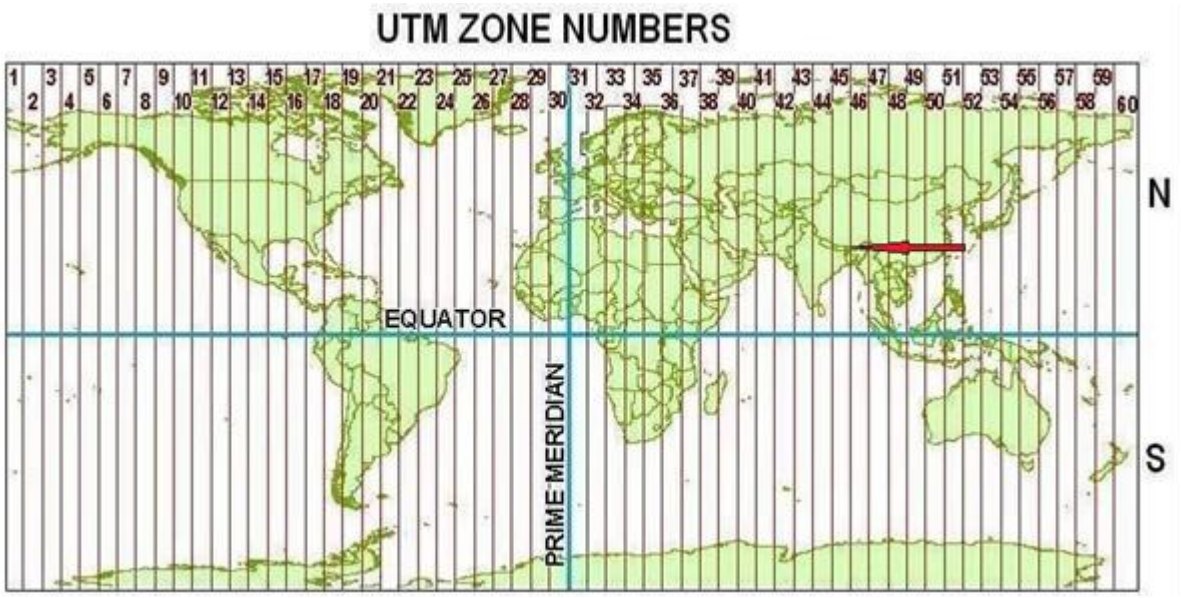


Figure 12: Location of the study area in the UTM zone, N46,the red arrow denotes the study area.[Image from National Geospatial – Intelligence agency(http://earth info.nga.mil/GandG/coordsys/grids/universal_grid_system.html#zza3)

Validation of the data is an important step in processing the snow cover maps, the downloaded MODIS Terra snow data needs to be reviewed for errors and problems in sensor readings with the help of the metadata and the flagged data files which comes along with the daily snow cover maps. The metadata is an important component in preparation for using the data because the metadata referred to as the 'data about the data' provides structured information about the quality and usability of the data. The metadata file contains information about the scale, resolution, source, processing and observation dates and contact information for further questions. The metadata file provides important information which allows the user to handle the data effectively and efficiently for further analysis. In the metadata file there is a section for flagged data ,if the data is flagged it indicates that there was a failure in the sensor where there was no surface reflectance input (Hall & Riggs, 2001). In the downloaded MOD10A1 for years 2003 to 2008, few days were flagged, so as a first screening step these flagged data were removed and not used for analysis. Also data in which majority of pixels covering the study area classified as zero (missing data0) and 1(no decision) were removed from analysis.

Since land cover is never homogenous, the pixel classification process used can never be 100 % accurate at any level of detail, even with a very good image resolution there is bound to be some variations within a pixel. The basic assumption is that the information within one pixel is considered the same throughout the pixel, but there are pixels which are not homogenous and its area consists of more than one class called the 'mixels'.The classification of these mixels are of importance here.Two main techniques are used to classify the mixels, the most common technique is to identify and assign the land class with highest percentage cover in that pixel, the other approach is to identify the land cover class at the centre of the pixel and to assign that land cover class to the whole pixel (Longley et. al., 2005).The pixels of the MODIS Terra snow data is classified using the first approach where the pixel is classified based on the land class with highest percent coverage since the resolution of the image is 500m and it is difficult to pin point the

land class at the centre of the pixel. The pixels of the MODIS snow products are divided into 11 classes represented using coded integers as shown in table 12 below.

Table 12:Land classification classes and pixel identification numbers [from (Riggs et al., 2006)

| Value | Description |
|---|---|
| 0 =missing data | Data is missing |
| 1 = no decision | No decision |
| 11 = Night | Darkness and polar night. |
| 25 = no snow | Snow free land. |
| 37 = lake | Lake or inland water. |
| 39 = ocean | Open water. |
| 50 = cloud | Obscured by clouds. |
| 100 = lake ice | Snow covered lake ice. |
| 200 = snow | Snow covered land |
| 254 = detector saturated | Detector saturated |
| 255 = fill | Data used to fill gaps in the swaths. |

MODIS being an optical sensor, cloud cover is one of the main obstacle in mapping snow. During the times of high cloud cover percentage there is greater possibility that clouds may be misclassified as snow and snow as cloud. Since the study area is a mountainous region experiencing monsoon in the summer months, the MODIS derived snow cover maps can be often influenced by cloud cover. Even with the improved snow mapping algorithm discussed in chapter 4, the MODIS Terra snow data downloaded for the entire analysis period from 2003 to 2010, the average cloud cover over the study area is found to be over 50 %.This large portion of cloud cover over the study period is a concern for data analysis and processing for snow cover mapping. The misclassification of snow and cloud occurs because parts of ice clouds appears yellow in bands 1, 4 and 6 colour display of the MODIS sensor, these three MODIS bands are used for snow classification. This error occurs when some of the clouds fall under the shadow of other clouds thereby leading to parts of the clouds not being recognized as cloud when the cloud mask is being generated because of the difference in the reflectance levels. The MODIS snow algorithm then processes these missed clouds as snow since their spectral features are nearer to 'snow ' than to 'no snow' but after the improvement of the snow algorithm in 2005,MODIS claims that this problem is typically very small (Riggs et al., 2006).

#### 5.1.3. Snow cover mapping:

Many intermediate steps are carried out to come up with final snow cover maps for the study area. Since the swath width of MODIS is 2330 km by 2330 km, the MODIS tile covering the study area is very large, therefore the study area needs to be extracted. The extract by mask feature in Arc GIS is used to extract only the study area, the catchment polygon is used for masking only the cells/pixels of the study area corresponding to the area defined by the catchment polygon as shown in figure 13.This process is implemented using the spatial model function in Arc GIS for all the downloaded images for the years 2003 to 2010.

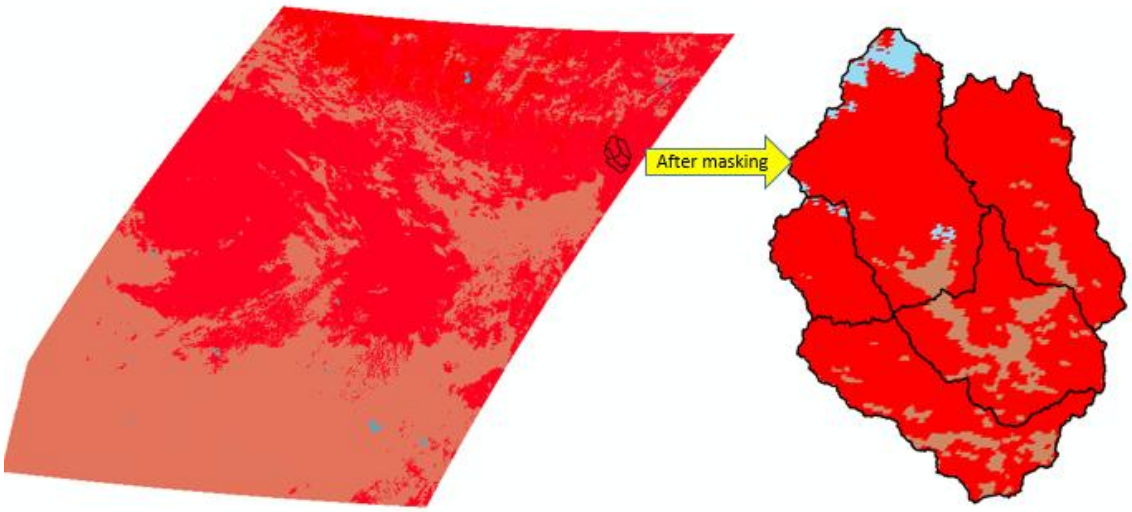


Figure 13:: MODIS tile covering the study area (left) and extracted snow cover map after masking the study area (right).

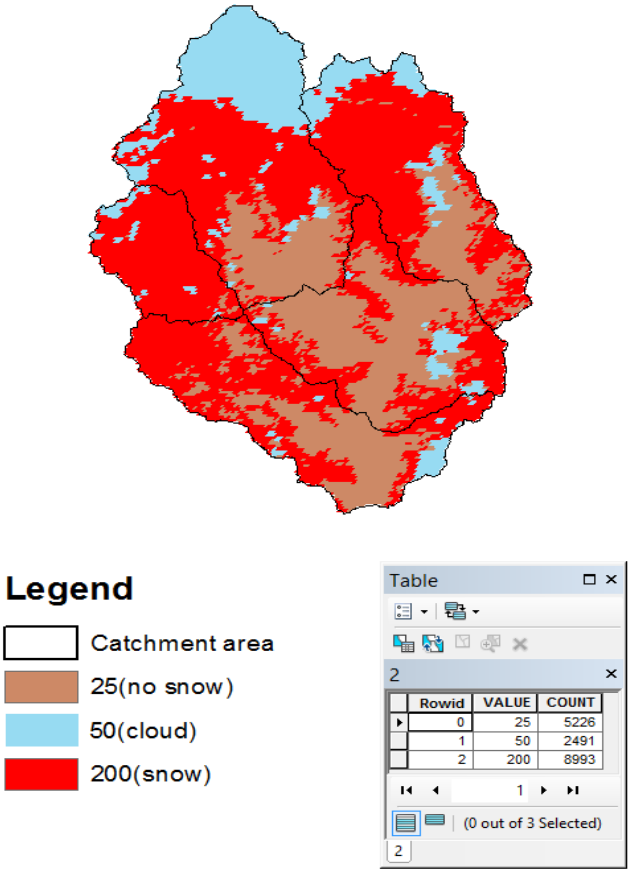


Figure 14: snow cover map on a particular day

Once the snow cover data of the study area has been extracted, the attribute table which contains information on the pixel count of the particular land cover classification: snow, no snow, lake, cloud and water as shown in table 10 above of each processed day was copied to excel and daily percentages of snow and cloud cover for the study area is calculated. Figure 14 above shows the snow cover map on a particular day, on that day three types of land classes were reported no snow (pixel 25),cloud (pixel 50) and snow (pixel 200).The number of pixel values of the land classes in the attribute table varied throughout the eight years of data period.

### 5.1.4. Analysis of MODIS derived snow cover Maps:

After all the attributes were imported to excel, various steps were involved in analysis of the snow cover data for checking the credibility and to assess the potential use of MODIS Terra MOD10A1 snow product for snow cover mapping applications for the Bhutan Himalayas. First to check the consistency of the data, percentages of pixels of land class groups like snow cover, cloud cover and areas without snow percentages were calculated and plotted. In figure 15 the daily percentage snow cover is plotted (see annex 1 for time series of snow and cloud cover for the years 2003-2010). It can be seen that the maximum total snow cover percentages vary largely from about almost 90% in 2004 to just over 50 % in 2007,this can be explained by the fact that there had been a change in the version of the MODIS TERRA snow product since 2007,the version 5 of the product began since 2007 and it had some changes in the snow detection algorithm where a conservative cloud mask was exclusively used and the consistent application of screens which reduced the occurrence of erroneous snow in various snow covered places which appeared in the previous version (Riggs et al., 2006),therefore for further analysis only the years 2007 to2010 will be used From the MODIS derived snow data, average snow cover in the basin estimated for the years 2003 to 2010 was around 4% of the total land area of the basin which corresponds to around 146 square kilometres of the total area.

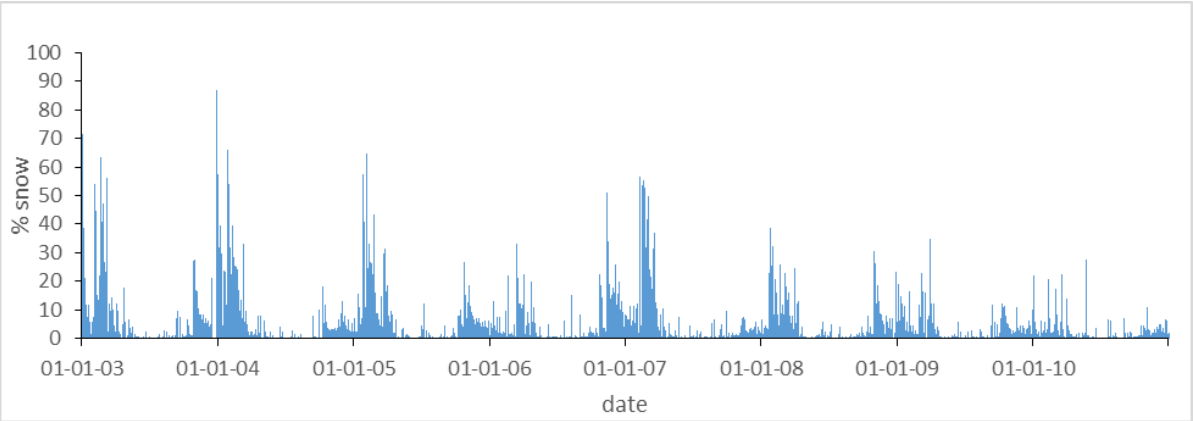


Figure 13: Snow cover percentage over the study area for the period 2003-2008.

The mean monthly distribution of the snow cover percentages for the study area was calculated and plotted as shown in figure16, the annual pattern of snow accumulation and melt can be observed, the snow starts to accumulate by end of September and gradually increases with the peak at February and starts to melt rapidly after it. Mean snow cover area trend in the basin was also calculated for the years 2003-2010 and were also plotted for visualization and to identify trends in the study basin.The mean monthly distribution of snow cover in the basin shows that the snow accumulation starts at around 4% of the total basin area and accumulates till it reaches a maximum of around 15% of the total area and depletes back to around 2% of the basin area by the end of the melt period. The yearly trend of snow

cover area in the basin shows a declining trend over the years which is in agreement with observations reported from the Western Himalayas( Kulkarni, et. al., 2003)

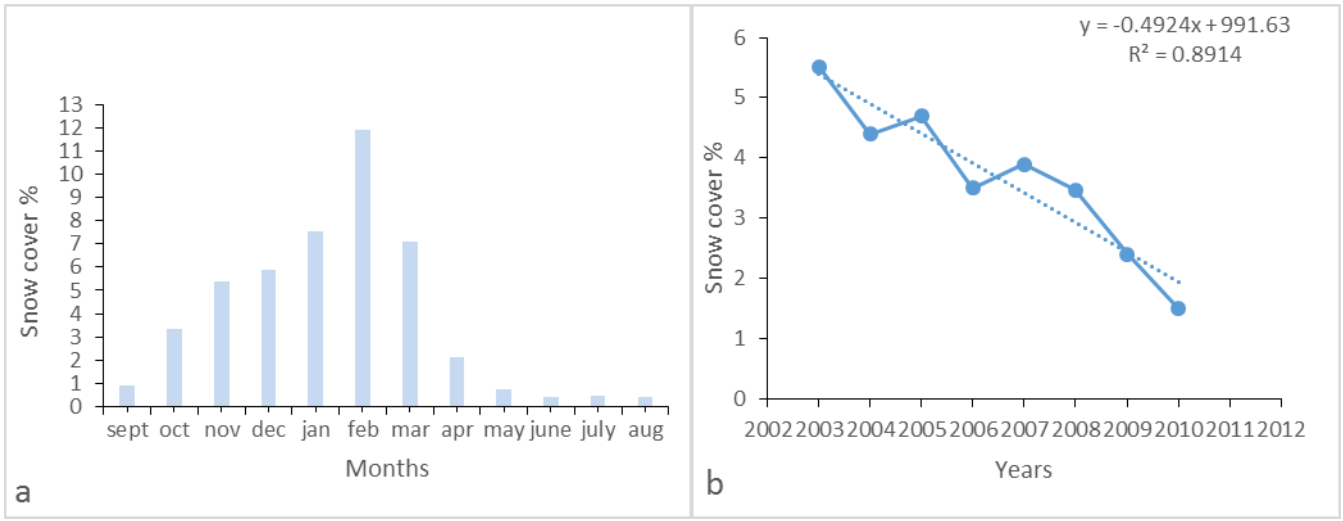


Figure 14: Mean monthly distribution of snow cover (a) and the yearly trend of snow cover in the basin (b).

#### 5.1.4.1. correlating MODIS derived snow cover percentages to station data

Since the climatological stations in the basin are located in the lower valleys and there are no stations in the higher elevation where it is covered by snow throughout the year, therefore to check how the MODIS TERRA derived snow cover data corresponds to ground station data, and to check if there is any correlation between the two, the MODIS TERRA derived snow cover data was compared to the mean annual average temperature of all the stations in the basin for the years 2007-2010 for every snow accumulation period as shown in figure 17.Then to cross check how the snow cover data represents for one particular pixel location, the Drugyel station was chosen as this is the station available at the highest elevation (2550m) in the basin. The Drugyel station pixel value was extracted from the MODIS derived snow cover maps for the basin for years 2007 to 2010 and it was found out that only during 3 days in the entire three years of data (2007-2010) the pixel was classified as snow(annex 2), from this analysis it can be inferred that the stations in the lower valleys are decoupled from the snow processes in the higher elevation.

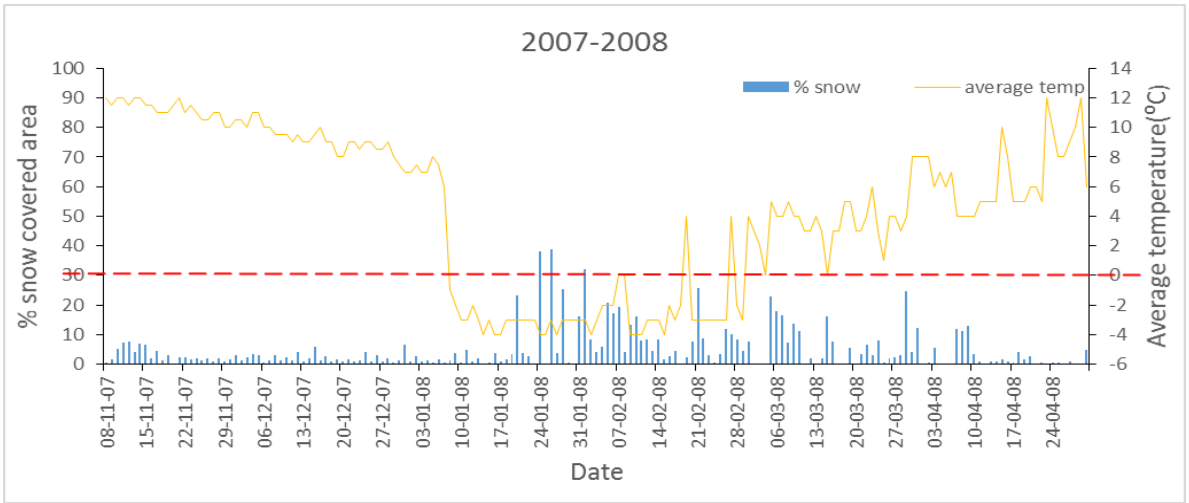


Figure 15: Comparison of snow cover area to mean average temperature in the basin.

### 5.1.5. Relationship between snow cover area distribution and runoff:

Snow cover area has been reported as a very important variable in understanding, modelling and predicting various atmospheric, ecological and hydrological processes in snow dominated basins(Jain et al.,2010:Sirguey, 2009:(Dietz et al., 2012) Monitoring of seasonal snow cover is an effective method of tracking spatial and temporal patterns in mountainous terrain since remotely sensed snow cover products can be viewed over large spatial regions.

In the study basin there are no insitu snow pack measurement stations and therefore no information on the spatial distribution and the snow water equivalent are available. The study area being mountainous, it is heterogeneous in nature and exhibit strong gradient in precipitation so understanding the spatial distribution of snow in the basin is the first step in understanding runoff generated from snowmelt. To identify spatial and temporal patterns of snow covered area and to identify relationships between snow cover distribution and runoff production in the study area, snow cover maps derived from the MODIS TERRA 8 day(MOD10A2) for the years 2007 to 2010 were used for analysis. The 8 day product is used because it gives the maximum snow cover extend over 8 day period and also the cloud cover is relatively lower than the daily maps. The snow covered area is used to characterize how snow spatial variability relates to snowmelt runoff generation in the Wangchhu basin across a large range of elevations. The snow covered areas and the runoff are compared directly without any prior defined relationship among the two so in this sense this study is solely data based. The melt season, which from the above analysis is observed to be occurring from mid-March up till when the snow cover percentage reduces to less than 1% of the entire basin which corresponds to around mid-June. A total of 57 images during the melt season were processed and used for further analysis for the years 2007-2010

To understand the relationship between snow cover area and runoff, snow cover area percentage for every sub catchment in the basin is calculated. Sub basins of the Wang Chhu basin ranges in elevation from 1837 m to over 7050m.Table13 shows the characteristics of the sub basins.This spatial sub division of dividing the basin into respective sub catchment is taken as the basis for analysing relationship between snow cover area and discharge.

Table 13: Sub catchments in the Wang Chhu basin with elevation range and area.

| | Elevation(m) | | |
|---|---|---|---|
| Sub basin | Minimum | Maximum | Area(km2) |
| Paro Chhu | 2124 | 7047 | 1044 |
| Haa Chhu | 2659 | 6734 | 318 |
| Lungten Phu | 2187 | 6430 | 763 |
| Damchhu | 2042 | 5127 | 746 |
| Chhukha | 1837 | 2567 | 719 |

First for the snow melt season of every year of 2007 to 2008, the snow covered area for every sub catchment was calculated and was compared with the discharge at the outlet of that particular basin. Regression analyses was used to compare these two variables. A total of 5 regressions per sub catchment per year was plotted to find the correlation between the snow cover area and the runoff in every sub catchment. Strength of the regression relationship was tested by choosing different regression equation either linear or nonlinear (exponential, logarithmic, polynomial or power) depending on which one resulted in the greatest coefficient of determination ($R^2$).

$$R^2 = \frac{\sum(S_i - \bar{S})^2}{\sum(O_i - \bar{O})^2}$$ Equation 15

Where S is the simulated value, $\bar{S}$ the average of simulated values the observed value and $\bar{O}$ the average of observed values. This $R^2$ provides the indication of degree of correlation between the spatial extent of snow cover and the discharge at every sub catchment. Higher the value of $R^2$ higher the degree of correlation between the two.

To study the distribution of snow cover in the basin based on elevation, the basin was divided into 10 elevation zones with each elevation zone covering an elevation range of around 550m.The area of the elevation zones ranges from less than 1km$^2$ to 847 km$^2$, with the upper most elevation covering the smallest area than all other zones as shown in table 14 below. The snow distribution for every elevation was plotted for analysis to check for the snow distribution pattern in the basin.

Table 14: Elevation zones and area for each elevation of Wang Chhu basin.

| | Elevation(m) | | |
|---|---|---|---|
| Elevation zone | Minimum | Maximum | Area(km2) |
| Zone 1 | 1800 | 2350 | 141.2 |
| Zone 2 | 2350 | 2900 | 614.8 |
| Zone 3 | 2900 | 3450 | 847.2 |
| Zone 4 | 3450 | 4000 | 704.2 |
| Zone 5 | 4000 | 4550 | 691.3 |
| Zone 6 | 4550 | 5100 | 488.8 |
| Zone 7 | 5100 | 5650 | 85.9 |
| Zone 8 | 5650 | 6200 | 10.9 |
| Zone 9 | 6200 | 6750 | 3.8 |
| Zone 10 | 6750 | 7300 | 0.9 |

## 5.2. Stream flow modelling

For the streamflow modelling, HBV-96 Model was used, this model has been discussed in detail in chapter 4.The following processes were followed.

### 5.2.1. Data pre-processing:

Before using the datasets as input for running the model, the collected datasets needs to be checked for consistency and pre-processed.

**Precipitation:**

Precipitation is one of the most important climatological parameters which is in two forms rain and snow. For the purpose of modelling it is necessary to have reliable precipitation data. Daily precipitation data for the study area was collected from the Department of Hydro met Services, Bhutan for the eight stations in the basin for 8 years, 2003 to 2010 considering the availability of satellite snow cover data for these years of Rain gauges were used to measure daily precipitation in millimetres, the daily rainfall is the measure of the rainfall accumulated over 24 hours, rainfall intensity is not measured. The daily precipitation time series had few days of missing data, these missing data have been filled in using the averages of the day before and the day after when it was few days of missing values and when there were many days in a row

with missing data, the missing data were filled depending on the similarities with the surrounding stations when the data of the surrounding station was consistent. Double mass curves ,which are used to check the consistency of many kinds of hydrological data by comparing data for a single station with that of a pattern composed of the data from several other stations in the area and also used to adjust inconsistent precipitation data (Searcy & Hardison, 1960) were used to check the consistency of the precipitation data, the cumulative precipitation of each station is plotted against the average cumulative precipitation of its surrounding stations for the eight years of study period. The double mass curves show that all the stations have good data consistency with regression coefficient, $R^2$ more than 0.9 for all the stations in the basin as shown in figure 18 below(ANNEX 3). This means that there has not been much changes in the location of the gauge station, in exposure or in observational methods. Table 15 shows the main station and its surrounding stations used for plotting the double mass curves.

Table 15:Main stations and the surrounding stations used for plotting the double mass curves.

| Sl no | Main Station | Surrounding Station |
|---|---|---|
| 1 | Chhukha | Paro,Haa,Drugyel,Betikha,Chapcha,Simtokha and Gidagom |
| 2 | Paro | Chhukha, Haa,Drugyel,Betikha,Chapcha,Simtokha and Gidagom |
| 3 | Haa | Chhukha,Paro, Drugyel,Betikha,Chapcha,Simtokha and Gidagom |
| 4 | Drugyel | Chhukha,Paro, Haa, Betikha,Chapcha,Simtokha and Gidagom |
| 5 | Betikha | Chhukha,Paro, Haa, Drugyel,Chapcha,Simtokha and Gidagom |
| 6 | Chapcha | Chhukha,Paro,Haa, Drugyel,Betikha,Simtokha and Gidagom |
| 7 | Simtokha | Chhukha,Paro,Haa, Drugyel,Chapcha,Betikha and Gidagom |
| 8 | Gidagom | Chhukha,Paro,Haa, Drugyel,Chapcha,Betikha and Simtokha |

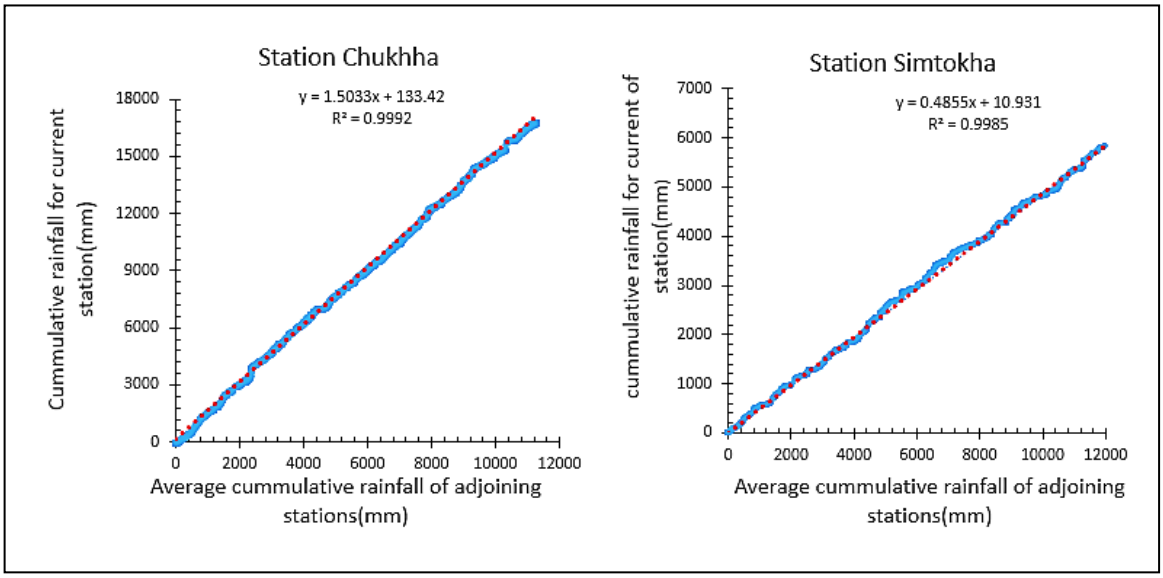


Figure 16: Double mass curves for station Chhukha and Simtokha.

**Temperature data:**

The climatic stations are used to record air temperatures, sunshine hours, relative humidity and wind speed and direction, temperatures are measured in degree Celsius. The climatological variables like maximum and minimum daily temperatures, the wind speed and the sun shine hours among others were also collected from the Department of Hydro Met services, Bhutan for the eight years of study period. There were days with missing data in these time series too. The missing temperature data were filled using normalization by

taking values from the nearby stations with little elevation difference since temperature is highly dependent on elevation(DeSilva et al., 2007).The mean monthly maximum, minimum and the average temperature was also calculated for the study area as shown in figure 19.

$$T_n = \frac{T_{pn}}{X} * \left(\frac{T_1}{T_{p1}} + \frac{T_2}{T_{p2}} + \cdots + \frac{T_x}{T_{px}}\right) \qquad \text{Equation 16}$$

Where:
$T_n$: is the missing daily temperature at station N,
$T_1, T_2, \ldots . T_x$:Daily temperature records of nearby stations when temperature is missing at station N,
$T_{p1}, T_{p2}, \ldots T_{px}$: previous year's similar season daily temperature data when $T_{pn}$ is used and
X :is the number of nearby stations used.

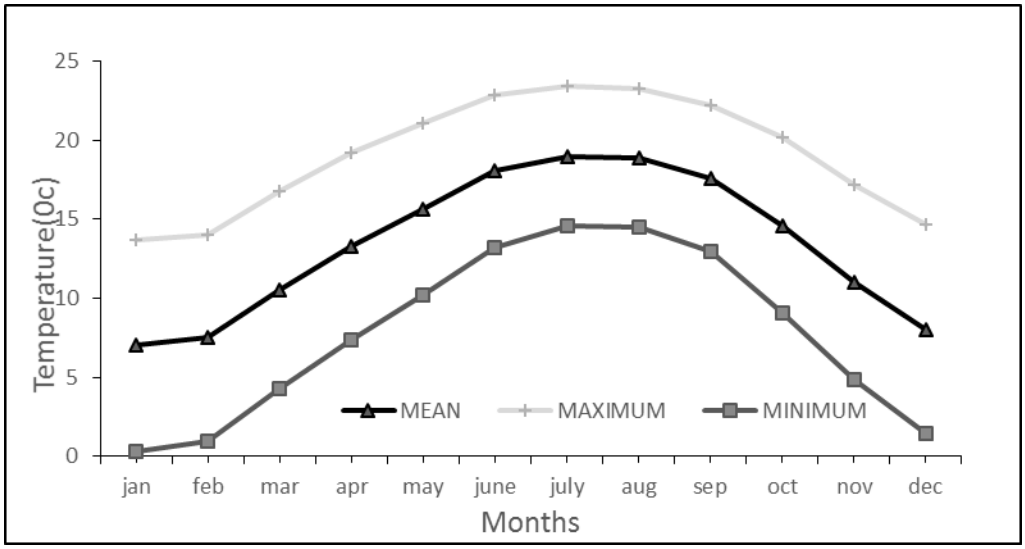


Figure 17:Mean, maximum and minimum temperatures in the study area(2000-2010)

**Stream Flow data:**
The stream flow data for the five stations in the study area was collected from the Department of Hydro Met Services, Bhutan, these stations measure water level (stage) and these water stages are converted to flow rates ($m^3/s$) by the proper stage-discharge curve. The stage discharge curves are developed and adjusted by the Department of Hydro met Services, Bhutan by using the measurements taken throughout the year Measurements of stage and discharge is an important part of operational hydrology and runoff data is vital in model calibration and verification(Seibert, 2000).A long time series of runoff helps in understanding the behavior and characteristics of the catchment.

The eight years (2003-2010) of data series collected for the study period was screened to test the reliability of the data. Composite hydrograph of each basin was plotted against the respective rainfall of that particular basin to screen the data. Only station Chhukha, Paro and Haa had the complete series of data so these three stations were used. As shown if figures 20 it can be observed that the discharge corresponds well in tune with the rainfall and there are few outliers in the data which can be explained as observational errors.

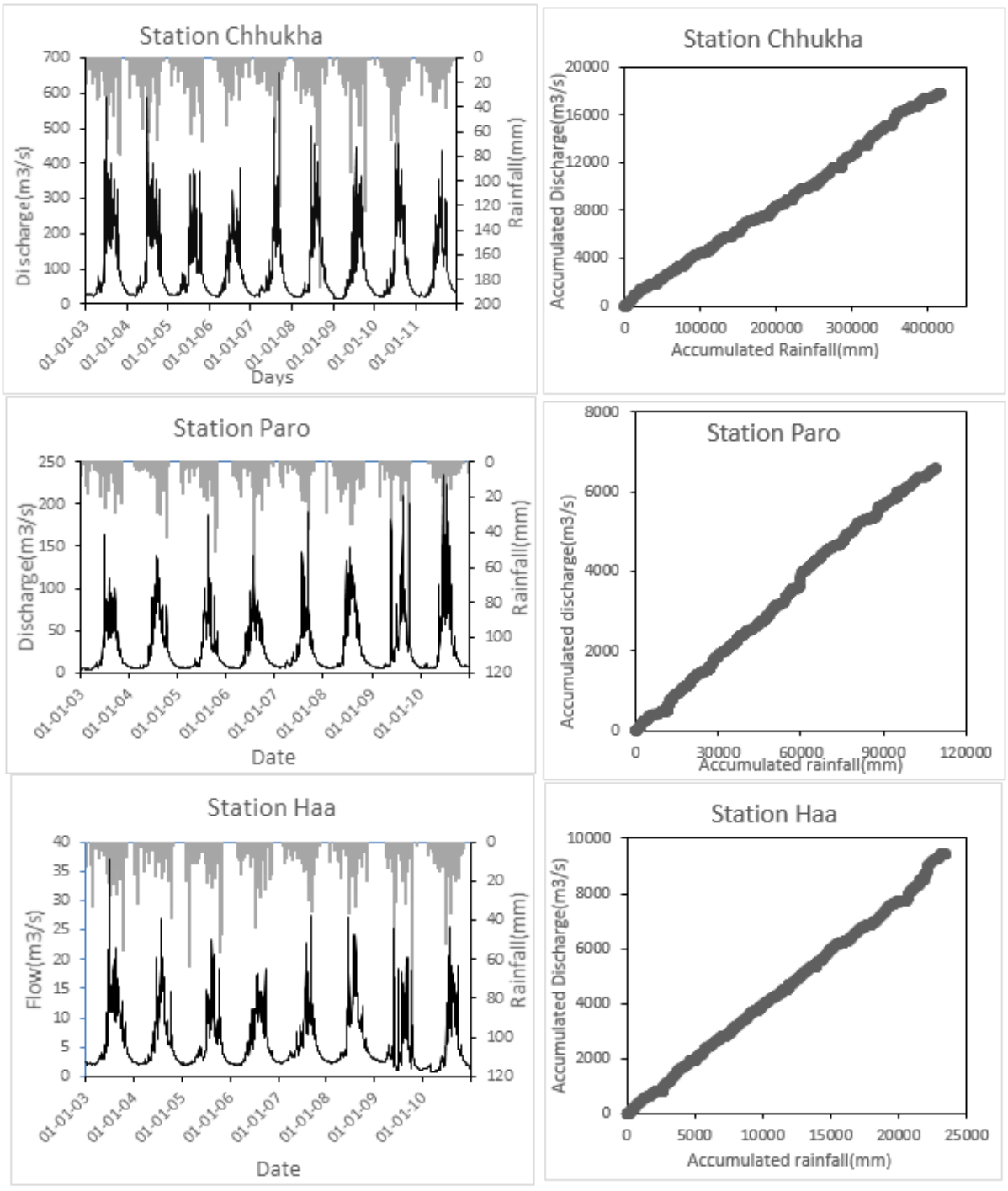


Figure 18: Discharge-Rainfall consistency plots.

**Monthly Potential Evapotranspiration:**

Evapotranspiration is the term used to describe two inseparable processes which occur simultaneously, Evaporation and transpiration. Evaporation is the process of conversion of liquid water to water vapor(vaporization) and removed from the evaporating surface and transpiration is the loss of water by plants(Haque, 2003).The actual and the maximum rate of evapotranspiration is called the actual and

potential evapotranspiration respectively. For the HBV model requires the mean monthly potential evapotranspiration (PET) as an input. There are various methods to calculate the potential evapotranspiration, some of the most widely used methods being Thornthwaite (1948), Blaney- Criddle (1950) and the Penman (1956) methods.The in situ reference evapotranspiration was calculated using the Penman Monteith(FAO-56,2007) equation using the meteorological variables like temperature, sunshine hours, wind speed and relative humidity data collected from the Department of Hydro met services,Bhutan. The FAO Penman-Monteith equation to calculate the reference evapotranspiration is as follows(after Allen et al., 1998):

$$ET_0 = \frac{\Delta(R_n - G) + \gamma * \frac{900}{T+273} * U_2 * (e_s - e_a)}{\Delta + \gamma * [1 + 0.34 * U_2]} \qquad \text{Equation 17}$$

Where $ET_0$ is the reference evapotranspiration (mm/day), $R_n$ is the net radiation at the crop surface(MJ/m²/day) , $U_2$ is the wind speed at 2m of height(m/sec),G the soil heat flux density(MMJ/m²/day),T the mean daily temperature at 2m height(°C), $e_s$ the saturation vapor pressure(kPa), $e_a$ the actual vapour pressure(kPa), $\gamma$ is the psychometric constant(kPa/°C) and $\Delta$ is the slope of the vapor pressure curve.

Solar radiation is estimated from the cloudiness conditions of the day after translating them into sunshine hours. The psychometric constant ($\gamma$), saturation vapor pressure ($e_s$), actual vapor pressure ($e_a$) and the slope of the vapor pressure ($\Delta$) are not measured directly in the field and needs to be estimated. Since the psychometric constant relates the partial pressure of water in the air to the air temperature (Łabędzki et al.,2011),it is estimated using the air pressure as shown below:

$\gamma = 0.665 * 10^{-3} * P$, Where P is the air pressure (kPa).

As saturation vapor pressure is related to air temperature, it can be calculated using the air temperature data and is expressed as following:

$$e_{(T)} = 0.6108\ exp\left[\frac{17.27\,T}{T+237.3}\right] \qquad \text{Equation 18}$$

Where, $e_{(T)}$ is the saturation vapor pressure (kPa) at air temperature T (°C).Mean saturation vapor pressure is calculated as the mean between the saturation vapor pressure at both the daily maximum and minimum air temperatures according to (FAO-56,2007) using the following equation:

$$e_s = \frac{eT_{max} + eT_{min}}{2} \qquad \text{Equation 19}$$

The actual vapor pressure is also calculated from the relative humidity data using the following equation,

$$e_a = e_s \left[\frac{RH_{mean}}{100}\right] \qquad \text{Equation 20}$$

where $RH_{mean}$ is the mean of the relative humidity (%).

And finally the slope of saturation vapor pressure curve was calculated using the following equation:

$$\Delta = \frac{4098[0.6108 exp\left(\frac{17.27 * T_{mean}}{T_{mean}+237.3}\right)}{(T_{mean}+273.3)^2} \qquad \text{Equation 21}$$

Where, $T_{mean}$ is the mean daily air temperature (°C) and exp is the base of natural logarithm (2.7183).

Since the HBV Model requires the monthly potential evapotranspiration, it has been calculated using the Thornwaite method because of its simplicity and applicability. To estimate the potential evapotranspiration by this method mean monthly temperature and the latitude of the site are the only parameters that need to be known and is therefore simple to calculate(Cruff & Thompson, 1967) and it is calculated using the following equation:

$$ET_0 = 16 * \left(\frac{10T_i}{I}\right)^a \left(\frac{N}{12}\right)\left(\frac{1}{30}\right)$$ Equation 22

$$I = \sum_{i=1}^{12} \left(\frac{T_i}{5}\right)^{1.514}$$

$$a = (492390 + 17920I - 771I^2 + 0.675I^3) * 10^{-6}$$

Where $T_i$ is the mean monthly temperature (°C), N the mean monthly sunshine hour, I the heat index and a is the cubic function of the heat index. The main advantage of using this method is the minimum parameter requirement of only temperature and the sunshine hours. The monthly potential evapotranspiration calculated for each station in the study area using this method is listed in table 16 below.

Table 16: Mean monthly Potential Evapotranspiration for the stations in the study area.

| Months | Chukha PET(mm /month) | Paro PET(mm /month) | Haa PET(mm/ month) | Betikha PET(mm/ month) | Simtokha PET(mm/ month) | Drugyel PET(mm/ month) | Chapcha PET(mm/ month) | Gidagom PET(mm/ month) |
|---|---|---|---|---|---|---|---|---|
| Jan | 1.94 | 1.78 | 0.98 | 1.61 | 1.35 | 1.1 | 1.96 | 1.52 |
| Feb | 2.65 | 2.23 | 1.51 | 1.7 | 2.2 | 2.09 | 2.52 | 2.23 |
| Mar | 4.86 | 4.04 | 3.16 | 3.49 | 3.72 | 3.72 | 3.49 | 3.79 |
| Apr | 6.7 | 5.99 | 4.99 | 5.27 | 6.11 | 5.15 | 4.8 | 5.83 |
| May | 8.64 | 7.85 | 6.89 | 6.7 | 8.16 | 7.65 | 6.26 | 7.88 |
| Jun | 10.44 | 9.97 | 8.82 | 8.35 | 10.54 | 9.97 | 8.17 | 9.9 |
| Jul | 10.5 | 10.68 | 9.63 | 8.75 | 11.32 | 10.48 | 8.54 | 10.19 |
| Aug | 9.37 | 10.17 | 9.22 | 8.7 | 10.95 | 9.82 | 8.17 | 9.57 |
| Sept | 8.52 | 8.57 | 7.55 | 7.45 | 9.11 | 8.1 | 7.39 | 8 |
| Oct | 7.01 | 5.47 | 4.72 | 5.08 | 6.08 | 5.28 | 6.06 | 5.64 |
| Nov | 4.71 | 3.13 | 2.57 | 3.33 | 3.29 | 2.81 | 4.34 | 3.19 |
| Dec | 2.96 | 1.86 | 1.37 | 2.56 | 1.81 | 1.28 | 2.78 | 2.09 |

### 5.2.2. GIS application for data extraction and preparation for HBV Model:

GIS(Geographic Information system),a tool for working with geographic system, is defined as an organized computer based system which is designed to efficiently capture, store, update, manipulate, analyze and display all forms of georeferenced data(de By,2009).GIS is used in this study for preparing data and maps for use as input data to the model. Arc GIS, ILWIS and ERDAS have been extensively used in preparation for the inputs

**DEM Hydro processing and Catchment extraction:**

For this study, 500mx500m Digital Elevation Model from the Shuttle Radar Topography Mission (SRTM) has been used for extraction of the catchment area. DEM characterizes the topography of the catchment and SRTM dataset is one of the freely available DEM datasets on the internet and is easy to use. In order to use the SRTM digital elevation model, it is necessary to project and clip the raw DEM to the study area. The DEM is re-projected and clipped to the projection of the study.(figure 19).

For catchment delineation the Hydrology Toolbox of Arc GIS has been used to perform terrain processes and extraction of the catchment. The hydro processing tools used for the catchment extraction are fill sinks, flow direction, flow accumulation, drainage network extraction and catchment merge. Each of these processing steps are discussed in detail below.

- **Fill Sink:**

The SRTM DEM data has some undefined values, cleaning of these local depressions from the DEM data is done by the fill sink operation where any pixel with a smaller height value than all of its 8 neighboring pixels is replaced by the height of the smallest value of the 8 neighboring pixels Also any group of adjacent pixels where the pixels have smaller height values than all the pixels that surround a depression will be increased to the smallest value of the pixel that is adjacent to the outlet of the depression and would discharge into the initial depression. By this fill sink process a sink/depression free DEM is created whereby for every pixel in the map a flow direction would be found towards the edges of the map.

- **Flow Direction:**

The flow direction operation determines into which neighboring pixel any water would flow from the central pixel in a sink free DEM. The flow direction is calculated for every central pixel from a group of 3 by 3 pixels by comparing the values of the central pixel with the value of its 8 neighboring pixels every time. The output map contains the various flow direction of the water from the central pixel.

- **Flow Accumulation:**

After the flow direction map has been created, the flow accumulation operation has been performed, it gets a cumulative count of the number of pixels that naturally drains into outlets, and this operation finds the drainage pattern of the terrain from the flow direction map. The flow accumulation map contains the cumulative hydrological flow values that represents the number of input pixels which contribute any water to any outlet, the outlets of the largest streams and rivers will have the largest values.

- **Stream network , stream links and stream ordering :**

The raster calculator is used to create a new raster map using the values of the flow accumulation map and a conditional function which extracts a Boolean raster basic drainage network map, the output raster map shows the basic drainage as pixels with value 'true' while all other pixels with value 'false'. This map contains the cumulative drainage count for each pixel. The stream link operation creates the stream link using the stream network and flow direction raster map as input. After this the stream ordering is done based on the Strahler method of stream ordering. From the drainage network map, the drainage network ordering operation examines all the drainage lines and locates the nodes where two or more streams converge and then it assigns a unique ID to all the streams in between these nodes and also to streams with just one node. A raster and a segment map with an attribute table

which uses the newly created ID domain is created as an output from the drainage network ordering operation.

- **Catchment extraction:**

The basin tool is used for constructing the catchment, a point map of the location of the outlet is specified a catchment will be calculated for each stream found in the output map of the drainage network ordering operation and the output map from the flow direction operation is used as a guide to locate the direction of flow. A raster, polygon and an attribute table are produced. To create sub catchments in the basin, the locations of the outlets (pour points) in the basin are specified and using the watershed tool, the sub catchments are created.

**Reclassification of Land cover maps:**

The land cover maps collected from the National soil and service Centre Bhutan as discussed in chapter 3 had 28 sub land cover classes. There are more land cover classes in this original classification than the HBV model can recognize, therefore the land cover map was reclassified into three classes as forest, non-forest and snow cover to be used as inputs to HBV Model. From the original land cover map, the land cover of the catchment was extracted using extract by mask function in Arc GIS and then applying the reclassify function was reclassified into forest non-forest and snow cover classes as shown in figure21 below. After the reclassification the areal percentage of each land cover type in each sub catchment in the study area was calculated. The basin has 84.7% of the area as forest, 6.2% as non-forested land and 9 % as snow covered area.

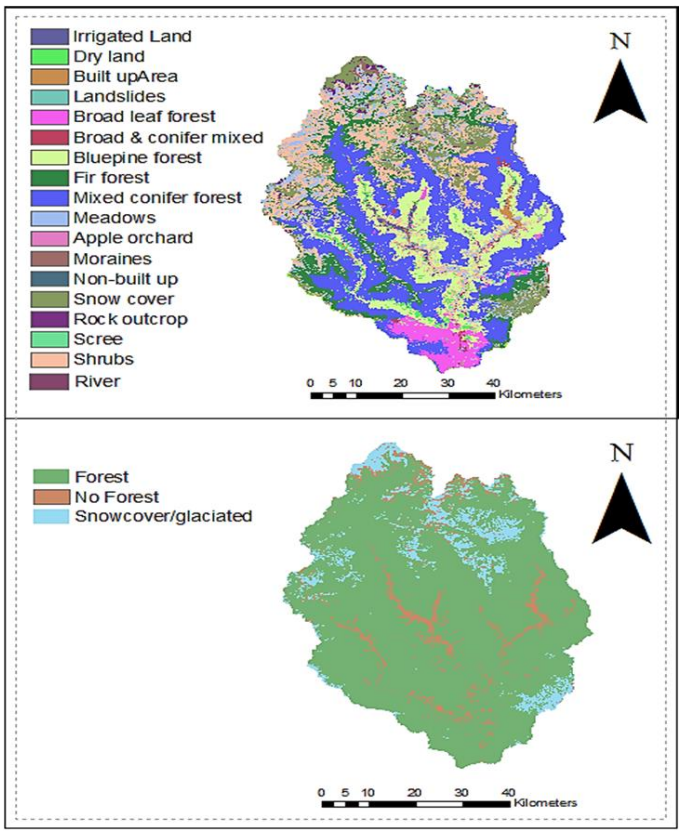


Figure 19: Land cover maps with all land covers and reclassified land cover map with 3 land covers

**Preparation of elevation zones:**

As the input to the HBV model the catchment needs to be divided into elevation zones, using the raster cross function in ILWIS, the raster map of the extracted catchment is crossed with the DEM to determine the elevation zone in each catchment. The catchment was divided into 19 elevation zones. To calculate the fraction of land cover for every elevation zone the reclassified land cover map with three land cover classes was resampled to the spatial resolution of the DEM and the extracted catchment area raster maps and then the land cover map was crossed with the elevation zone raster map. The fraction land cover for every elevation zone in each sub catchment is needed as an input to HBV model, this information is used in the soil moisture routine of the model to estimate the amount of soil moisture by having the correct elevation and land cover.

### 5.2.3. Processing of meteorological data forcing's for application in the HBV-96 Model:

Rainfall, temperature and potential evapotranspiration data are the meteorological data forcing's used in the HBV model. Since the ground measurement stations are point data, they are not representative of the whole basin, therefore to cover the entire basin area thiessen polygons have been used to calculate station weights in each sub catchment to obtain the areal average values of temperature, potential evaporation and precipitation in that particular basin.

### 5.2.4. Model calibration and validation:

**Model Calibration:**

Model calibration is the process by which the parameters of the model are systematically adjusted or changed in order to get model outputs that closely resemble the observed data (Eckhardt & Arnold, 2001).The main aim of calibration is to reduce the uncertainty associated with the model parameters, there is a possibility of maximum uncertainty when the parameters are assigned their initial range and it improves when a single set of optimized parameters is found. HBV 96 model calibration is a manual trial and error process where the model parameters are optimized usually one at a time. This is a very tedious and time consuming procedure but it provides valuable and significant insights into parameter sensitivity and interaction.

When the model calibration is started with the default values, the simulated and the observed stream flow does not show a good match. Therefore to start the calibration process first the volume parameters are adjusted until the volume looks reasonable. Next the snow parameters which affects the accumulation and melt of snow are adjusted followed by adjusting the soil parameters and finally the response parameters. The parameter calibration is carried out until the observed stream flow matches that of the model simulated. But because of various sources of errors and uncertainties such as errors due to the meteorological forcing, initial conditions, boundary conditions, the structure of the model and other factors which contribute to the overall efficiency of the model, these two are not always a good fit.

To decide if the optimized parameter gives the best fit for the model or to adjust the parameters further, a method of criterion to determine the goodness of fit is needed. There are different objective functions used for model evaluation in streamflow modelling (Lemke et al., 2007).In the HBV 96 model the goodness of fit is tested using subjective and objective methods. The subjective methods includes studying plots of input forcing data, observed and simulated hydrographs, graphs of accumulated difference between observed and simulated runoff which helps in understanding the volumetric bias. The subjective method is helpful during the initial stages of calibration when several parameters needs to be changed simultaneously. Once the simulated and the observed hydrograph shows a reasonable fit, the

objective method is used to further fine tune the model when the parameters are almost at their optimal value.

To understand the model performance when using an objective method, statistical criterion usually the $R^2$ value according to Nash Sutcliffe (NSE) (1970) and Relative volumetric Error (RVE) are the most widely used for evaluation of hydrological uncertainties. The value of Nash Sutcliffe ,often termed as the model efficiency criterion ranges from '-∞' to +1,the higher the value the better is the model fit,R2 will have a value of 1 if the observed and the simulated values agrees completely. The model is considered to be a good performing model if the value of 'NSE'ranges from 0.8 to 0.9 and is said to be a fair performing model when the values of

'NSE' ranges from 0.6-0.8.On the other hand Relative volumetric error (RVE) is a representation of the relative volume between the simulated and the observed discharge and it assesses the mass balance error between them.. The values of RVE ranges from '- ∞ to+∞'.A good performing model will have RVE value in the range of -5% to 5 % and models with reasonable performance will result in a RVE between -5% and -10% or +5% to +10%,and the best performance will be when the value of RVE is 0 since the accumulated difference between the observed and the simulated discharge is then zero. These objective functions can be expressed mathematically as follows:

$$NSE = 1 - \frac{\sum(Q_{obs} - Q_{sim})^2}{\sum(Q_{obs} - \overline{Q_{obs}})^2} \qquad \text{Equation 23}$$

$$RVE = \frac{\sum(Q_{obs} - Q_{sim})}{\sum Q_{obs}} * 100 \qquad \text{Equation 24}$$

Where:

$Q_{obs}$: Observed stream flow at the gauge station ($m^3$/sec)

$Q_{sim}$: Simulated stream flow at the gauged station ($m^3$/sec)

$\overline{Q_{obs}}$: mean of observed stream flow at the gauge station ($m^3$/sec).

A split sample test is carried out after achieving the optimal parameter set, where by 2/3 of the available time series of forcing factors are used for calibrating the model and the remaining 1/3 for validation of the model.

Therefore for this study the calibration was performed for the years 2004-2008.

**Model Validation:**

Model validation is an important procedure in the process of modelling(Carson, 2002)(Carson, 2002)(Carson, 2002)(Carson, 2002)(Carson, 2002). After the calibration of the model, the parameters might still be over or under optimized because the model may not be accurate enough to represent the real world conditions. So to test the applicability of the optimized parameters during calibration it must be tested with an independent set of forcing variables (Carson, 2002). If the model performs well with the second set of independent forcing factor then the model is said to be validated. Model validation is carried out to check if the optimized model parameters perform as well as it did during calibration when the input forcing are changed, to ensure that the boundary conditions for algorithm development have been properly implemented and to minimize the model errors.

For this study, model validation was carried out for the Wang Chhu basin for the years 2009 and 2010 following a split sample. To check the performance during validation the above discussed objective functions were used. When the optimized parameters during the calibration were not valid during the

process of validation the model was recalibrated until the objective functions during the validation phase gave objective function values in the acceptable range thereby validating the model.

# 6. RESULTS AND DISCUSSIONS:

## 6.1. Snow cover mapping:

Daily snow cover maps for the study area was derived as mentioned in chapter 5.The total average cloud cover for the years 2007 to 2010 was calculated to be over 50%.Table 17 below gives the summary of cloud and snow cover percentages in the basin for the years 2007-2010.An average of 101 km$^2$ of the total area of the basin is covered by snow.

Table 17: Yearly snow and cloud cover percentages in the basin.

| Years | Snow cover percentage | Cloud cover percentage |
|---|---|---|
| 2007 | 3.9 | 52 |
| 2008 | 3.4 | 54.7 |
| 2009 | 2.4 | 48.2 |
| 2010 | 1.6 | 50.5 |

### 6.1.1. Correlation of snow cover percentages observed by MODIS Terra snow product to the station data:

Comparing the snow cover area with the mean temperatures measured at the stations, it can be said that the timing of the minimum temperature in the basin shows good correlation with the snow accumulation period. It can also be explained by observation that the snow cover area decreases with the increase in mean air temperatures as shown in figure 17.

### 6.1.2. Relationship between snow cover area distribution and runoff:

For the determination of spatial snow cover distribution in the basin, the basin was divided into 10 elevation zones and snow cover area percentage for each elevation zone was calculated. It was found that the maximum area of the basin was in the elevation zone 2 which ranges from 2350m to 2900m and the upper most elevation zone covered the smallest portion of the basin which always had the highest percentage of its area under snow cover. Cloud cover percentage was seen to be increasing with elevation with an average of 2% in zone 1 to about 20% in zone 10.The percentage of area covered by snow during the melt period had been calculated and plotted as in figure 22 It can be observed that when the basin was divided into elevation zones the snow cover area increases with increase in elevation with the highest elevation having the maximum area with snow cover while the lowest elevation showed lower percent of its area covered by snow.

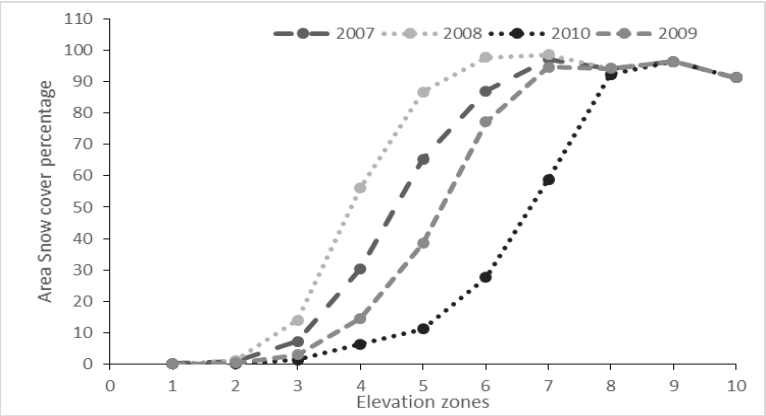


Figure 20:Snow cover per elevation zones.

For deriving relationship between the snow cover area and the runoff the study area was spatially divided into sub catchments as discussed in chapter 5.The melt season was taken into consideration for this analysis and a total of 57 images from the melt season of years 2007 to 2010 was processed and analysed. Cloud cover percentages for the melt season ranged from 0 to 54% for the entire basin with an average of 17% for the entire melt season. Average of snow cover and cloud cover for each sub catchment is summarized in table 18 and 19 below:The Paro chhu sub catchment showed the highest area of snow covered area and the Chhukha sub catchment with the lowest snow cover percentage.

Table 18: Percentage of cloud cover for the 5 sub catchments.

| | Percentage cloud cover | | | |
|---|---|---|---|---|
| Sub basin | 2007 | 20008 | 2009 | 2010 |
| Paro Chhu | 5.4 | 20.2 | 19.4 | 20.5 |
| Haa Chhu | 12.5 | 27.8 | 22.7 | 23.8 |
| Lungten Phu | 11.1 | 31.7 | 22.7 | 27.5 |
| Damchhu | 5.7 | 10.8 | 12.6 | 13.2 |
| Chhukha | 11.3 | 13.1 | 16.2 | 15.1 |

Table 19:Percentage of snow cover in the 5 sub catchments.

| | Percentage snow cover | | | |
|---|---|---|---|---|
| | 2007 | 20008 | 2009 | 2010 |
| Paro Chhu | 15.3 | 17.4 | 11.6 | 9.3 |
| Haa Chhu | 11.2 | 15.9 | 13.7 | 9.1 |
| Lungten Phu | 15.9 | 13.8 | 11.7 | 5.8 |
| Damchhu | 2.5 | 4.1 | 2.5 | 2.3 |
| Chhukha | 6.9 | 6.8 | 6.1 | 3.0 |

Snow cover depletion curves were plotted for the melt season of the years 2007 to 2010(figure 23).The snow cover area gradually decreases through spring but it can be seen that sometimes spring snow storms often result in temporary increase in the snow cover percentage.

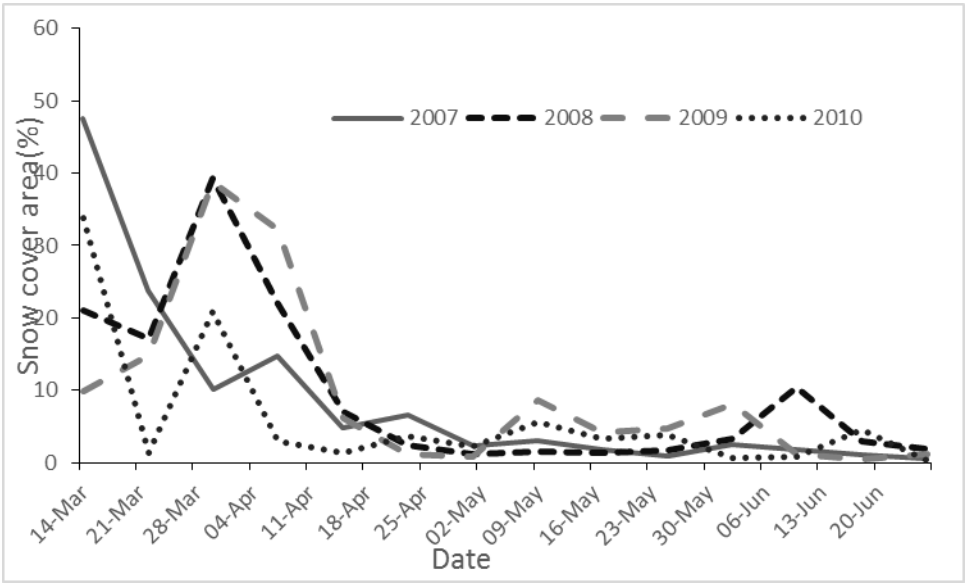


Figure 21: Snow depletion curves during the melt season for years 2007-2010.

Regression analysis between snow covered area and discharge from every sub catchment for the three year melt season resulted in a wide range of correlation strength,$R^2$ ranging from 0.02 to 0.63. The yearly sub catchment regressions of snow cover area and discharge showed lower range of correlation than the average of all the years. An example of good correlation between the snow cover area and discharge is shown in figure 24(ANNEX 4)This regression analysis shows that there is a nonlinear increase in discharge as the snow cover area depletes. The highest discharge rates cause the highest scatter in the regression relationship of snow cover area and discharge. Figure 25 shows the ranges of regression correlation strengths while comparing snow cover area and discharge in each sub catchment The strongest correlation between the snow cover area and discharge were for the Paro Chhu sub catchment with a correlation strength ranging from 0.2 to o.63 while the lowest strength of correlation between the snow cover area and the discharge was seen in Damchhu sub catchment with correlation strength ranging from 0.04 to 0.4 The strength of correlation for the sub catchments varied largely over the three years of melt period and in general it could be said that with increase in the snow cover resulted in a decrease in the stream flow .

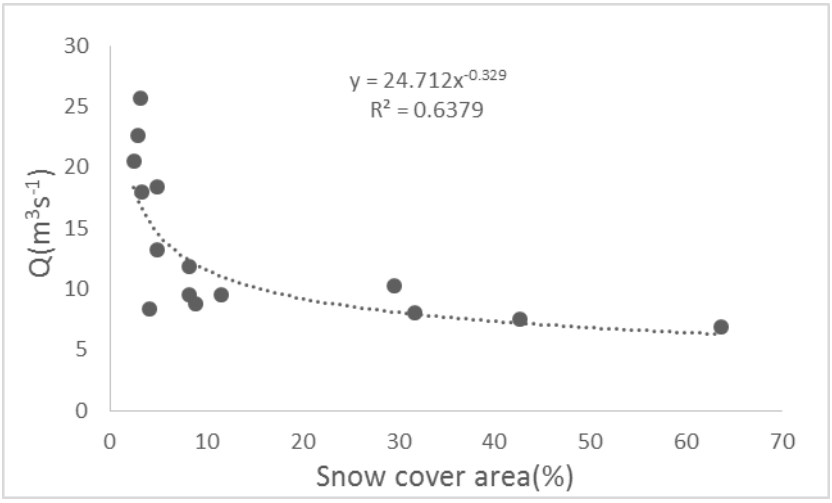


Figure 23: Regression for snow cover area vs the discharge at Paro Chhu sub catchment during 2007 melt year.

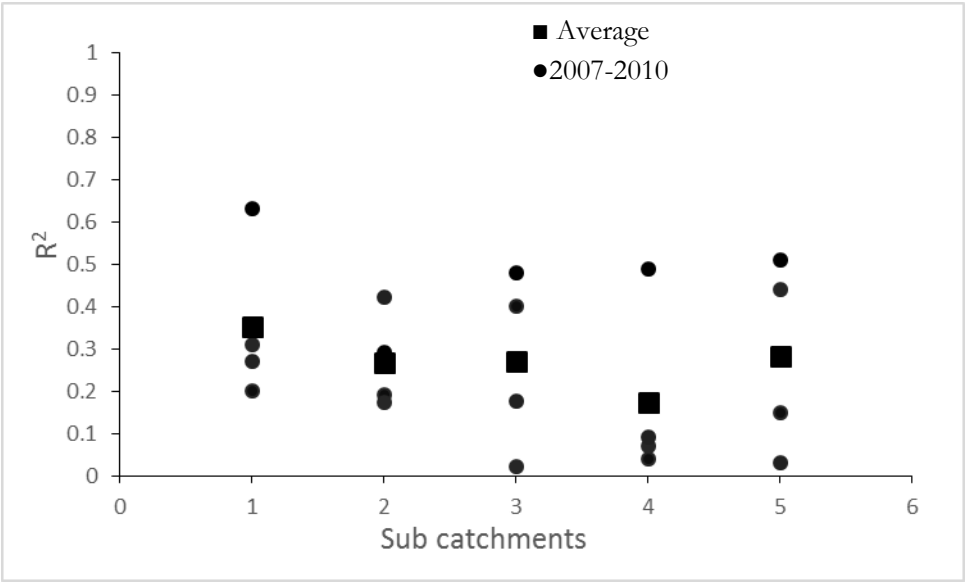


Figure 22:The correlation strength($R^2$) for snow cover area and discharge relationship for the five sub catchments.

The analyses of the snow cover area in the basin for the melt period using the 8 day MODIS Terra images were generally less affected by cloud cover as compared to the daily images. Although snow cover area is not indicative of the snow water equivalent in the basin, the snow cover area analysis was found useful for identifying the spatial and temporal patterns of snow cover in the basin. It was found out from the above analysis that the snow cover area is elevation dependant. Figure 26 shows the temporal and spatial variability of the snow cover area in the basin for the accumulation and the melt year 2007-2008.It can be observed that the snow cover area gradually increased through the accumulation period with the maximum snow cover area during the month of February after which the snow cover area gradually decreases. This trend is in agreement with the average temperature data from the basin which shows that the minimum temperature in the basin occurs during the months of January and February where it is expected that precipitation falls in the form of snow. It can be observed that cloud cover tends to increase during the summer seasons and are relatively lower during the winter months.

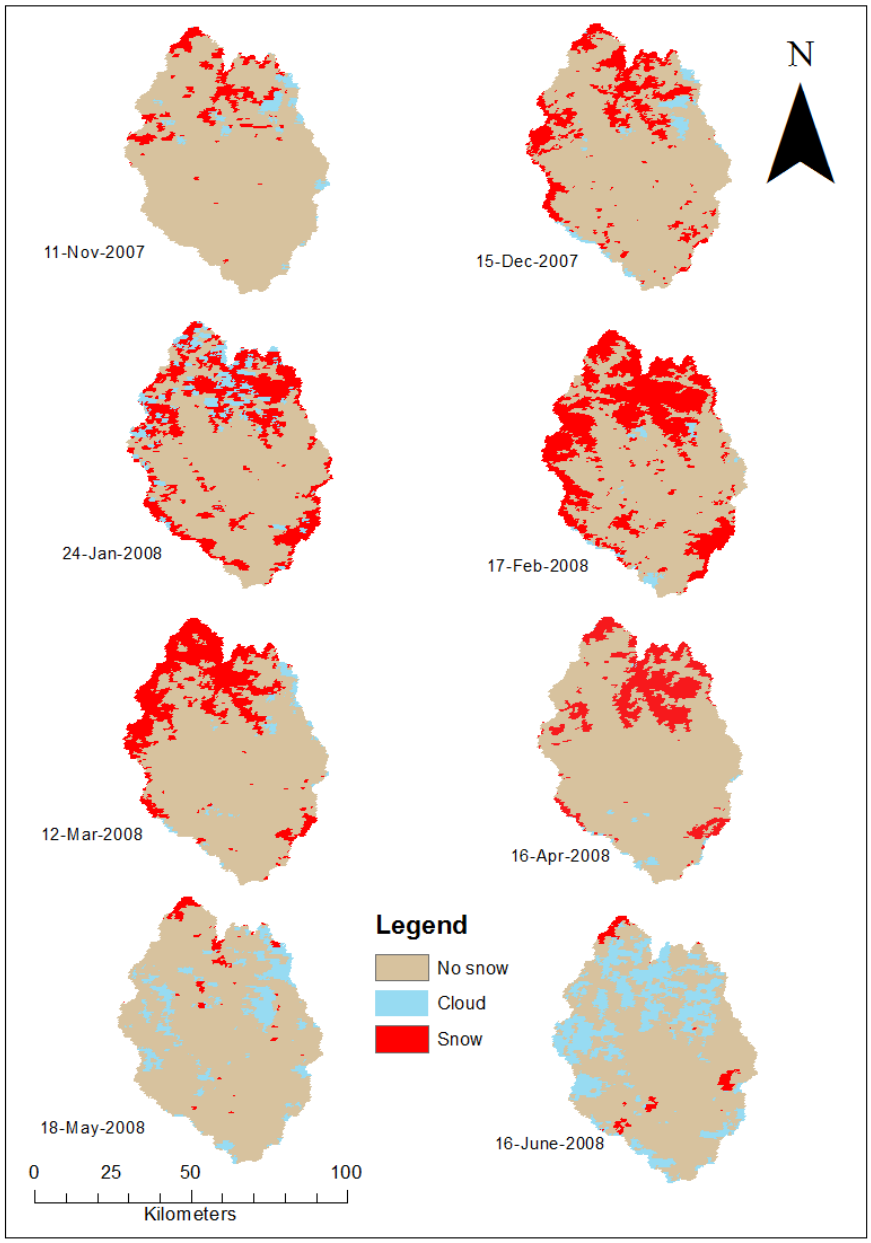


Figure 24: Spatial and temporal variation of snow cover area in the basin during the accumulation and melt year 2007-2008.

## 6.2. Results of HBV 96 Model Calibration and Validation:

**Calibration Results:**

The year 2003 was taken as the warm up period of the model and after warming up the model, calibration of the model was performed for the years 2004-2008.Manual calibration was carried out by trial and error changing one model parameter at a time. Model performance was evaluated by visual inspection of the goodness of fit between the simulated and the observed hydrographs and also the objective functions were taken into consideration while calibrating the model to get the best fit between the simulated and the observed hydrographs. The Nash Sutcliffe(NSE) objective function is used to evaluate the overall fit between the simulated and the observed hydrograph and the model parameters are optimized one by one until the highest possible value of NSE is achieved that happens when ,either increase or decrease in the model parameters does not bring any more changes to the NSE.

Using the rain gauge measured data as input to the model, the model parameters are optimized, and figure 25 shows the streamflow simulation results for the Wang Chhu basin .The model calibration for the years 2004 to 2008 resulted in a NSE of 0.80 which indicates a high ability of the model to simulate streamflow. Overall visually inspecting the hydrograph shape shows that the observed and the simulated hydrographs show matching pattern, the model was able to reproduce the base flow quite satisfactorily but the peaks could not be reproduced fairly(figure27) this may be caused by two main factors first one being errors in the observation during the measurement of the discharge or it could be due to uncertainties in the model. Table 20 gives the optimized parameter values used for calibrating the model with the default parameter range which was specifically for the Scandinavian conditions but the optimized parameters fell in the described range.

The snow accumulation and melt is also well represented by the model, a threshold temperature for rainfall and snowfall was set at -1°C meaning rain fall would occur as snow below -1°C temperature. The model could handle the snowfall quite fairly where it exhibited maximum snowpack in the coldest months of February and gradual decrease over the melt period.Maximum snow cover was exhibited when the temperature was at its lowest and it also agrees that during the melt phase temperature increases resulting in the decrease of the snow.(Figure 28)

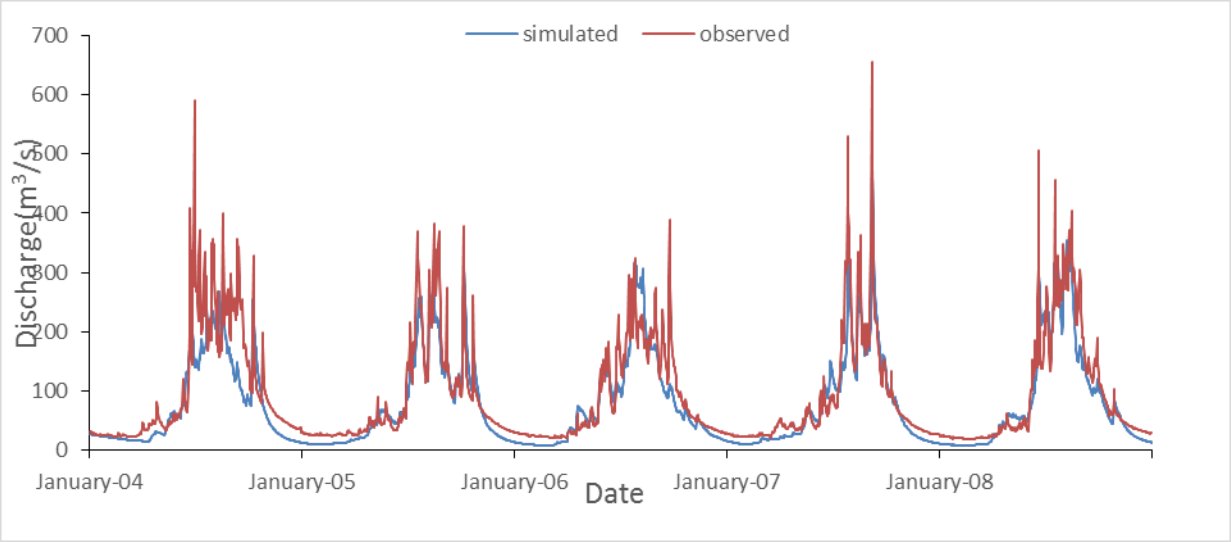


Figure 25: HBV Model calibration for the years 2004-2008.

Table 20: Optimized model parameters for the Wangchhu basin

| Model Parameters | Default Parameter range | Optimized model parameters |
|---|---|---|
| Alfa(α) | 0-1.5 | 0.9 |
| Beta(β) | 1-4 | 1.5 |
| Cflux | 0-2 | 0.1 |
| FC | 100-1500 | 400 |
| LP | <=1 | 0.9 |
| K4 | 0.001-0.1 | 0.02 |
| Khq | 0.005-0.5 | 0.015 |
| Perc | 0.1-2.5 | 1.5 |
| Gmelt | <5 | 3.5 |
| Cfmax | 2-5 | 3 |
| Sfcf | 0.7-1.4 | 1.11 |
| Rfcf | 0.8-1.3 | 0.95 |

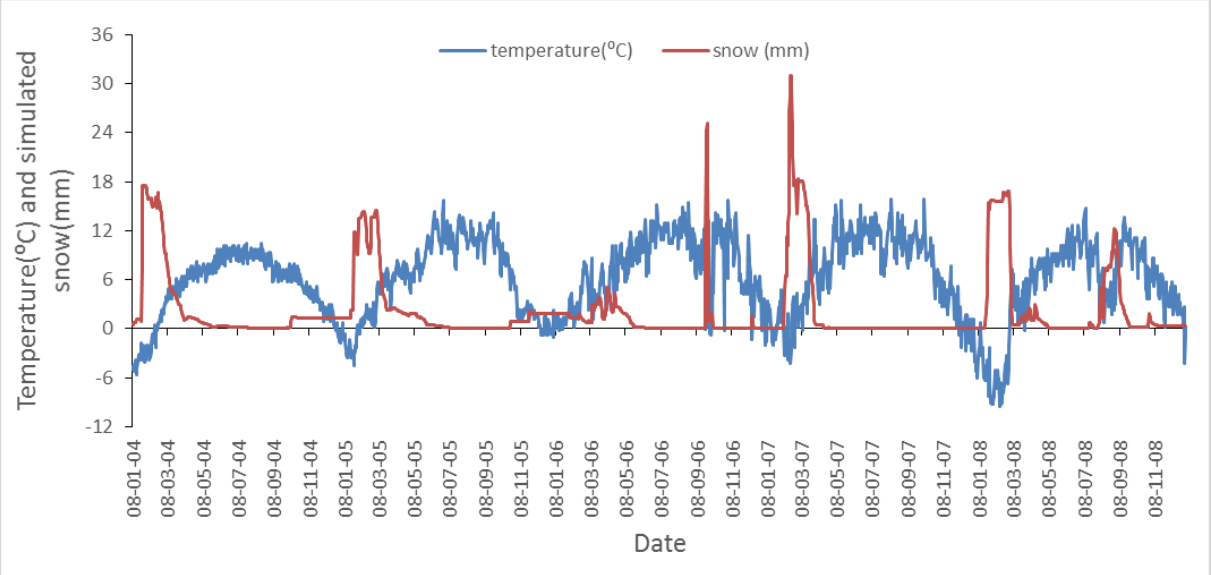


Figure 26: Comparison of the mean average temperature and simulated snow.

**Model validation results:**

After the calibration of the model, the optimized parameter set was applied to a different set of hydro meteorological dataset for the years 2009-2010.Figure 29 shows the validation process of the model of the model. It can be observed that there is a fair match between the observed and the simulated hydrographs, the base flows are represented fairly well while the peaks of the simulated hydrograph seems to be under estimating. The under and over estimation of the peaks and the recession limbs may not be entirely due to errors in the model, it may be caused by the fact that one of the stations used for the thiessen polygon weights to estimate the areal average precipitation was out of the study area and this may have caused the error .The Nash Sutcliffe model efficiency of 0.75 obtained for the validation period is lower compared to 0.80 obtained during the calibration of the model, however it still shows a satisfactory model performance.

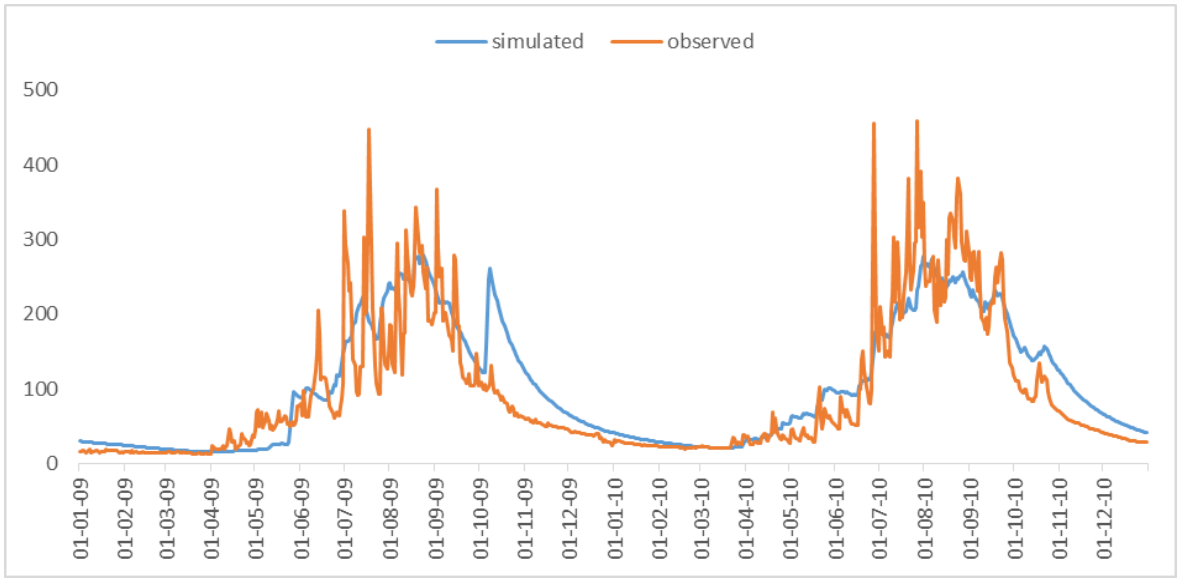


Figure 27: Model validation for the years 2009-2010.

### 6.3. Comparision of snow cover area derived from the MODIs Terra Snow Product and the HBV 96 simulated snow cover:

For checking how the MODIS derived snow cover map relates to the snow cover simulated by the model, it was found out in the earlier analysis of the MODIS snow cover maps that the snow cover maps show accumulation period starting late October with the peak of maximum snow cover area at around February and then the gradual melting phase, this temporal variability is also seen in the snow cover area simulated by the model as shown in figure 28 above .

# 7. CONCLUSIONS AND RECOMMENDATIONS

## 7.1. Conclusions:

The main objective of this research work was to access the runoff regime in the Wang Chhu basin by the methods of snow cover mapping and stream flow modelling using a semi distributed conceptual hydrological model. HBV-96 Model. This research objective will be full filled by mainly two steps, first the snow cover mapping of the study area using MODIS TERRA daily and 8 day composite products and secondly the stream flow modelling.

Remote sensing is currently the best way to monitor snow cover mainly because it is of its easy accessibility, reasonable accuracy and better spatial and temporal coverage especially in remote and inaccessible topography like in Bhutan.MODIS sensor on the Terra platform was chosen because of its easy access, good results for snow cover mapping reported from many tested basins and its temporal and spatial coverage. However the study basin being located in high altitude had high cloud cover over the study area which proved to be a challenge with MODIS being an optical sensor the cloud cover affected the snow data interpretation significantly.

Analysis were carried out during the melt and the accumulation period of snow in the basin and it was found out that the snow cover maps derived from the daily MODIS Terra product had large areas of snow cover over the study area and the cloud cover slightly improved when the 8 day composite MODIS Terra snow product was used.

Mountain snowpack's that contribute to streamflow may have high spatial variability but due to the lack of snow stations and snowpack measurement stations in the basin there is no data to determine snow spatial and temporal variability in the basin. To determine the relationship between the snow cover area and the runoff, the basin was divided into five sub catchments and snow cover area for each basin was calculated and compared with the stream flow at the outlet of each sub catchment. Regression analysis between the snow cover area and stream flow for the five sub catchments for the melt season for years 2007 to 2010 was carried out. The strength of correlation among the snow cover area and the stream flow varied hugely with,$R^2$ values ranging from 0.01 to 0.63,even though the strength of correlation was not conclusive, the general trend showed that with increase in snow cover area over time resulted in slight decrease in the streamflow.

Analysis of the snow cover distribution for the high range of elevation in the basin was carried out by dividing the basin into elevation zones from the lowest elevation to the highest elevation, the highest elevation zone showed the maximum percent of land area covered by snow almost throughout the year and the lowest elevation zone with the least amount of its area under snow cover. The snow cover area is altitude dependant whereby increase in elevation resulted in increase in snow cover area throughout the basin;

Snow cover depletion curves during the melt season showed that the snow cover area in the basin decreases gradually throughout spring but were sometimes affected by spring snow storms which often resulted in increase of the snow cover percentages.

The comparison of the snow cover maps derived from MODIS Terra satellite and the simulated snow cover by the model both shows the correct time of snow accumulation and melt in the basin.

## 7.2. Recommendations:

- The MODIS Terra images were highly affected by cloud cover for the study area, for future studies combination of the Aqua and Terra snow products could be considered which may help in reducing the cloud cover over the study area.

- The MODIS snow cover maps cannot be used for quantifying the snow melt, it can only be used for spatial and temporal snow cover patterns and for qualitative analyses, other snow water equivalent products may be used for quantitative studies.

- The HBV-96 Model proves to be a powerful tool in simulating the stream flow in the study basin so it might be useful in snowmelt runoff modelling in other similar mountainous basins in Bhutan which have the same physical characteristics.

- 

- Installation of hydro meteorological stations in the higher elevation in the basin can be useful for future snow and hydrological modelling studies where by there is better representation of the basin.

# REFERENCES


Ageta, Y., Iwata, S., Yabuki, H., & Naito, N. (2000). Expansion of glacier lakes in recent decades in the Bhutan Himalayas. *IAHS …*, (264). Retrieved from http://books.google.com/books?hl=en&lr=&id=ghn8LV2CZ20C&oi=fnd&pg=PA165&dq=Expansion+of+glacier+lakes+in+recent+decades+in+the+Bhutan+Himalayas&ots=RtmEBeSMI4&sig=lIfOzxb5N-Ocjgr-5ACe7joK-AY

Allen, R., Pereira, L. S., Raes, D., & Smith, M. (1998). Crop evapotranspiration: Guidelines for computing crop requirements. *Irrigation and Drainage Paper No. 56, FAO*, (56), 300. doi:10.1016/j.eja.2010.12.001

Basist, A., Garrett, D., Ferraro, R., Grody, N., & Mitchell, K. (1996). A Comparison between Snow Cover Products Derived from Visible and Microwave Satellite Observation. *Journal of Applied Meteorology*, *35*(2), 163–177. doi:10.1175/1520-0450(1996)035<0163:ACBSCP>2.0.CO;2

Beldring, S., & VoksØ, A. (2012). Climate Change Impact on Flow Regimes of Rivers in Bhutan and Possible Consequences for Hydropower Development. *Hydro Nepal: Journal of Water, Energy and …*. Retrieved from http://www.nepjol.info/index.php/HN/article/viewFile/7167/5795

Bergstrom, S. (1997). hydrological model, *201*, 272–288.

Beven, K. (1989). [41 changing i d e a s in h y d r o l o g y - p h y s i c a l l y - b a s e d models the case of, *105*, 157–172.

Bhutan-Water-Policy-Eng.pdf. (2007).

Bormann, H., Breuer, L., & Giertz, S. (2009). Spatially explicit versus lumped models in catchment hydrology–experiences from two case studies. … *and Consequences for …*, 3–26. Retrieved from http://link.springer.com/chapter/10.1007/978-90-481-2636-1_1

Brubaker, K. (2001). Snow and glacier hydrology. *Eos, Transactions American Geophysical Union*. doi:10.1029/01EO00355

Burnash, R. (1995). The NWS River Forecast System -- Catchment Modeling.

Carson, J. S. (2002). Model Verification and Validation. *Proceedings of the 2002 Winter Simulation Conference*, 52–58.

Chelamallu, H. P., Venkataraman, G., & Murti, M. V. R. (2013). Accuracy assessment of MODIS/Terra snow cover product for parts of Indian Himalayas. *Geocarto International*, (February 2015), 1–17. doi:10.1080/10106049.2013.819041

Chokmani, K., Bernier, M., Dever, K., Gauthier, Y., & Royer, A. (2006). Snow mapping over Eastern Canada for climate change studies purpose using historical NOAA- AVHRR and SSM / I data, 738–741.

Clyde, G. (1931). Snow melting characteristics. *Techinical Bullet*, 92–95.

Cruff, R. W., & Thompson, T. H. (1967). A Comparison of Methods of Estimating Potential Evapotranspiration From Climatological Data in Arid and Subhumid Environments. *Report*, 32.

Dai, L., Che, T., Wang, J., & Zhang, P. (2012). Snow depth and snow water equivalent estimation from AMSR-E data based on a priori snow characteristics in Xinjiang, China. *Remote Sensing of Environment*, *127*, 14–29. doi:10.1016/j.rse.2011.08.029

Denoth, A. (2003). Structural phase changes of the liquid water component in Alpine snow. *Cold Regions Science and Technology*, *37*, 227–232. doi:10.1016/S0165-232X(03)00066-1

DeSilva, R. P., Dayawansa, N. D. K., & Ratnasiri, M. D. (2007). A comparison of methods used in estimating missing rainfall data. *Journal of Agricultural Science*, *3*(May), 101–108.

Dietz, A. J., Kuenzer, C., Gessner, U., & Dech, S. (2012). Remote sensing of snow – a review of available methods. *International Journal of Remote Sensing*, *33*(13), 4094–4134. doi:10.1080/01431161.2011.640964

Division, W. M., & Services, P. (n.d.). Rapid Classification of Watersheds in the Wang Chhu Basin.

Dorothy K. Hall and Jaroslav Martinec. (1985). *Remote Sensing of Ice and Snow* (Vol. 1).

Dorothy K. Hall and Jaroslav Martinec. (1986). Remote sensing of ice and snow by Dorothy K. Hall and Jaroslav Martinec, Chapman and Hall, London, 1985. No. of pages: 189. Price: £25 (hardback). *Geological Journal*, *21*(4), 427–428. doi:10.1002/gj.3350210410

E. T. Engman and R. J. Gurney. (2000). *Remote Sensing in Hydrology and Water Management*. (G. A. Schultz & E. T. Engman, Eds.) (pp. 85–102). Berlin, Heidelberg: Springer Berlin Heidelberg. doi:10.1007/978-3-642-59583-7

Eamer, J., & Prestrud, P. (2007). *Global outlook for ice and snow*. *New York* (Vol. 27, p. 238). doi:10.1111/j.1751-8369.2008.00046.x

Eckhardt, K., & Arnold, J. G. (2001). Automatic calibration of a distributed catchment model. *Journal of Hydrology*, *251*, 103–109. doi:10.1016/S0022-1694(01)00429-2

Fernandes, R., Zhao, H., Wang, X., Key, J., Qu, X., & Hall, A. (2009). Controls on Northern Hemisphere snow albedo feedback quantified using satellite Earth observations. *Geophysical Research Letters*, *36*. doi:10.1029/2009GL040057

Franz, K. J., & Karsten, L. R. (2013). Calibration of a distributed snow model using MODIS snow covered area data. *Journal of Hydrology*, *494*, 160–175. doi:10.1016/j.jhydrol.2013.04.026

Frei, A., Tedesco, M., Lee, S., Foster, J., Hall, D. K., Kelly, R., & Robinson, D. a. (2012). A review of global satellite-derived snow products. *Advances in Space Research*, *50*(8), 1007–1029. doi:10.1016/j.asr.2011.12.021

Gao, J., Williams, M. W., Fu, X., Wang, G., & Gong, T. (2012). Spatiotemporal distribution of snow in eastern Tibet and the response to climate change. *Remote Sensing of Environment*, *121*, 1–9. doi:10.1016/j.rse.2012.01.006

Gardner, A. S., & Sharp, M. J. (2010). A review of snow and ice albedo and the development of a new physically based broadband albedo parameterization. *Journal of Geophysical Research: Earth Surface*. doi:10.1029/2009JF001444

Gelfan, A. N., Pomeroy, J. W., & Kuchment, L. S. (2004). Modeling Forest Cover Influences on Snow Accumulation, Sublimation, and Melt. *Journal of Hydrometeorology*. doi:10.1175/1525-7541(2004)005<0785:MFCIOS>2.0.CO;2

Geographica, A. U. C. (2012). Modelling snow accumulation and snowmelt runoff – present approaches and results, (2), 15–24.

Ghedira, H., Arevalo, J., Lakhankar, T., Khanbilvardi, R., & Blake, R. (2011). Snow Cover Mapping Using Satellite Remote Sensing Data, *1*(6), 37–42.

H.J. Kramer. (2002). *Observation of the Earth and Its Environment: Survey of Missions and Sensors, Third Edition*. *Eos, Transactions American Geophysical Union* (Vol. 77, p. 292). doi:10.1029/96EO00211

Hall, D. K., Riggs, G. a, Salomonson, V. V, DiGirolamo, N. E., & Bayr, K. J. (2002). MODIS snow-cover products. *Remote Sensing of Environment*, *83*(1-2), 181–194. doi:10.1016/S0034-4257(02)00095-0

Hall, D. K., & Riggs, G. A. (2007). Accuracy assessment of the MODIS snow products †, *1547*, 1534–1547. doi:10.1002/hyp

Hall, D. K., Riggs, G. A., & Salomonson, V. V. (1998). Development of Methods for Mapping Global Snow Cover Using Moderate Resolution Imaging Spectroradiometer Data, *4257*(95).

Hall, D., & Riggs, G. (2001). *Algorithm theoretical basis document (ATBD) for the MODIS snow and sea ice-mapping algorithms*. *NASA GSFC, …* (pp. 1–45). Retrieved from https://eospso.gsfc.nasa.gov/sites/default/files/atbd/atbd_mod10.pdf

Hansen, M. C., Defries, R. S., Townshend, J. R. G., & Sohlberg, R. (2000). *Global land cover classification at 1 km spatial resolution using a classification tree approach*. *International Journal of Remote Sensing* (Vol. 21, pp. 1331–1364). doi:10.1080/014311600210209

Haque, A. (2003). Estimating actual areal evapotranspiration from potential evapotranspiration using physical models based on complementary relationships and meteorological data. *Bulletin of Engineering Geology and the Environment*, *62*(1), 57–63. doi:10.1007/s10064-002-0170-5

Hock, R. (2003). Temperature index melt modelling in mountain areas. *Journal of Hydrology*, *282*(1-4), 104–115. doi:10.1016/S0022-1694(03)00257-9

Hyvärinen, O. (2006). Intercomparison of satellite products and in-situ analysis for snow.

Immerzeel, W. W., Droogers, P., de Jong, S. M., & Bierkens, M. F. P. (2009). Large-scale monitoring of snow cover and runoff simulation in Himalayan river basins using remote sensing. *Remote Sensing of Environment*, *113*(1), 40–49. doi:10.1016/j.rse.2008.08.010

*Integrated Hydrological Modelling System*. (n.d.).

Jain, S. K., Goswami, A., & Saraf, a. K. (2010). Snowmelt runoff modelling in a Himalayan basin with the aid of satellite data. *International Journal of Remote Sensing*, *31*(24), 6603–6618. doi:10.1080/01431160903433893

Jonas, T., Marty, C., & Magnusson, J. (2009). Estimating the snow water equivalent from snow depth measurements in the Swiss Alps. *Journal of Hydrology*, *378*, 161–167. doi:10.1016/j.jhydrol.2009.09.021

K.Beven, A. C. &E. M. M. (n.d.). The Institute of Hydrology Distributed Model.

Kelly, R., & Hall, D. (2008). Remote Sensing of Terrestrial Snow and Ice for Global Change Studies. *Earth Observation of Global Change*. Retrieved from http://link.springer.com/chapter/10.1007/978-1-4020-6358-9_9

Kirkbride, M. (2011). *Landscapes of glacial erosion*. doi:10.1007/978-90-481-2642-2

Ko, M., & Winther, J. (2001). MEASURING SNOW AND GLACIER ICE PROPERTIES FROM SATELLITE, (1999), 1–27.

Komori, J. (2008). Recent expansions of glacial lakes in the Bhutan Himalayas. *Quaternary International*, *184*(1), 177–186. doi:10.1016/j.quaint.2007.09.012

Kripalani, R. H., Kulkarni, A., & Sabade, S. S. (2003). Western Himalayan snow cover and Indian monsoon rainfall: A re-examination with INSAT and NCEP/NCAR data. *Theoretical and Applied Climatology*, *74*, 1–18. doi:10.1007/s00704-002-0699-z

Kulkarni, a. V., Singh, S. K., Mathur, P., & Mishra, V. D. (2006). Algorithm to monitor snow cover using AWiFS data of RESOURCESAT-1 for the Himalayan region. *International Journal of Remote Sensing*, *27*(12), 2449–2457. doi:10.1080/01431160500497820

L. Feyen, R. Vázquez, K. Christiaens, O. Sels, J. F. (n.d.). Applocation of a distributed physically based hydrological model to a medium size catchment.

Łabędzki, L., & Kanecka-Geszke, E. (2011). Estimation of Reference Evapotranspiration using the FAO Penman-Monteith Method for Climatic Conditions of Poland. … *Fao-Penman-Monteith* …. Retrieved from http://cdn.intechweb.org/pdfs/14190.pdf

Lemke, P., Ren, J., Alley, R. B., Allison, I., Carrasco, J., Flato, G., … Zhang, T. (2007). Observations: Changes in snow, ice and frozen ground. In *Climate Change 2007: The Physical Science Basis. Contribution of Working Group I to the Fourth Assessment Report of the Intergovernmental Panel on Climate Change* (pp. 337–383). doi:10.1016/j.jmb.2004.10.032

LI, H., BELDRING, S., XU, C., & JAIN, S. (2013). Modelling runoff and its components in Himalayan basins, *2014*(February), 1–7. Retrieved from http://folk.uio.no/hongli/pdf/Modelling runoff and its components in Himalayan basins.pdf

Lopez, P., Sirguey, P., Arnaud, Y., Pouyaud, B., & Chevallier, P. (2008). Snow cover monitoring in the Northern Patagonia Icefield using MODIS satellite images (2000–2006). *Global and Planetary Change*, *61*(3-4), 103–116. doi:10.1016/j.gloplacha.2007.07.005

M.B.Abbott, J.C.Bathurst, J.A.Cunge, P. E. O. &J. R. (1986). AN INTRODUCTION TO THE E U R O P E A N HYDROLOGICAL SYSTEM - - SYSTEME HYDROLOGIQUE E U R O P E E N , " SHE ", 2 : MODELLING SYSTEM The Syst ~ me Hydrologique Europ ~ en , or European Hydrological System ( SHE ), is an advanced , physically-based , distri, *87*, 61–77.

Marshall, L., Nott, D., & Sharma, A. (2005). Hydrological model selection: A Bayesian alternative. *Water Resources Research*, *41*(10), n/a–n/a. doi:10.1029/2004WR003719

Maskey, S., Uhlenbrook, S., & Ojha, S. (2011). An analysis of snow cover changes in the Himalayan region using MODIS snow products and in-situ temperature data. *Climatic Change*, *108*(1-2), 391–400. doi:10.1007/s10584-011-0181-y

MEIER, M. F. (1979). Remote sensing of snow and ice.

Mhawej, M., Faour, G., Fayad, A., & Shaban, A. (2014). Towards an enhanced method to map snow cover areas and derive snow-water equivalent in Lebanon. *Journal of Hydrology*, *513*, 274–282. doi:10.1016/j.jhydrol.2014.03.058

Mool, P., & System, I. C. for I. M. D. M. E. and N. R. I. (2001). *Inventory of glaciers, glacial lakes, and glacial lake outburst floods: monitoring and early warning systems in the Hindu Kush-Himalayan Region, Bhutan* (p. 227). International Centre for Integrated Mountain Development, Mountain Environment and Natural Resources' Information Systems. Retrieved from http://books.google.com/books?ei=7dD5U-XYJcakO-6igZAN&id=pmlNAQAAIAAJ&pgis=1

Naito, N., Suzuki, R., & Komori, J. (2012). Recent glacier shrinkages in the Lunana region, Bhutan Himalayas. *Global Environmental …*, 13–22. Retrieved from http://www.airies.or.jp/attach.php/6a6f75726e616c5f31362d31656e67/save/0/0/16_1-3.pdf

Nolin, A. W. (2010). Recent advances in remote sensing of seasonal snow. *Journal of Glaciology*, *56*(200), 1141–1150. doi:10.3189/002214311796406077

Office, B. C. S. (2006). Statistical Yearbook of Bhutan. Retrieved from http://scholar.google.com/scholar?hl=en&btnG=Search&q=intitle:Statistical+Yearbook+of+Bhutan#1

Paper, W. (2014). Perspectives for a European Satellite-based Snow Monitoring Strategy.

Parajka, J., & Blöschl, G. (2008a). Spatio-temporal combination of MODIS images - potential for snow cover mapping. *Water Resources Research*, *44*(3), n/a–n/a. doi:10.1029/2007WR006204

Parajka, J., & Blöschl, G. (2008b). The value of MODIS snow cover data in validating and calibrating conceptual hydrologic models. *Journal of Hydrology*, *358*(3-4), 240–258. doi:10.1016/j.jhydrol.2008.06.006

Paul A.Longley, Michael F.Goodchild, D. J. M. and D. W. R. (2005). *Geographic Information Systems and Science* (p. 517). John Wiley & Sons. Retrieved from https://books.google.com/books?id=-FbVI-2tSuYC&pgis=1

Pouliot, D., Latifovic, R., Zabcic, N., Guindon, L., & Olthof, I. (2014). Development and assessment of a 250m spatial resolution MODIS annual land cover time series (2000–2011) for the forest region of Canada derived from change-based updating. *Remote Sensing of Environment*, *140*, 731–743. doi:10.1016/j.rse.2013.10.004

Prasch, M., Mauser, W., & Weber, M. (2013). The Cryosphere Quantifying present and future glacier melt-water contribution to runoff in a central Himalayan river basin, 889–904. doi:10.5194/tc-7-889-2013

Rango, a. (1994). Application of remote sensing methods to hydrology and water resources. *Hydrological Sciences Journal*, *39*(4), 309–320. doi:10.1080/02626669409492752

Rango, A. (1993). II. Snow hydrology processes and remote sensing. *Hydrological Processes*, *7*, 121–138. doi:10.1002/hyp.3360070204

Rientjes, T. H. M., Muthuwatta, L. P., Bos, M. G., Booij, M. J., & Bhatti, H. a. (2013). Multi-variable calibration of a semi-distributed hydrological model using streamflow data and satellite-based evapotranspiration. *Journal of Hydrology*, *505*, 276–290. doi:10.1016/j.jhydrol.2013.10.006

Riggs, G. A., Hall, D. K., & Salomonson, V. V. (2006). MODIS Snow Products User Guide to Collection 5, *6*, 1–80.

Rikiishi, K., & Nakasato, H. (2006). Height dependence of the tendency for reduction in seasonal snow cover in the Himalaya and the Tibetan Plateau region, 1966–2001. *Annals of Glaciology*. Retrieved from http://www.ingentaconnect.com/content/igsoc/agl/2006/00000043/00000001/art00055

Rupper, S., Schaefer, J. M., Burgener, L. K., Koenig, L. S., Tsering, K., & Cook, E. R. (2012). Sensitivity and response of Bhutanese glaciers to atmospheric warming. *Geophysical Research Letters*, *39*(19), n/a–n/a. doi:10.1029/2012GL053010

Safari Shad, M., Habibnejad Roshan, M., & Ildoromi, A. (2013). Integration of the MODIS Snow Cover Produced Into Snowmelt Runoff Modeling. *Journal of the Indian Society of Remote Sensing*, *42*(1), 107–117. doi:10.1007/s12524-013-0279-y

Salomonson, V. V., & Appel, I. (2004). Estimating fractional snow cover from MODIS using the normalized difference snow index. *Remote Sensing of Environment*, *89*, 351–360. doi:10.1016/j.rse.2003.10.016

Searcy, J. K., & Hardison, C. H. (1960). Double-Mass Curves. *WaterSupply Paper 1541B*, 66. doi:http://udspace.udel.edu/handle/19716/1592

Seibert, J. (2000). Multi-criteria calibration of a conceptual runoff model using a genetic algorithm. *Hydrology and Earth System Science*. doi:10.5194/hess-4-215-2000

Seidel, K., & Martinec, J. (2004). *Remote Sensing in Snow Hydrology: Runoff Modelling, Effect of Climate Change* (p. 150). Springer Science & Business Media. Retrieved from https://books.google.com/books?id=N99MuO98gAMC&pgis=1

Sharma, V., Mishra, V. D., & Joshi, P. K. (2012). Snow cover variation and streamflow simulation in a snow-fed river basin of the Northwest Himalaya. *Journal of Mountain Science*, *9*(6), 853–868. doi:10.1007/s11629-012-2419-1

Siderius, C., Biemans, H., Wiltshire, a, Rao, S., Franssen, W. H. P., Kumar, P., … Collins, D. N. (2013). Snowmelt contributions to discharge of the Ganges. *The Science of the Total Environment*, *468-469 Su*, S93–101. doi:10.1016/j.scitotenv.2013.05.084

Sirguey, P. (2009). Monitoring Snow Cover and Modelling Catchment Discharge With Remote Sensing in the Upper Waitaki Basin , New Zealand, (December).

Snyder, J. P. (1987). Map Projections: A Working Manual. *U.S. Geological Survey Professional Paper 1395*, 154–163. doi:10.2307/1774978

Tadono, T., & Kawamoto, S. (2012). Development and validation of new glacial lake inventory in the Bhutan Himalayas using ALOS "DAICHI." *Global Environmental …*, 31–40. Retrieved from http://www.airies.or.jp/attach.php/6a6f75726e616c5f31362d31656e67/save/0/0/16_1-5.pdf

Tahir, A. A., Chevallier, P., Arnaud, Y., Neppel, L., & Ahmad, B. (2011). Modeling snowmelt-runoff under climate scenarios in the Hunza River basin, Karakoram Range, Northern Pakistan. *Journal of Hydrology*, *409*(1-2), 104–117. doi:10.1016/j.jhydrol.2011.08.035

Taylor, P., Dietz, A. J., Kuenzer, C., & Gessner, U. (n.d.). International Journal of Remote Remote sensing of snow – a review of available methods, (May 2013), 37–41.

Techel, F., & Pielmeier, C. (2011). Point observations of liquid water content in wet snow – Investigating methodical, spatial and temporal aspects. *Cryosphere*, *5*, 405–418. doi:10.5194/tc-5-405-2011

Tekeli, a. E., Akyürek, Z., Şorman, a. A., Şensoy, A., & Şorman, a. Ü. (2005). Using MODIS snow cover maps in modeling snowmelt runoff process in the eastern part of Turkey. *Remote Sensing of Environment*, *97*, 216–230. doi:10.1016/j.rse.2005.03.013

UN Water: KWIP. (n.d.). Retrieved August 06, 2014, from http://www.unwater.org/kwip

UNEP. (2007). *Global outlook for Ice & snow*.

US Department of Commerce, NOAA, N. O. and A. A. (n.d.). National Oceanic and Atmospheric Administration (NOAA) Home Page. Retrieved January 12, 2015, from http://www.noaa.gov/

Wigmosta, M., & Nijssen, B. (2002). The distributed hydrology soil vegetation model. … *Models of Small* …, 7–42. Retrieved from http://www.hydro.washington.edu/pub/lxb/asdf/Wigmostaetal.2002.pdf

Wilson, W. (1941). An outline of the thermodynamics of snowmelt. *Trans. AGU, 182-195.*, *23*, 2293–2306. doi:10.1175/2009JCLI2951.1

Yang, C., Zhao, Z., Ni, J., Ren, X., & Wang, Q. (2012). Temporal and spatial analysis of changes in snow cover in western Sichuan based on MODIS images. *Science China Earth Sciences*, *55*(8), 1329–1335. doi:10.1007/s11430-011-4336-5

Yerdelen, C. (2005). Study on prediction of snowmelt using energy balance equations and comparing with regression method in the Eastern part of Turkey, *64*(July), 520–528.

Yu, Z. (2002). Modeling and Prediction, 1–8. doi:10.1006/rwas.2002.0172

# APPENDICES:

ANNEX 1:Daily time series of cloud and snow cover derived from modis terra snow products for years 2003-2010

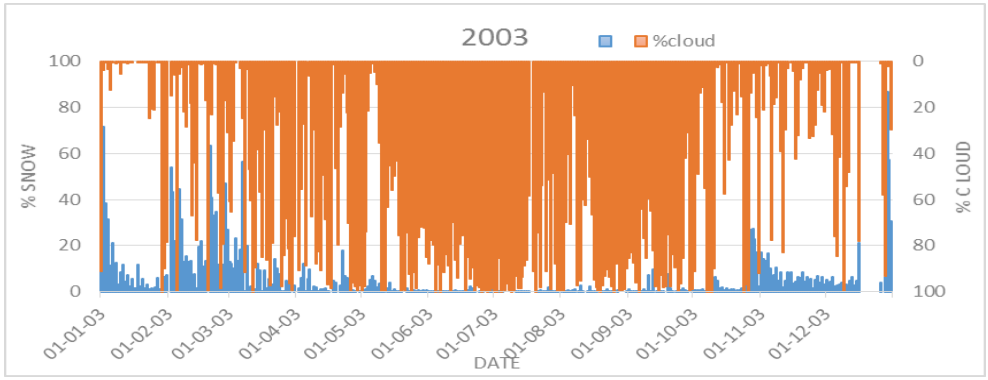


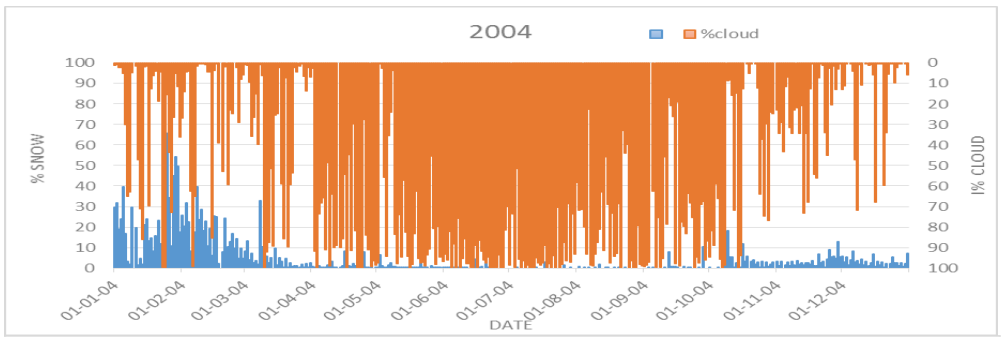


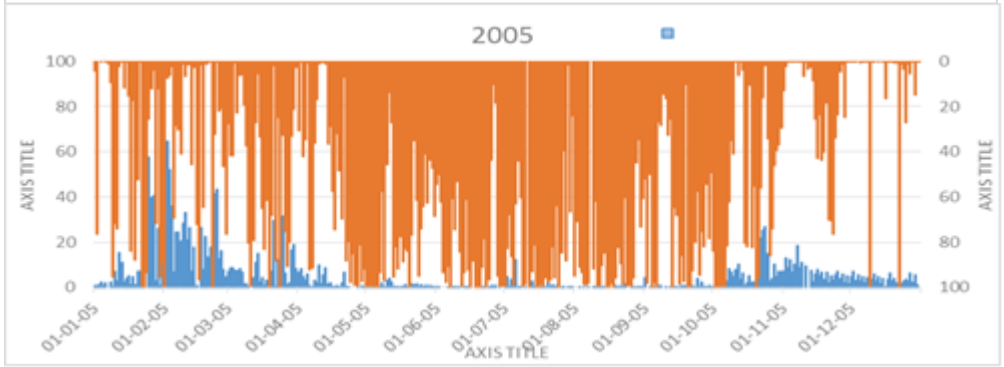


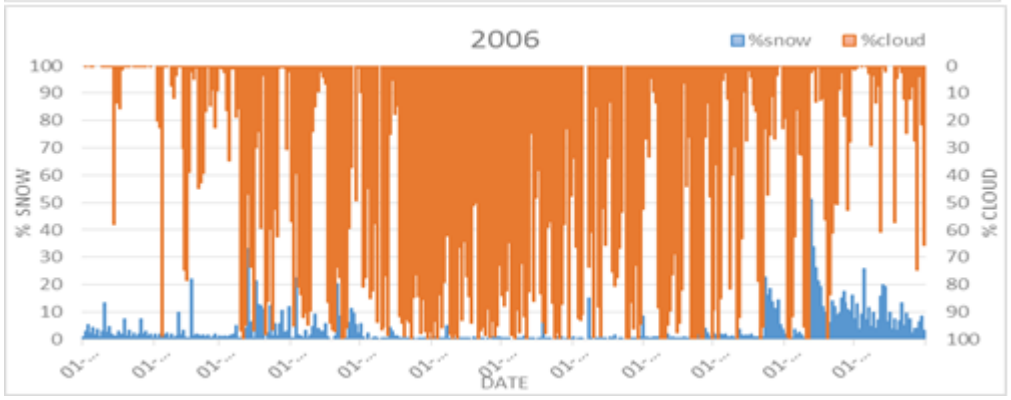

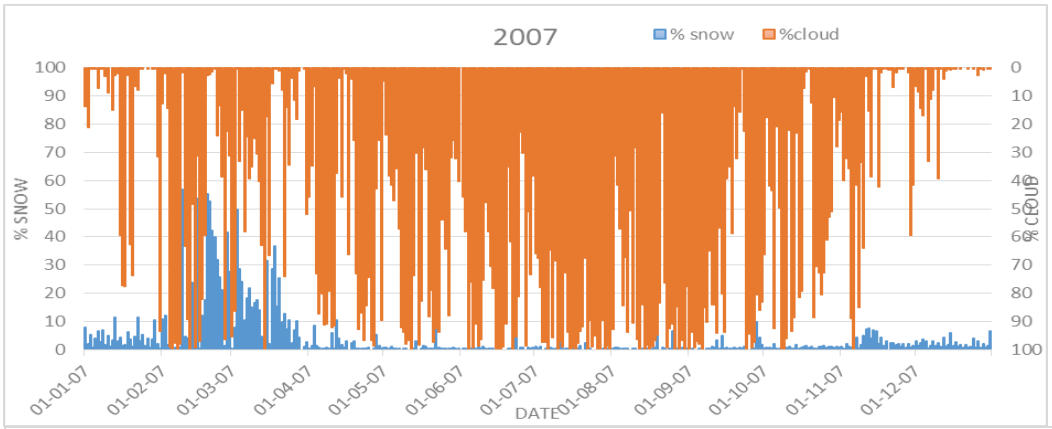
2007
% snow
%cloud
% SNOW
% CLOUD
DATE
01-01-07
01-02-07
01-03-07
01-04-07
01-05-07
01-06-07
01-07-07
01-08-07
01-09-07
01-10-07
01-11-07
01-12-07

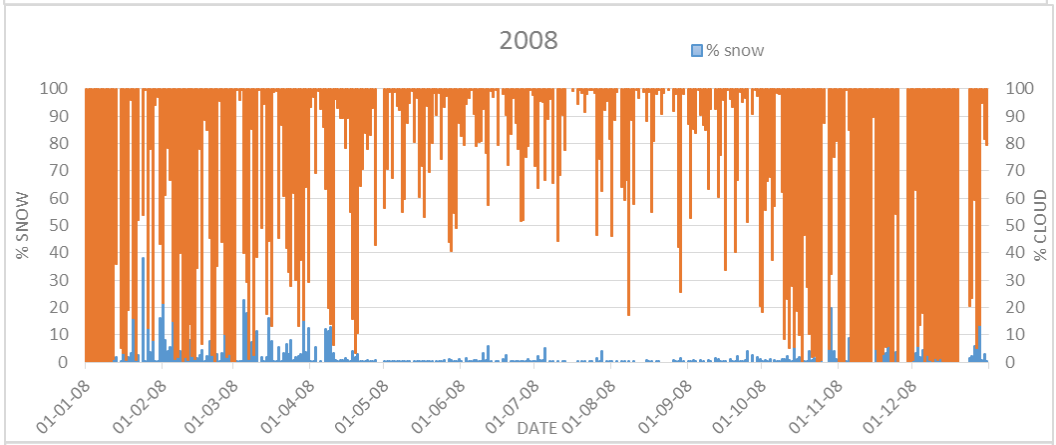
2008
% snow
% SNOW
% CLOUD
DATE
01-01-08
01-02-08
01-03-08
01-04-08
01-05-08
01-06-08
01-07-08
01-08-08
01-09-08
01-10-08
01-11-08
01-12-08

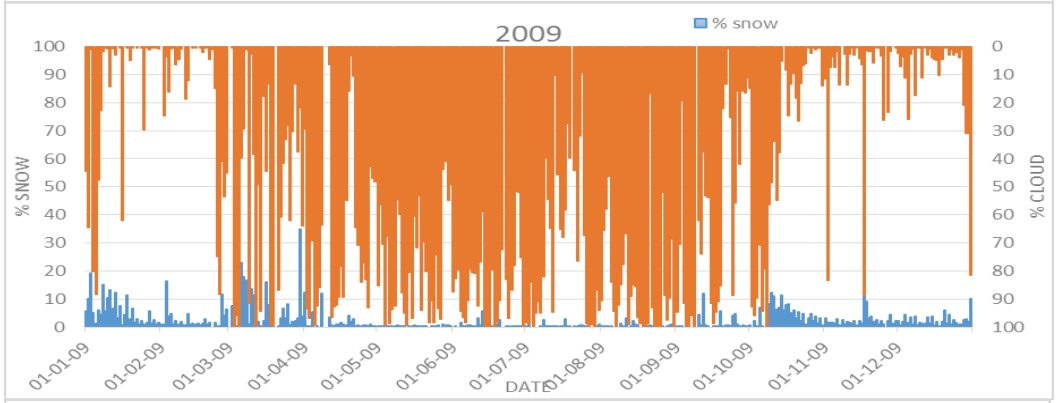
2009
% snow
% SNOW
% CLOUD
DATE
01-01-09
01-02-09
01-03-09
01-04-09
01-05-09
01-06-09
01-07-09
01-08-09
01-09-09
01-10-09
01-11-09
01-12-09

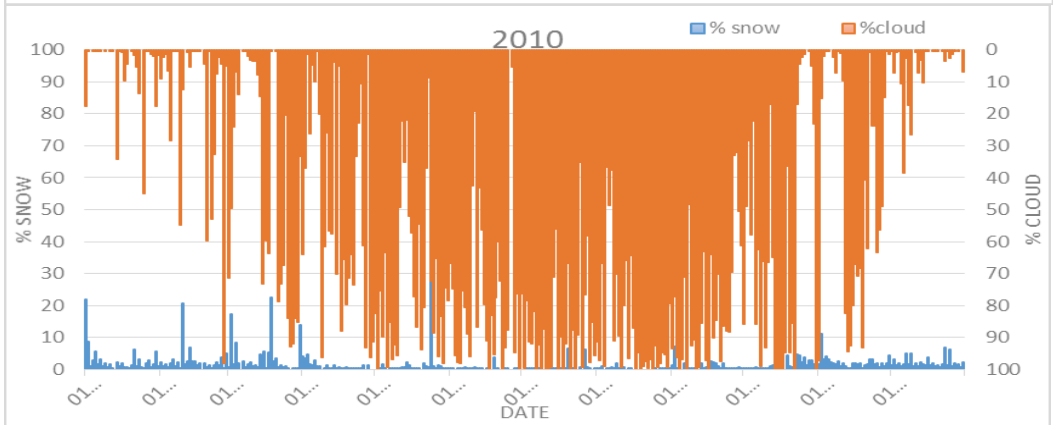
2010
% snow
%cloud
% SNOW
% CLOUD
DATE

ANNEX 2 :Pixel value of station Drugyel extracred from the MODIS snow procuct,200 is the pixel value of snow,50 for cloud 25 for land and other unclassiefied are 0.

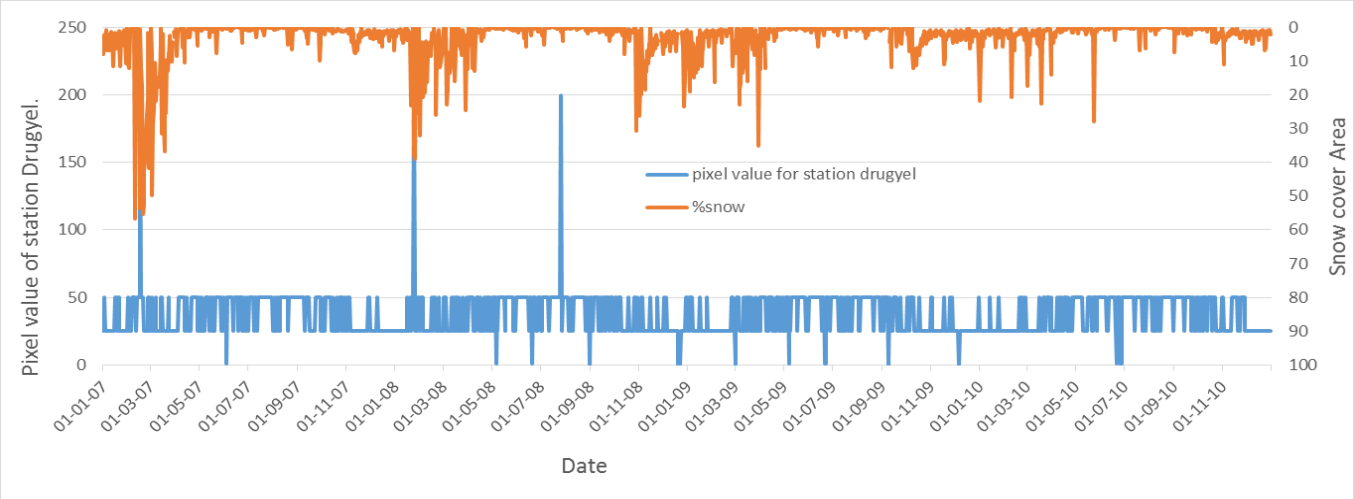

ANNEX 3:double mass curves frot the stations in the basin.

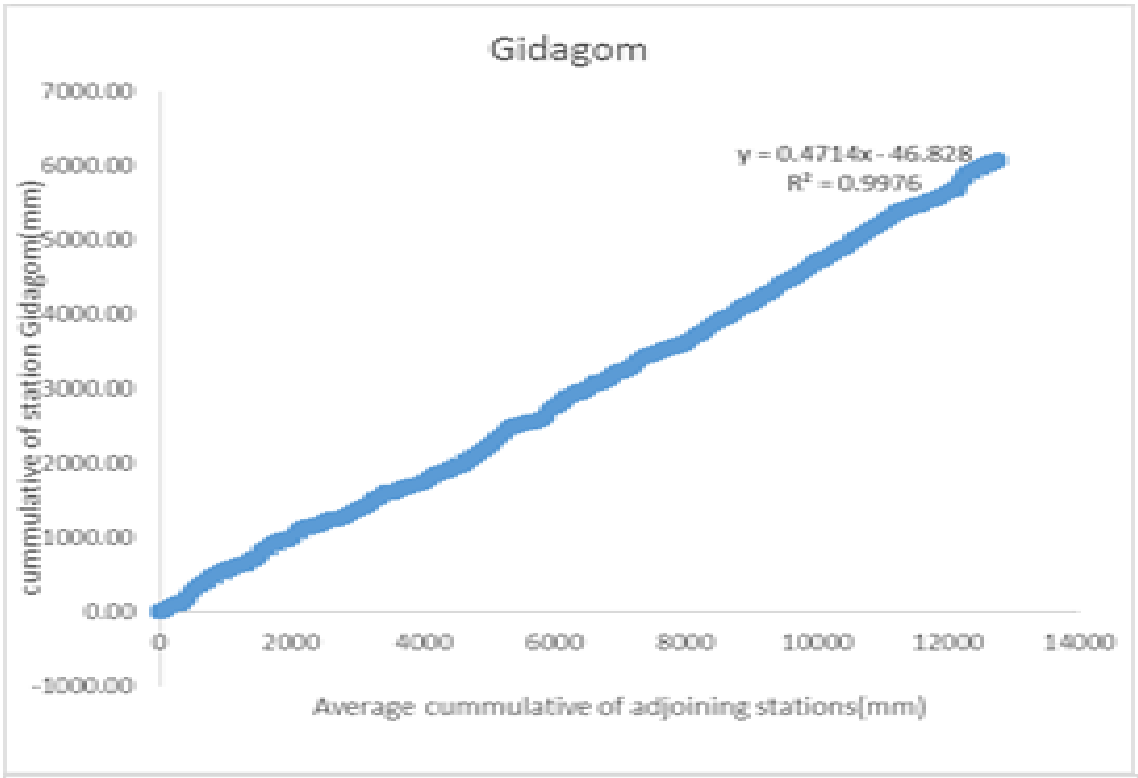


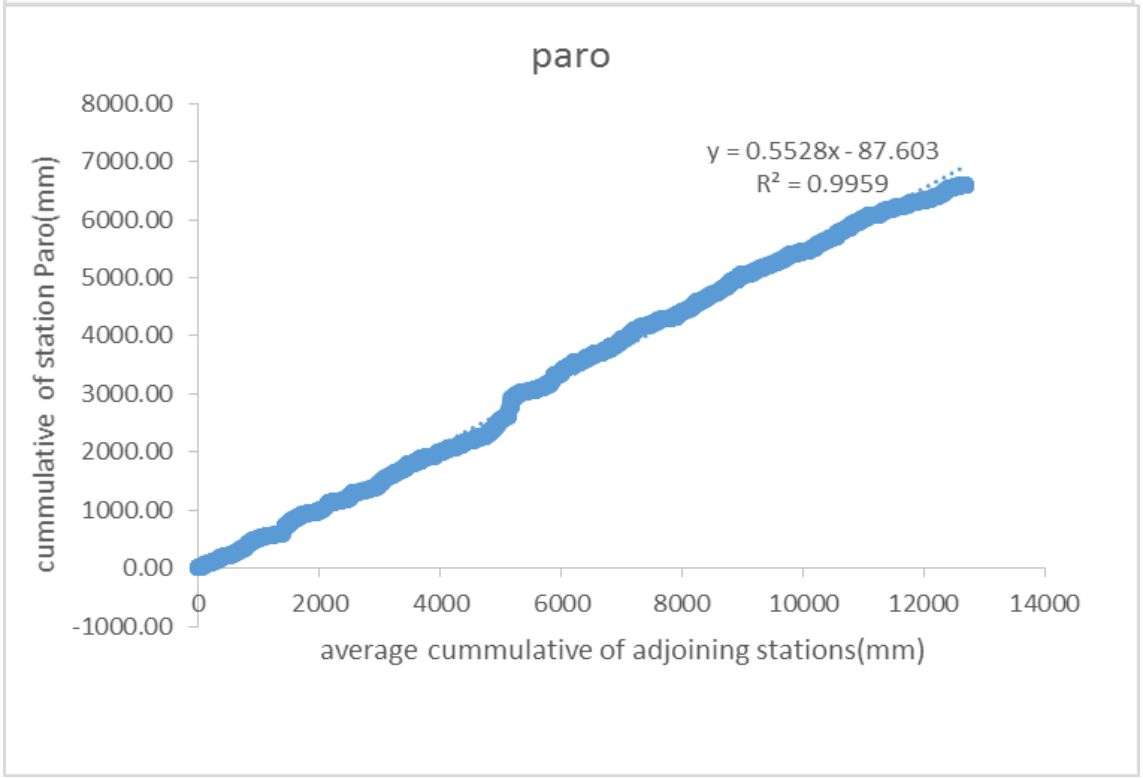

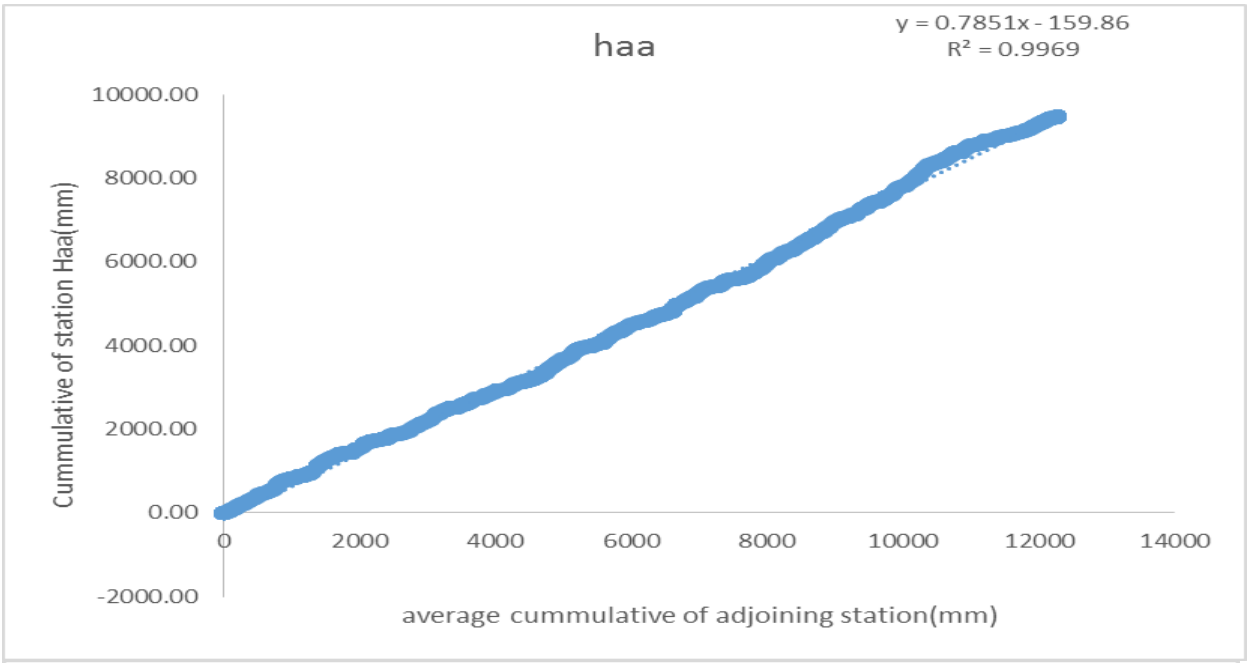
haa
y = 0.7851x - 159.86
R² = 0.9969
10000.00
8000.00
6000.00
4000.00
2000.00
0.00
-2000.00
Cummulative of station Haa(mm)
0
2000
4000
6000
8000
10000
12000
14000
average cummulative of adjoining station(mm)

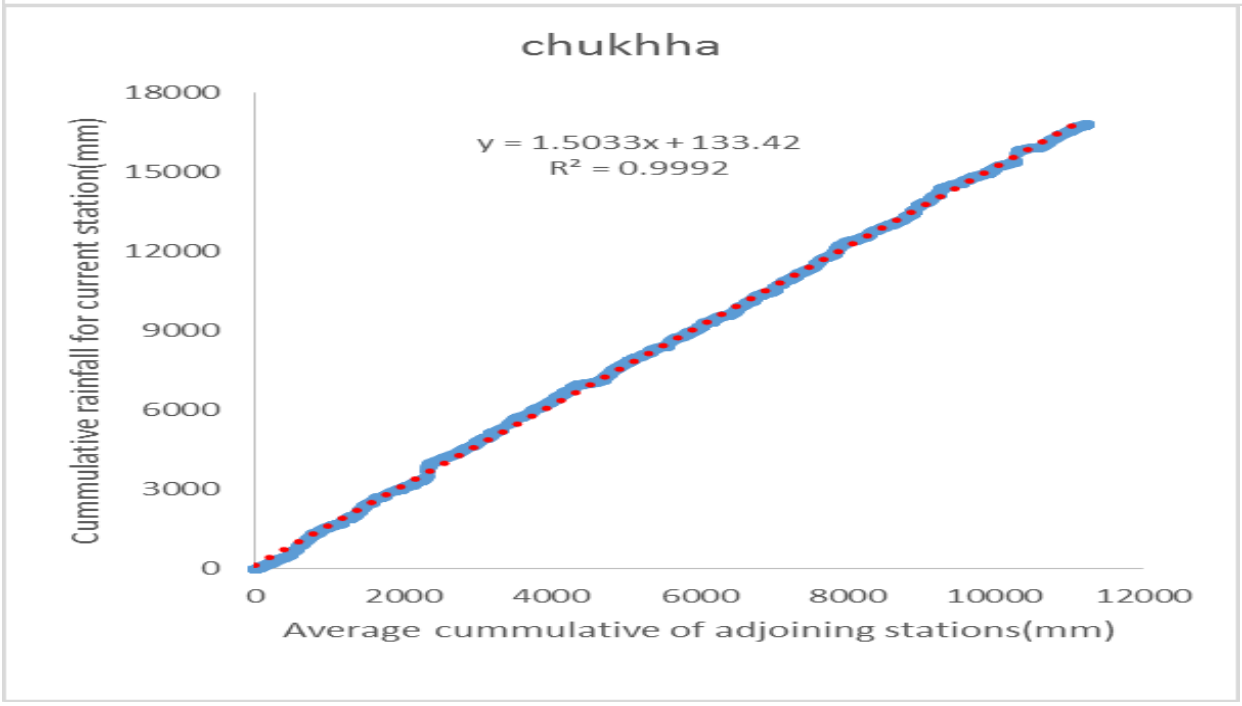
chukhha
y = 1.5033x + 133.42
R² = 0.9992
18000
15000
12000
9000
6000
3000
0
Cummulative rainfall for current station(mm)
0
2000
4000
6000
8000
10000
12000
Average cummulative of adjoining stations(mm)

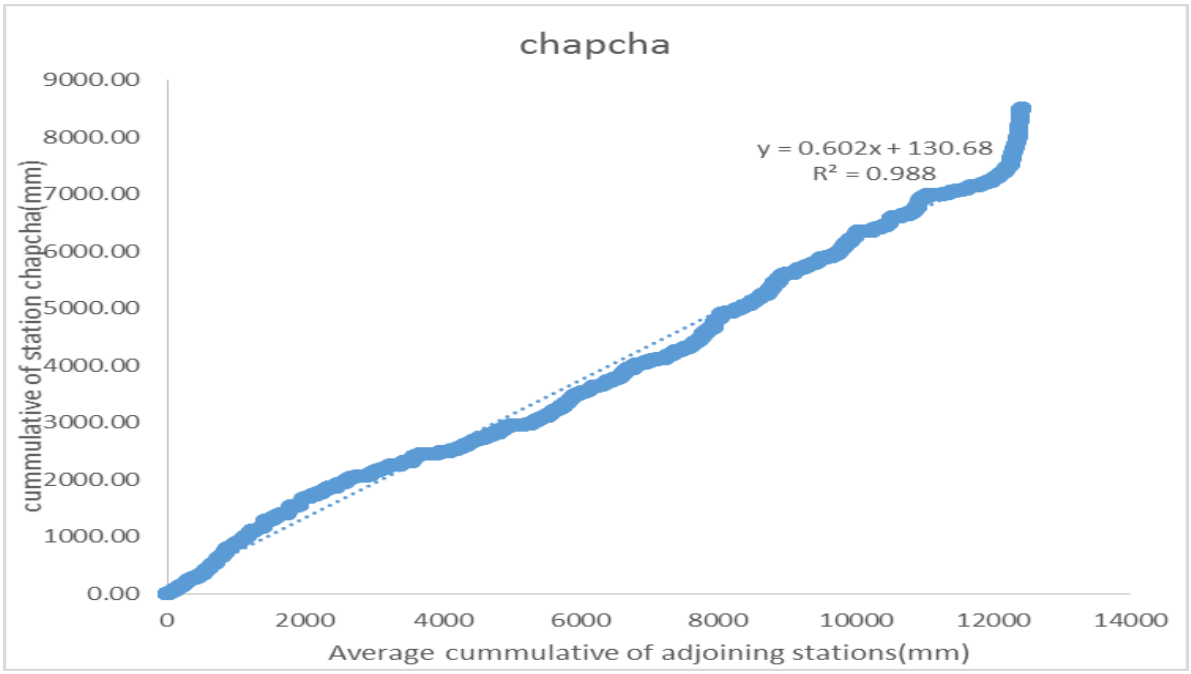
chapcha
y = 0.602x + 130.68
R² = 0.988
cummulative of station chapcha(mm)
9000.00
8000.00
7000.00
6000.00
5000.00
4000.00
3000.00
2000.00
1000.00
0.00
0
2000
4000
6000
8000
10000
12000
14000
Average cummulative of adjoining stations(mm)

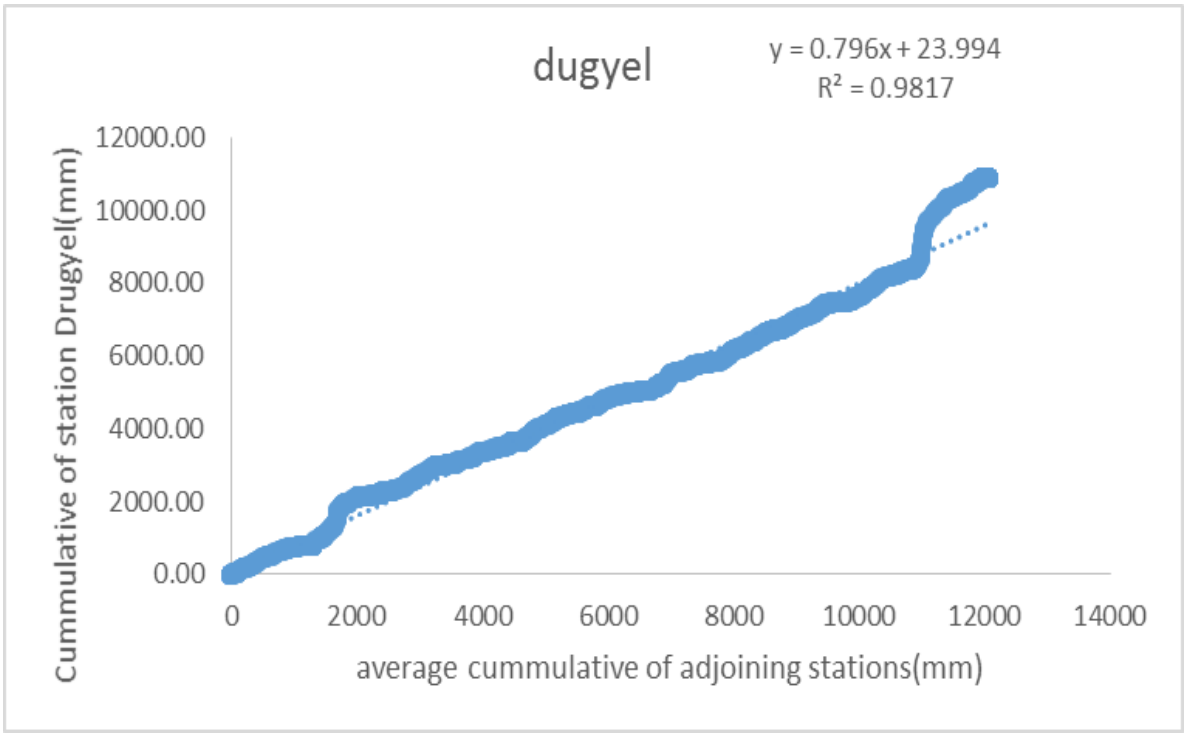
dugyel
y = 0.796x + 23.994
R² = 0.9817
Cummulative of station Drugyel(mm)
12000.00
10000.00
8000.00
6000.00
4000.00
2000.00
0.00
0
2000
4000
6000
8000
10000
12000
14000
average cummulative of adjoining stations(mm)

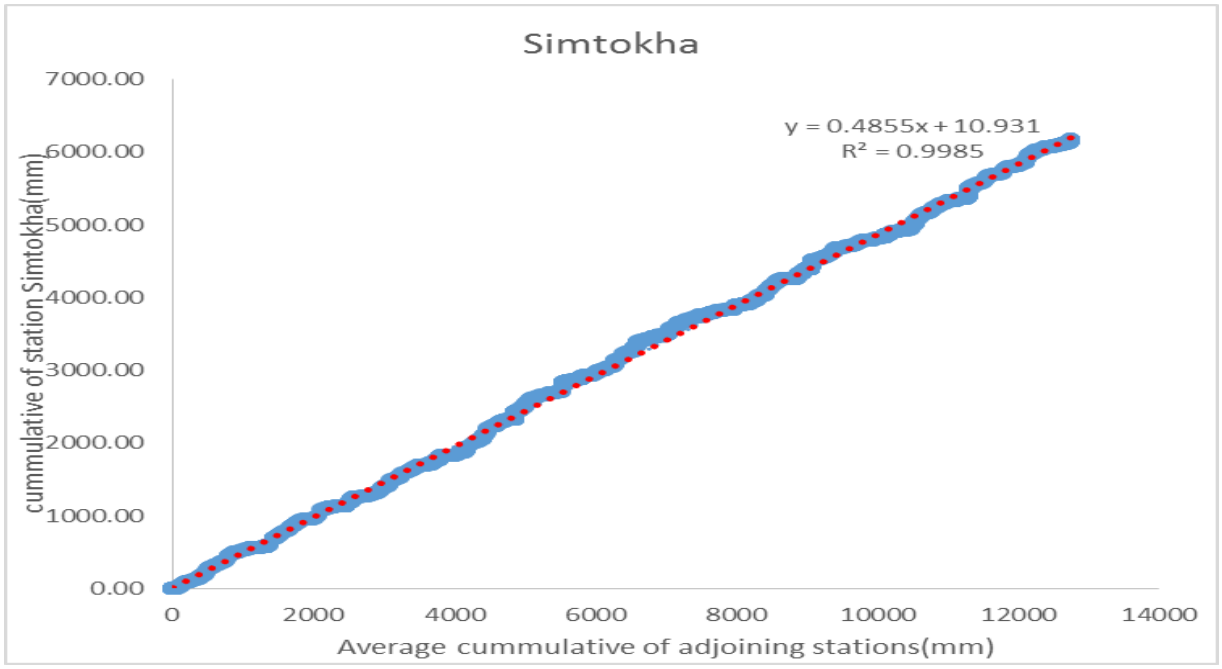
Simtokha
y = 0.4855x + 10.931
R² = 0.9985
cummulative of station Simtokha(mm)
7000.00
6000.00
5000.00
4000.00
3000.00
2000.00
1000.00
0.00
0
2000
4000
6000
8000
10000
12000
14000
Average cummulative of adjoining stations(mm)

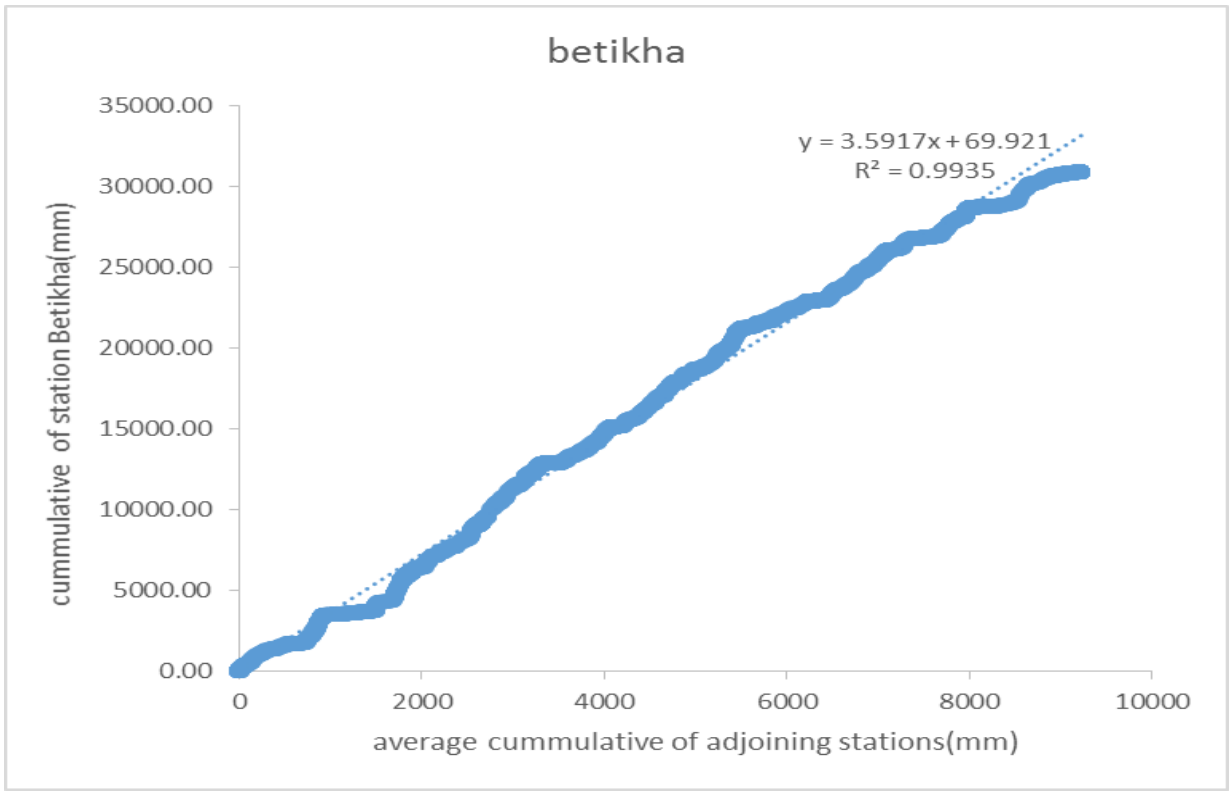
betikha
y = 3.5917x + 69.921
R² = 0.9935
cummulative of station Betikha(mm)
35000.00
30000.00
25000.00
20000.00
15000.00
10000.00
5000.00
0.00
0
2000
4000
6000
8000
10000
average cummulative of adjoining stations(mm)

Annex 4:Regression analysisfor snow cover area and streamflow for all five subcatchments in the basin for the melt season 2007-2010.

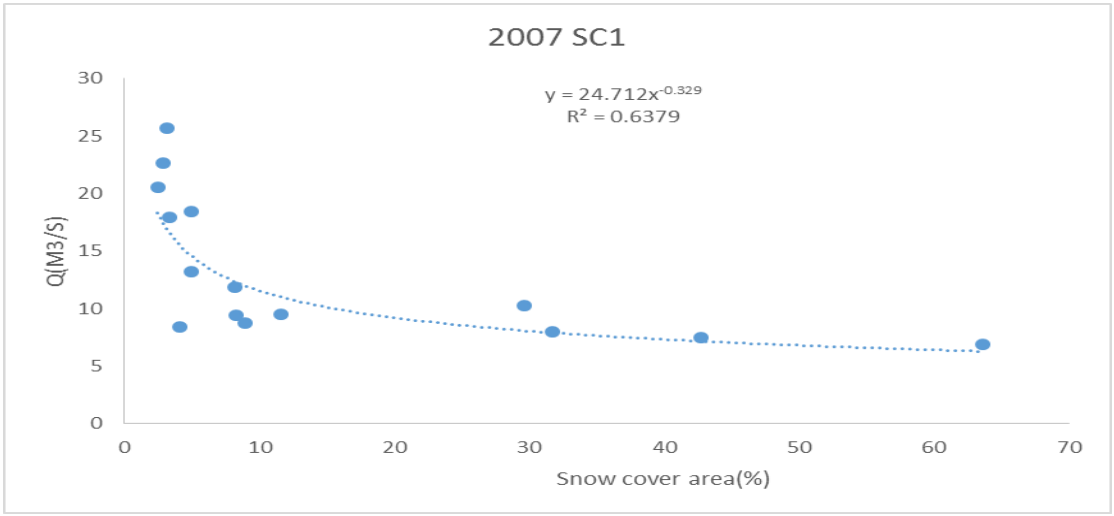


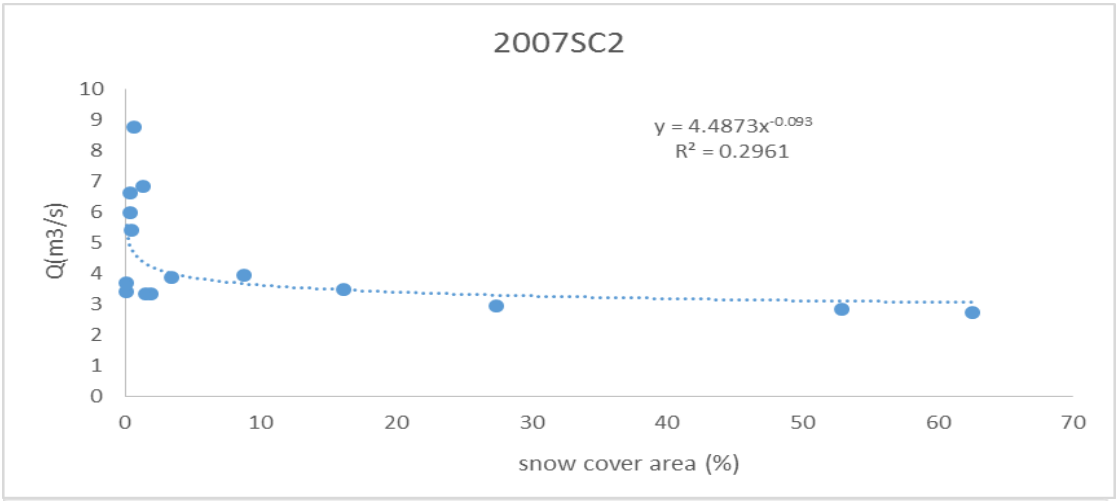


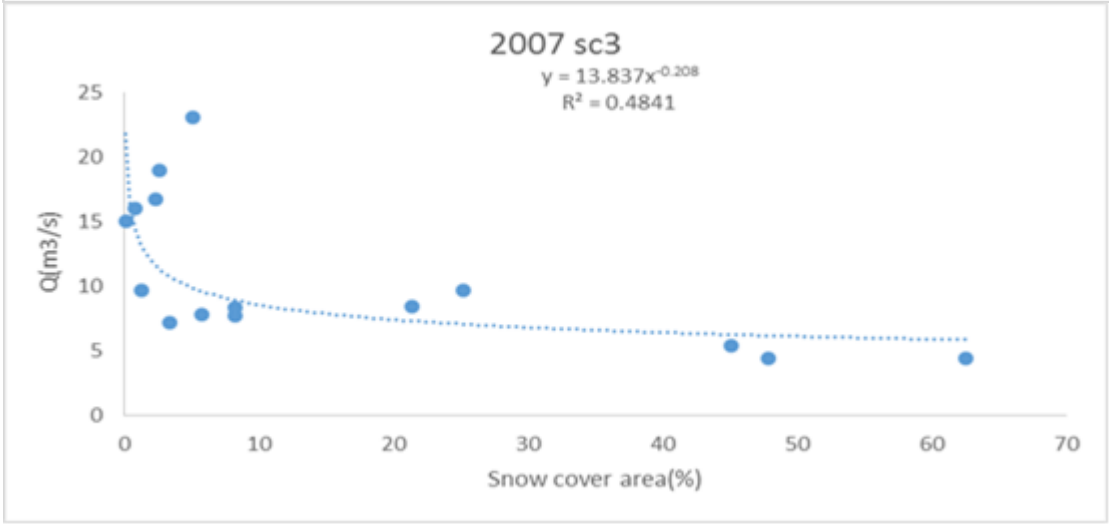

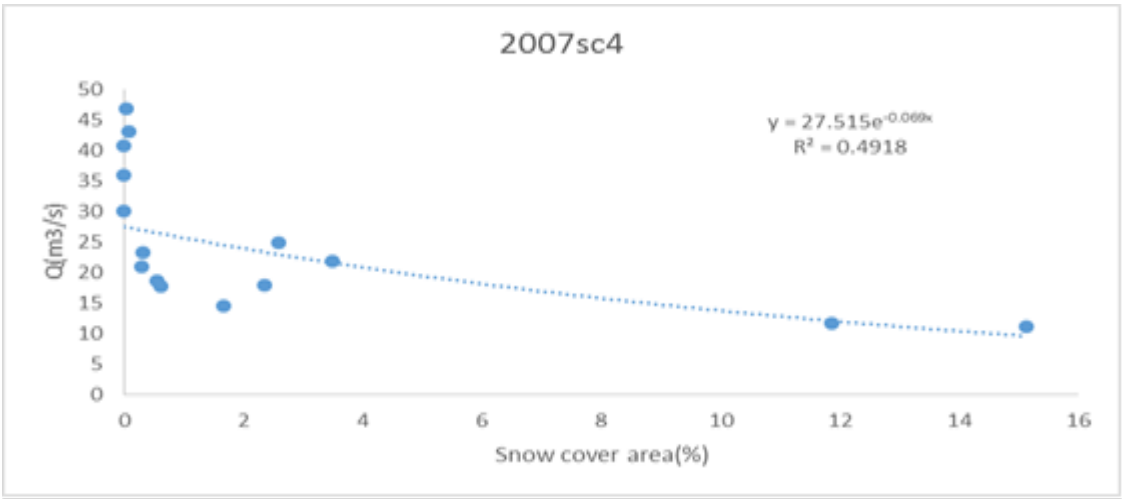
2007sc4
y = 27.515e-0.069x
R² = 0.4918
Q(m3/s)
Snow cover area(%)
0
5
10
15
20
25
30
35
40
45
50
0
2
4
6
8
10
12
14
16

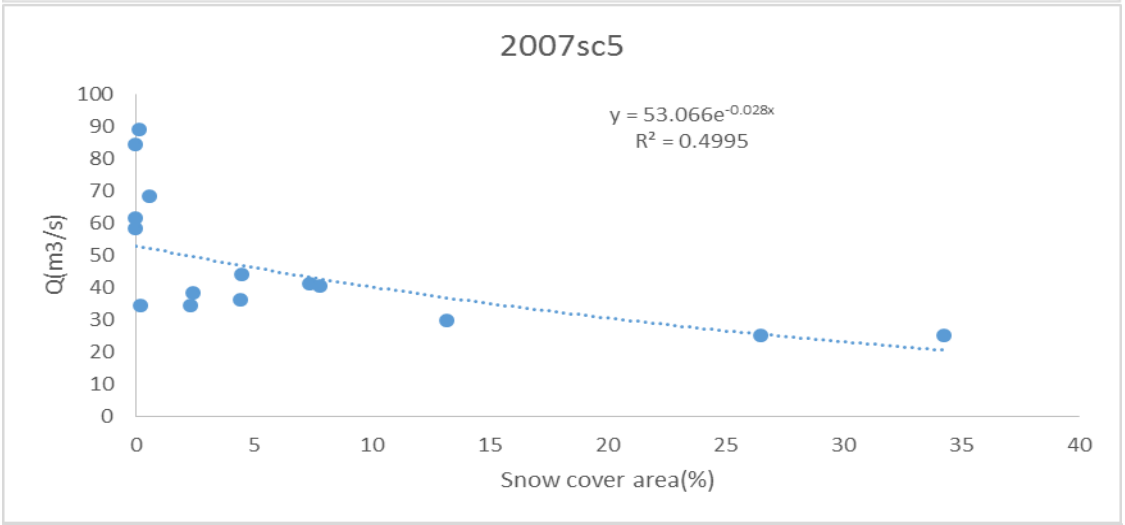
2007sc5
y = 53.066e-0.028x
R² = 0.4995
Q(m3/s)
Snow cover area(%)
0
10
20
30
40
50
60
70
80
90
100
0
5
10
15
20
25
30
35
40

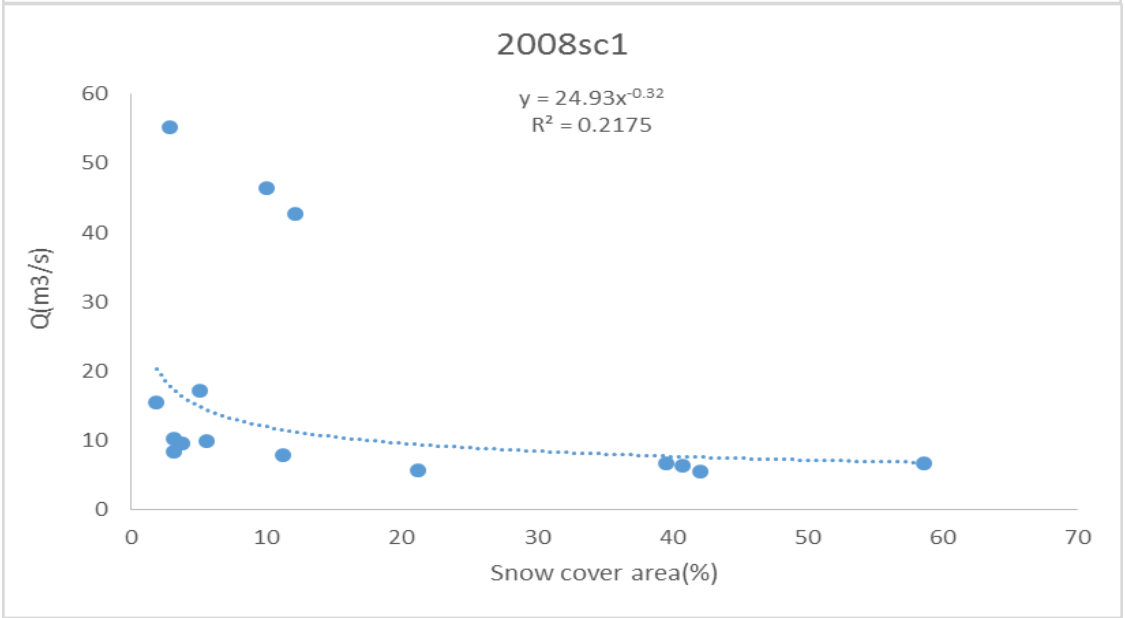
2008sc1
y = 24.93x-0.32
R² = 0.2175
Q(m3/s)
Snow cover area(%)
0
10
20
30
40
50
60
0
10
20
30
40
50
60
70

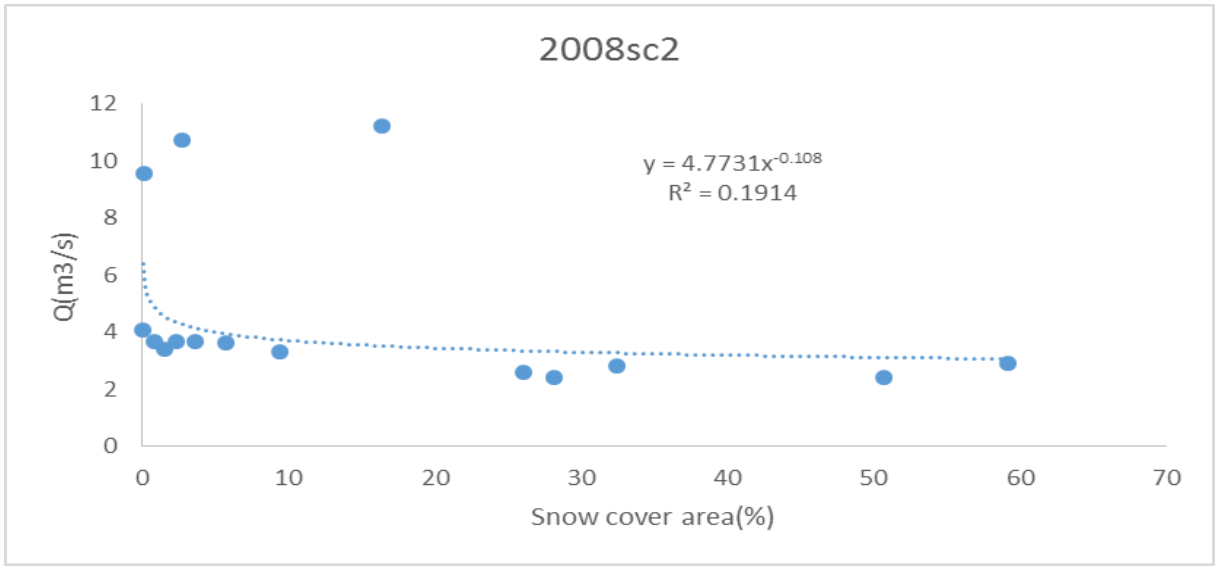
2008sc2
y = 4.7731x-0.108
R² = 0.1914
Q(m3/s)
Snow cover area(%)
0
2
4
6
8
10
12
0
10
20
30
40
50
60
70

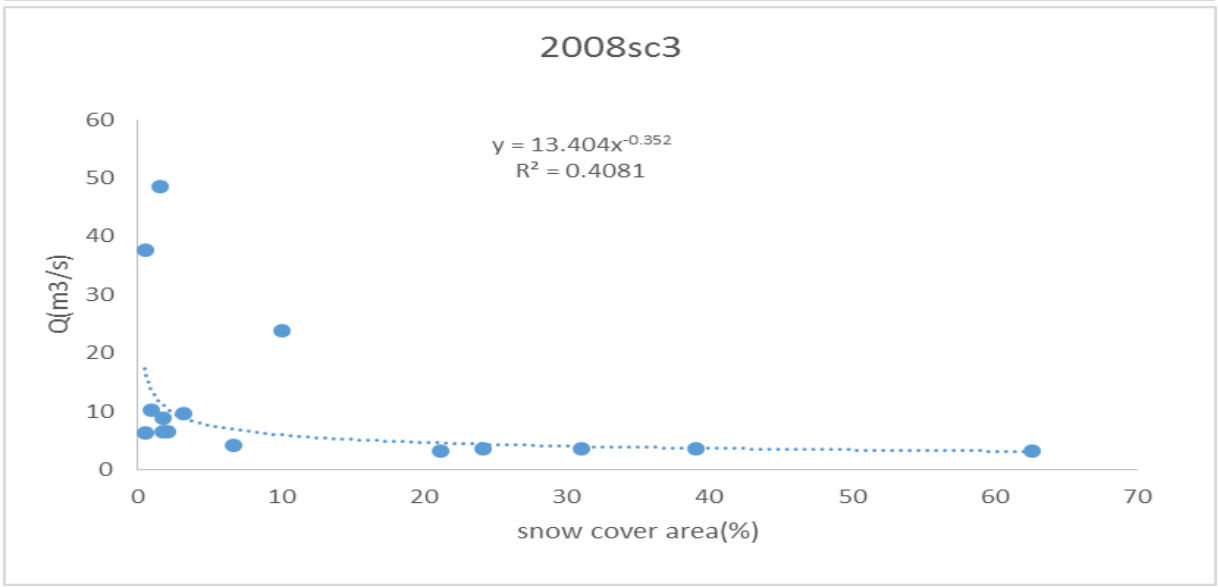
2008sc3
y = 13.404x-0.352
R² = 0.4081
Q(m3/s)
snow cover area(%)
0
10
20
30
40
50
60
0
10
20
30
40
50
60
70

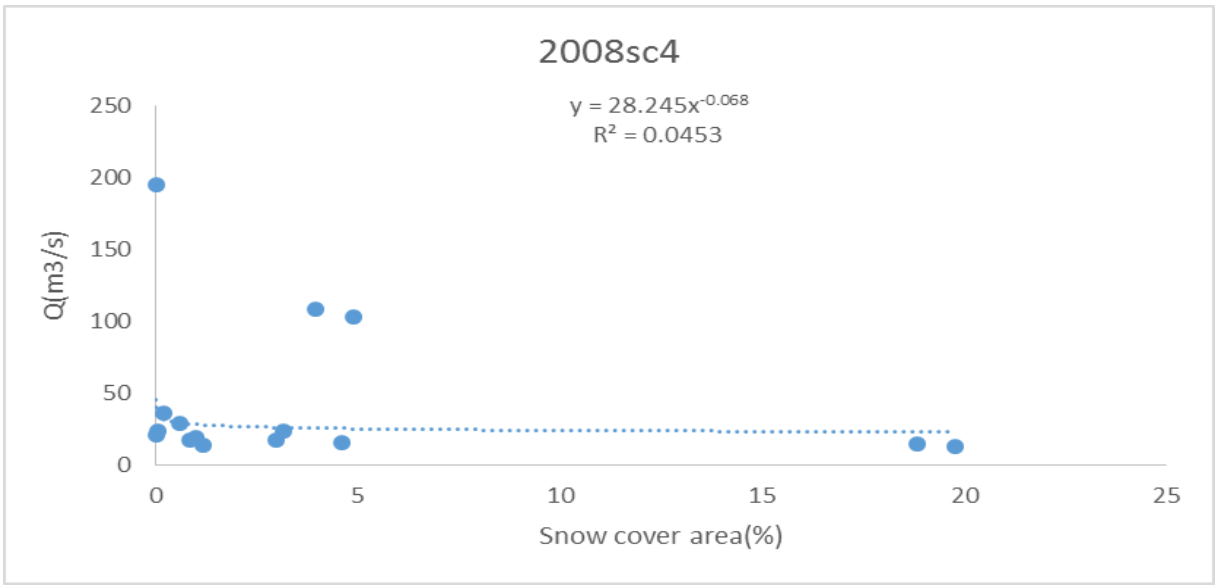
2008sc4
y = 28.245x-0.068
R² = 0.0453
Q(m3/s)
Snow cover area(%)
0
50
100
150
200
250
0
5
10
15
20
25

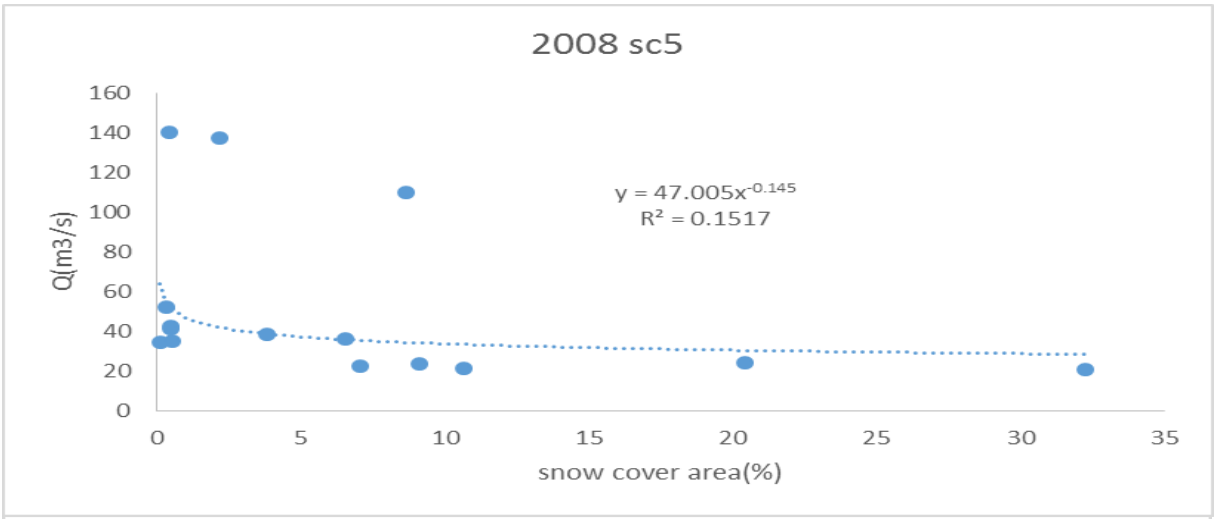
2008 sc5
Q(m3/s)
snow cover area(%)
y = 47.005x-0.145
R² = 0.1517

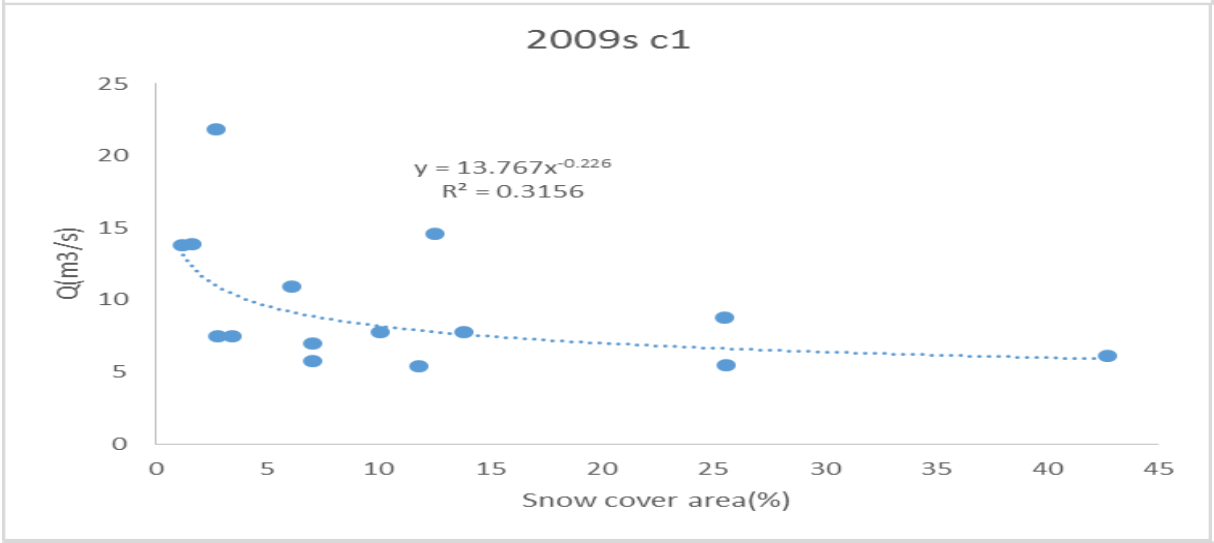
2009s c1
Q(m3/s)
Snow cover area(%)
y = 13.767x-0.226
R² = 0.3156

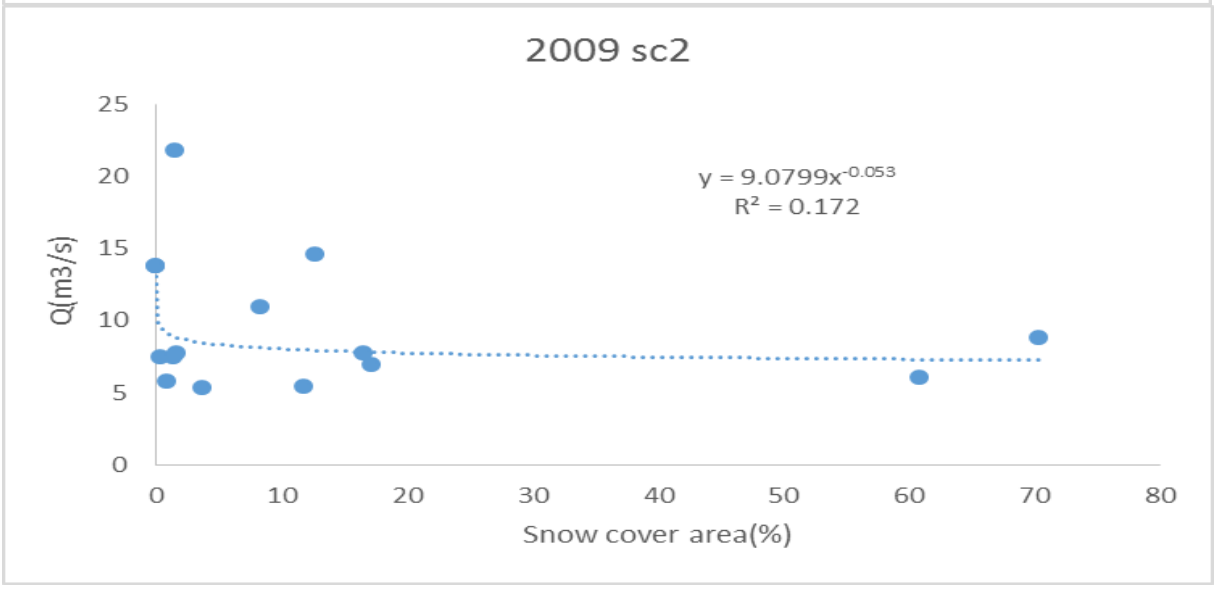
2009 sc2
Q(m3/s)
Snow cover area(%)
y = 9.0799x-0.053
R² = 0.172

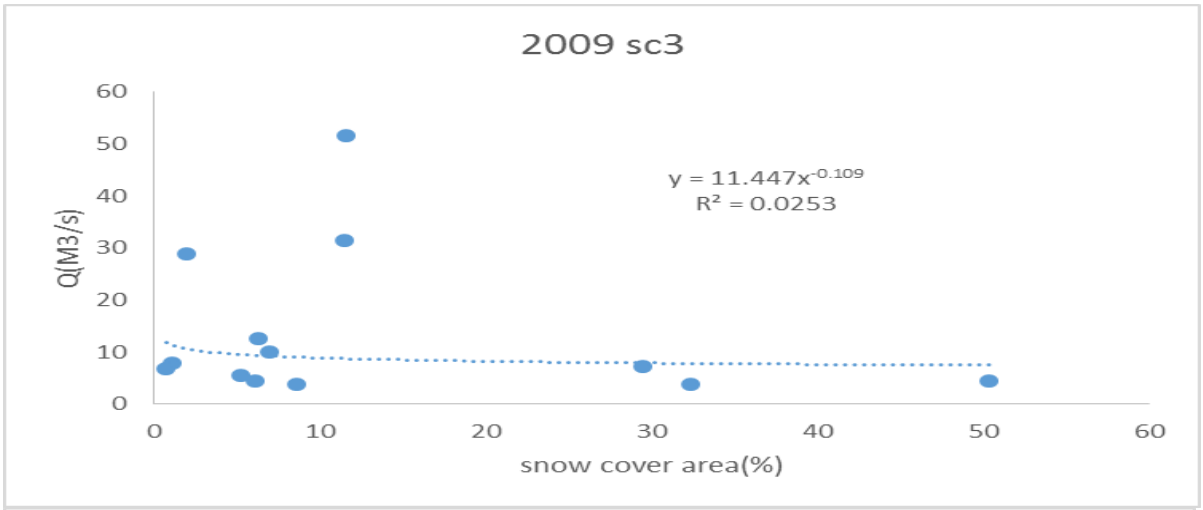
2009 sc3
y = 11.447x^-0.109
R² = 0.0253
Q(M3/s)
snow cover area(%)
0
10
20
30
40
50
60

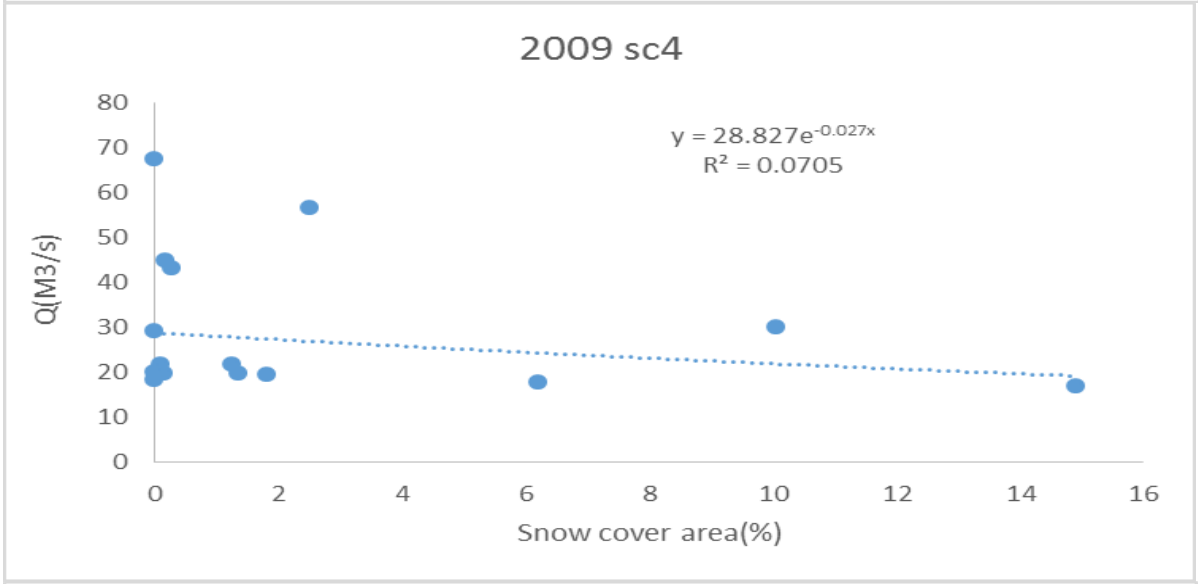
2009 sc4
y = 28.827e^-0.027x
R² = 0.0705
Q(M3/s)
Snow cover area(%)
0
2
4
6
8
10
12
14
16
70
80

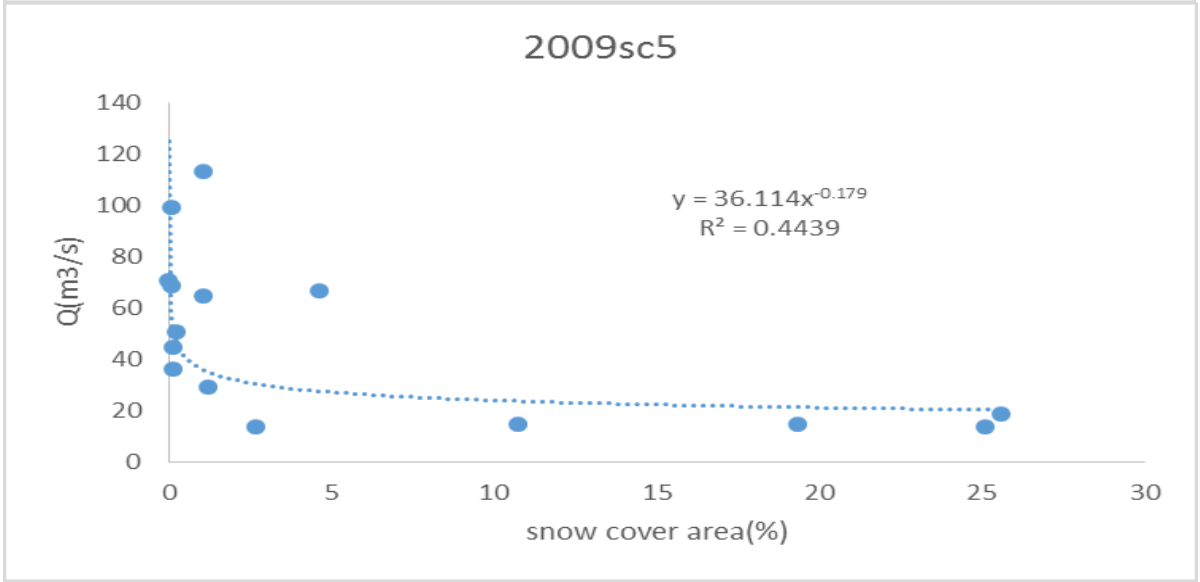
2009sc5
y = 36.114x^-0.179
R² = 0.4439
Q(m3/s)
snow cover area(%)
0
5
10
15
20
25
30
120
140

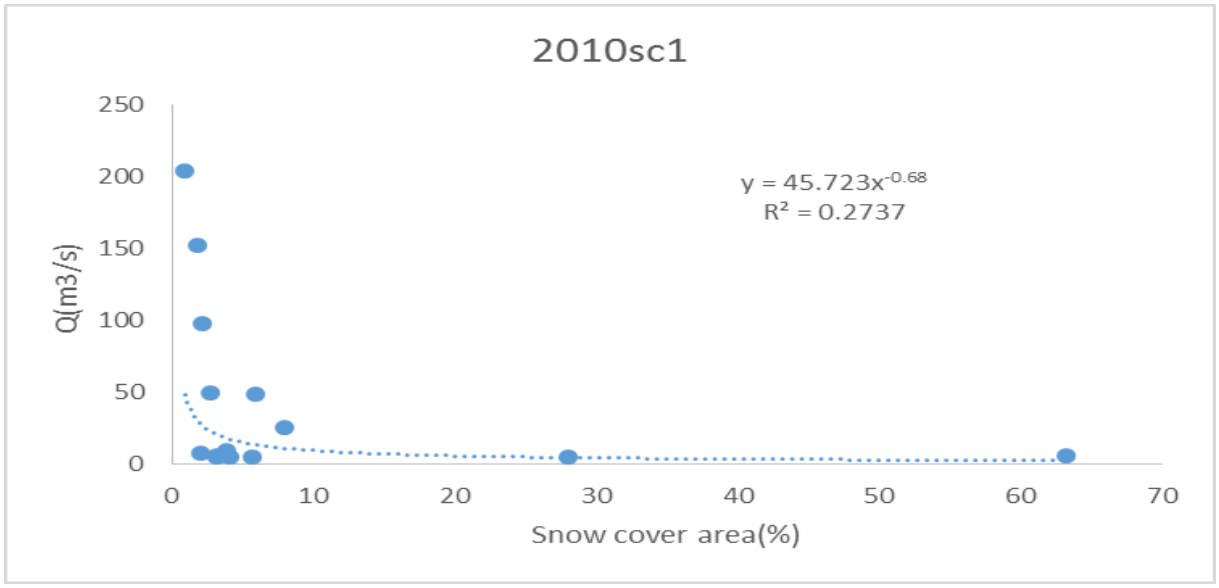
2010sc1
y = 45.723x-0.68
R² = 0.2737
Q(m3/s)
Snow cover area(%)
0
50
100
150
200
250
0
10
20
30
40
50
60
70

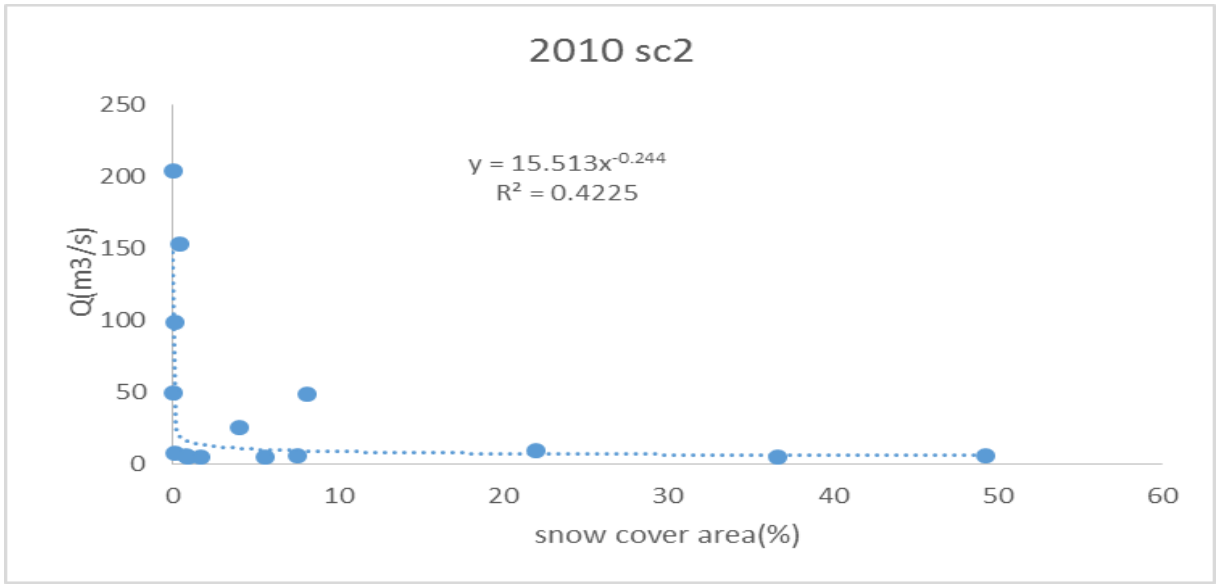
2010 sc2
y = 15.513x-0.244
R² = 0.4225
Q(m3/s)
snow cover area(%)
0
50
100
150
200
250
0
10
20
30
40
50
60

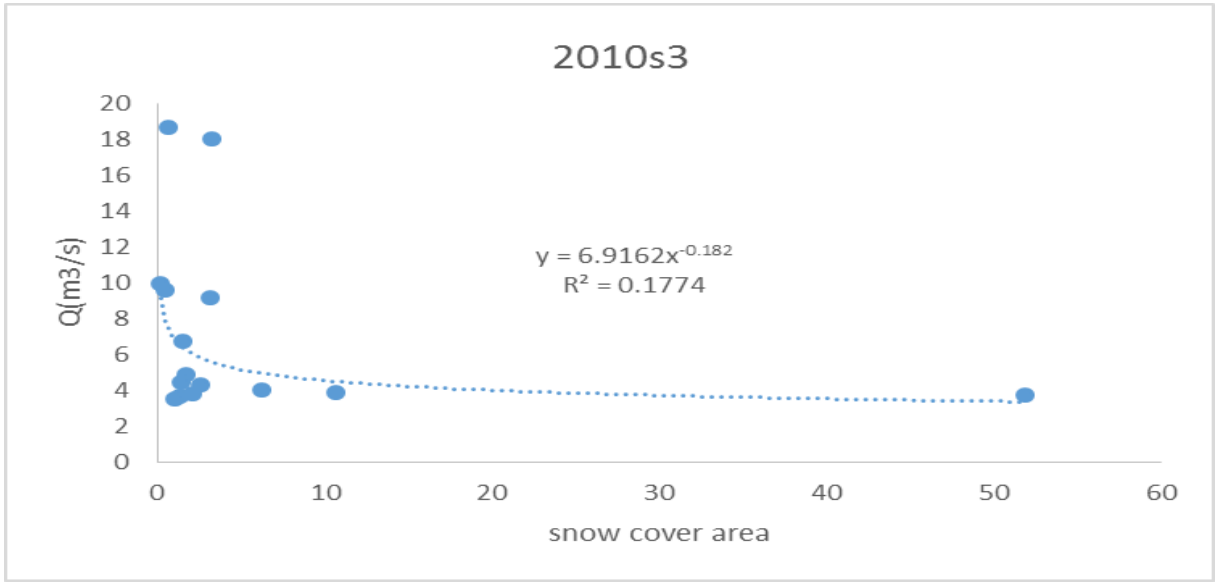
2010s3
y = 6.9162x-0.182
R² = 0.1774
Q(m3/s)
snow cover area
0
2
4
6
8
10
12
14
16
18
20
0
10
20
30
40
50
60

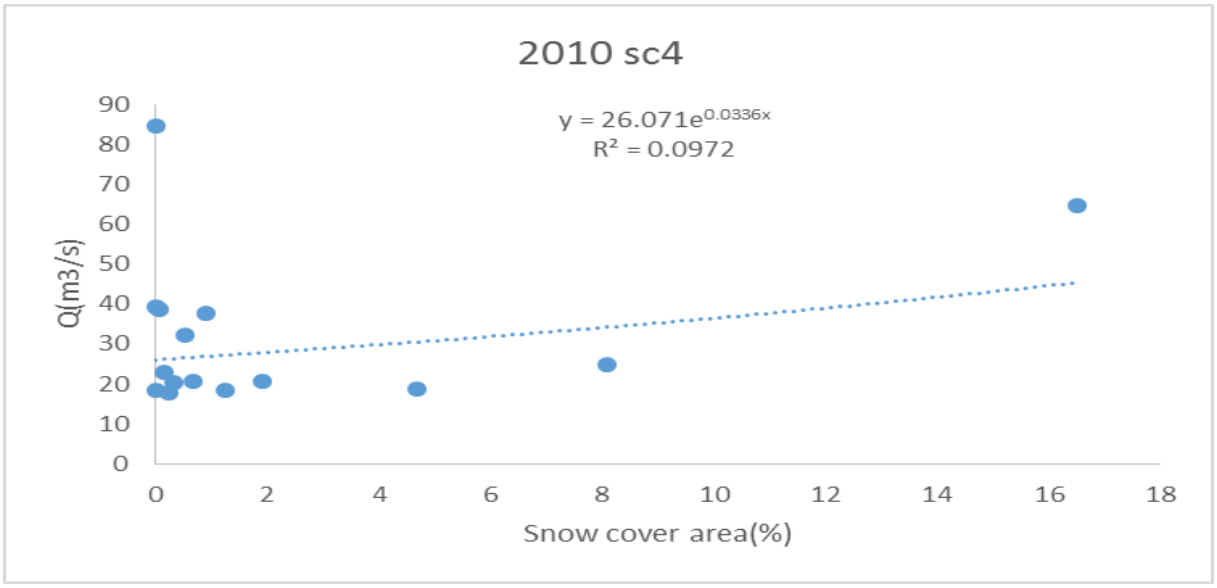
2010 sc4
y = 26.071e^0.0336x
R² = 0.0972
Q(m3/s)
Snow cover area(%)
0
10
20
30
40
50
60
70
80
90
0
2
4
6
8
10
12
14
16
18

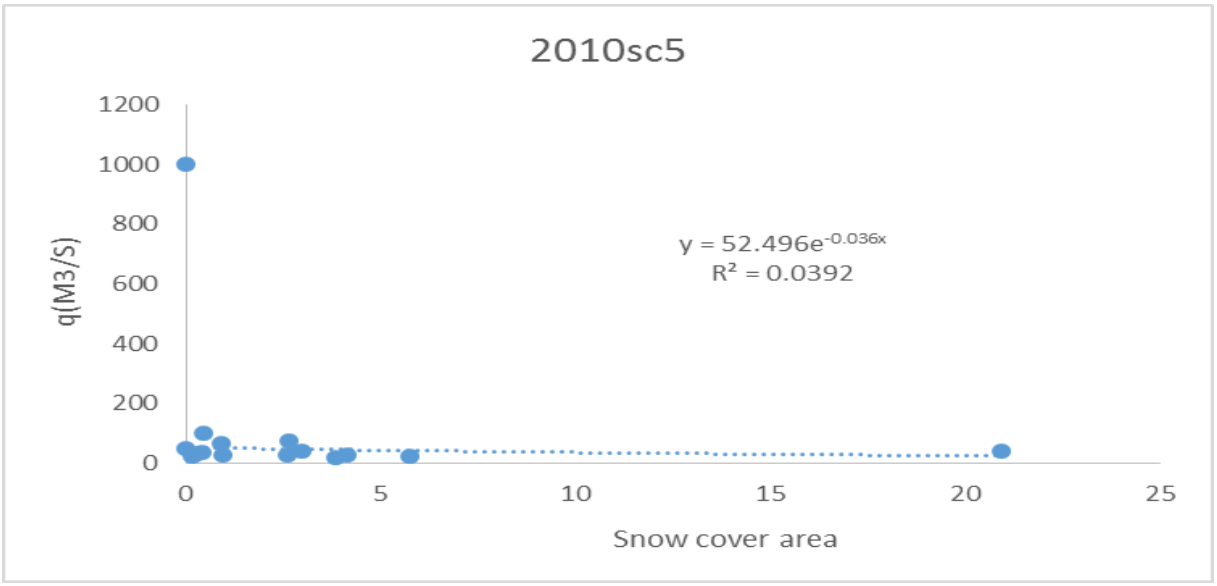
2010sc5
y = 52.496e^-0.036x
R² = 0.0392
q(M3/S)
Snow cover area
0
200
400
600
800
1000
1200
0
5
10
15
20
25